AN INVESTIGATION INTO THE
ACCURACY OF METROGON PHOTOGRAPHY

CHARLES FREDERICK WILLETT

AN INVESTIGATION INTO THE ACCURACY

OF METROGON PHOTOGRAPHY

A Thesis

Presented in Partial Fulfillment of the Requirements
for the Degree Master of Science

By

CHARLES FREDERICK WILLETT, B.A.
Lieutenant Commander, U. S. Navy

The Ohio State University

1959

TABLE OF CONTENTS

INTRODUCTION

The purpose of this thesis is to determine, by computation, the accuracy limitations of metrogon photography for use in stereo plotting instruments such as the Wild Autograph A7. This will be done by analyzing the error curves of lenses for which data can be obtained. These data will then be compared to a standard metrogon correction plate curve, as verified by observation, to determine residual errors. Then error curves within the stereo model will be constructed for X and Z coordinates and a y-parallax curve determined. Error curves from observation of an actual set of metrogon photographs will then be constructed and compared with the computed curves.

GENERAL DISCUSSION OF METROGON ACCURACY

In order to discuss the accuracy of metrogon photography, several letters were written to governmental agencies and metrogon lens manufacturers requesting data on these lenses. The only reply received with any usable information was from the National Bureau of Standards, enclosing data on all (25) metrogon lenses tested during fiscal year 1959.

The distortion values, which were taken from the original data, are tabulated in microns, normally the Bureau reports distortion values to the nearest ± 0.02 mm. These lenses were tested at their maximum aperture, f/6.3, and the measurements were made with a collimated incident light using a K-3 filter, a tungsten source and Eastman Kodak spectroscopic emulsion type V-F. Development was done in D-19 at 68°F for three minutes with continuous agitation. Tables I, II, and III are the tables of data provided by the National Bureau of Standards.

The data in Tables II and III are based on angular displacement from the principal point. This data was converted to radial distances in Table IV in order to provide a basis of comparison with the correction plate. The data of Tables III and IV were then used to construct the distortion curves of the best, average, and worst lenses, in Figures 5 through 8. These curves indicate the displacement of the image from the distortion free

position. The abscissa indicates radial distance of the distortion free position from the photo center. A positive distortion value indicates a displacement away from center.

There has been considerable discussion concerning the establishment of a standardized calibrated focal length for metrogon lenses. Insofar as could be determined, there has been no formalized decision on this matter. It is apparent from the reconstructed curves of the 25 lenses that the National Bureau of Standards has adopted the calibrated focal length to produce zero distortion at the $42\frac{1}{2}^{\circ}$ circle, as all curves plot out through this point.

Table V is a table of lens distortions, based on radial distance in mm, taken from the reconstructed curves of distortion of the lenses. Figure 9 is the distortion compensation curve of the correction plate manufactured by Wild. The offset abscissa chosen for construction of the plates was used in order to reduce the thickness of glass. The shifted abscissa requires that the calibrated focal length of metrogon plates used with the correction plates must be increased by 0.066 mm. However the values, taken in reference to the original abscissa, can be used for comparison with curves of lenses whose calibrated focal length is set for zero distortion at $42\frac{1}{2}^{\circ}$.

After a comparison of the correction plate curve with the curves of distortion of the lenses, the amount of distortion which the correction plates would leave uncompensated was tabulated in Table VI. It is realized that 25 lenses is a small sampling of the number which has been manufactured. However, this is the entire

number submitted to the National Bureau of Standards, for testing, over a one year period, regardless of manufacturer or source. With this in mind, it is interesting to note that only two lenses (8%) have distortion curves sufficiently close to the correction plate curve, which is apparently a fairly widely accepted standard curve, to provide uncompensated errors less than ±10 microns. Thirteen (62%) would have uncompensated errors less than ±20 microns. Two (8%) of the lenses would have uncompensated errors in excess of 40 microns.

In order to determine the effect the above errors would have on a stereo model, an assumed elevation of 4,000 meters above terrain was chosen and elevation errors were computed using the basic relief displacement relationship, $d = \frac{rh_p}{H}$ for computing an approximate elevation discrepancy which would result from the values in Table VI. This approximation is undoubtedly accurate enough for the number of significant digits used. These values, tabulated in Table VII, would not necessarily be the errors measured in a stereo model, as they would depend on the relative orientation achieved which in turn would depend upon the location of the chosen orientation points. This is true because, except along the line through the two principal points, the lens distortion will cause a varying amount of y-parallax. If this parallax is removed at the orientation points, the projected images will not have the true spatial relationship, and the effects of lens distortion at any given point in the model may be exaggerated or diminished

depending on the specific case. On the other hand, if the distortion at the chosen orientation points which are not on the line connecting the principal points happens to be zero from both projectors, the relative orientation will be true and the lens distortion will have full effect.

The values in Table VI will be the maximum possible elevation error at any given point, that is the larger of the two elevation errors at that point will be the maximum. This can be best demonstrated by diagramming the relationship of true and distorted rays at a point along the line connecting the principal points, as in Figure 1.

As can be seen from Figure 1, the maximum elevation error occurs when the elevation errors at a given point are equal which is true along the line equidistant from both principal points, and there will be an error in the X direction whenever the elevation errors are unequal. The same thing occurs at points which are not equidistant from both principal points or on lines through L_1 and L_2 parallel to this line, except that y-parallax is introduced. This can be seen in Figure 2. In Figure 2, point A" is not actually a point of intersection as the two rays pass through the vertical line through A-A' at different points. A" is the point on both lines at which there is no X or elevation separation and thus is the point which would be chosen in a stereo instrument as the true point with only y-parallax present. Actually, the ray from L_1 is in front of the ray from L_2, as Figure 1 is drawn. The range of possible y positions in a stereo instrument would be between points

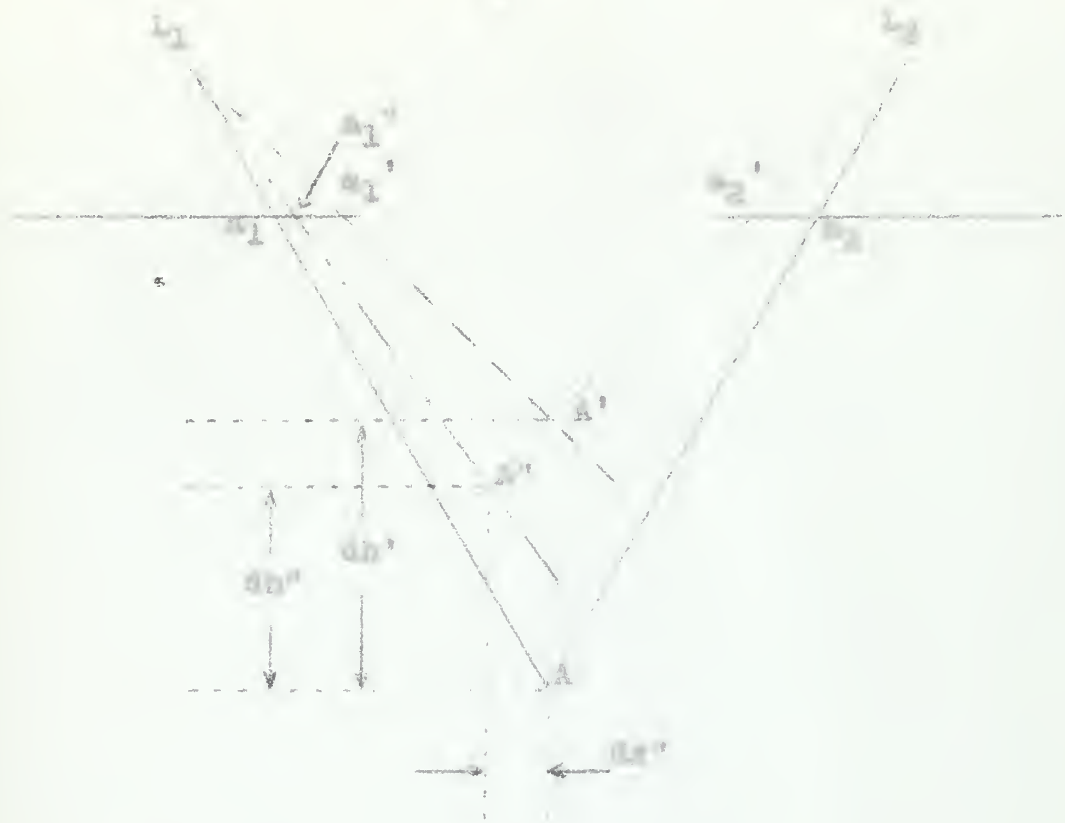

True rays

Distorted rays of equal elevation error

Distorted ray of unequal elevation error to ray from right projector

a_1 a_2 — undistorted positions

a_1' a_2' — equally distorted positions

a_1'' a_2' — unequally distorted positions

A — true projected image
A' — projected image with equal distortions
A" — projected image with unequal distortions
dh' — elevation error with equal distortions
dh" — elevation error with unequal distortions
dx" — X error with unequal distortions

Figure 1

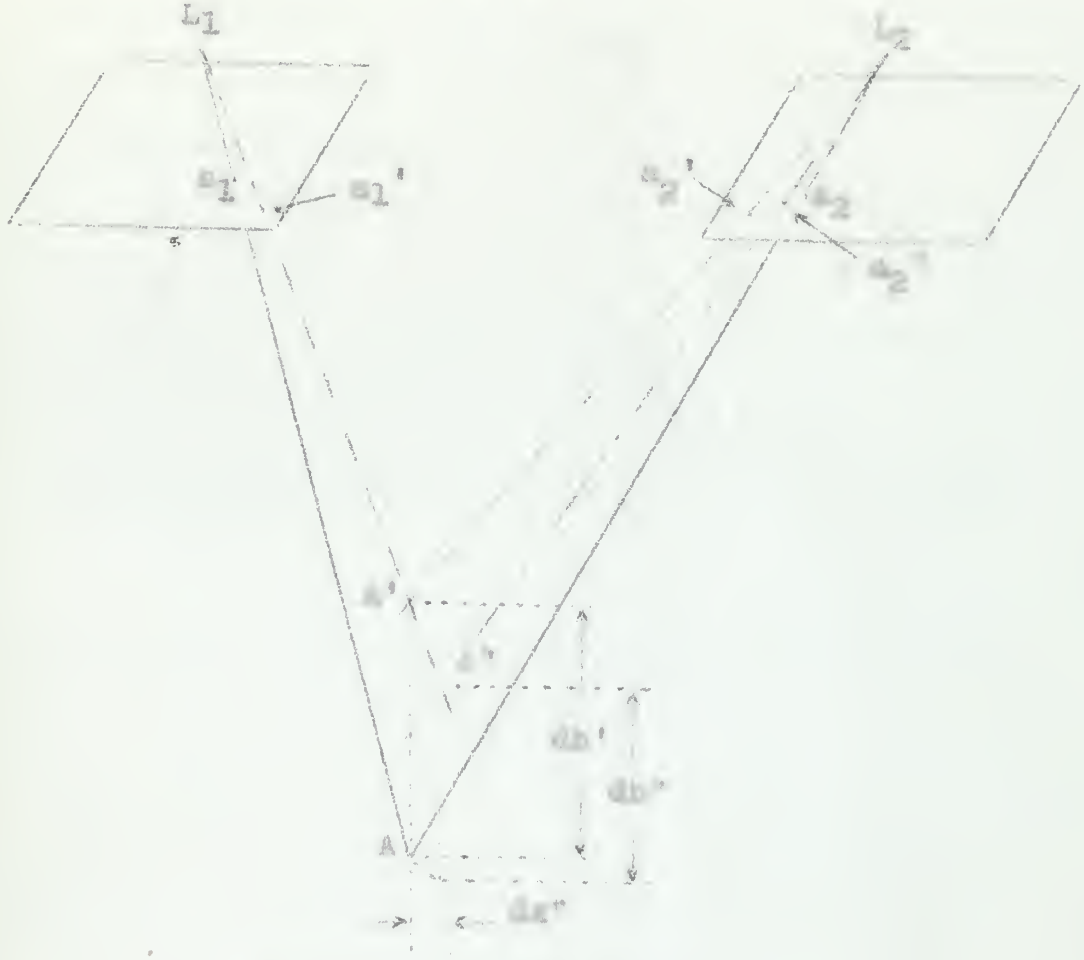

Symbols as used in Figure 1

Figure 2

A" on rays from L_1 and L_2. The exact position would depend on the relative orientation procedure. The point will be displaced by dX" which will be zero in the event of equal elevation errors from both projectors, as at point A'.

There will be no X displacement of the image along a line equidistant from both principal points or lines through L_1 and L_2 parallel to this line as the points along the equidistant line will

have equal distortion and thus equal elevation error at any given point along it, and the projection from either point parallel to the y-axis will have no X displacement.

As can be seen from Figures 1 and 2, the X displacement will always be toward the projector having the lowest (algebraically) elevation error at the point in question. The magnitude of the X displacement is computed as follows:

A drawing of a horizontal projection of the rays involved onto a plane containing both camera axes is constructed.

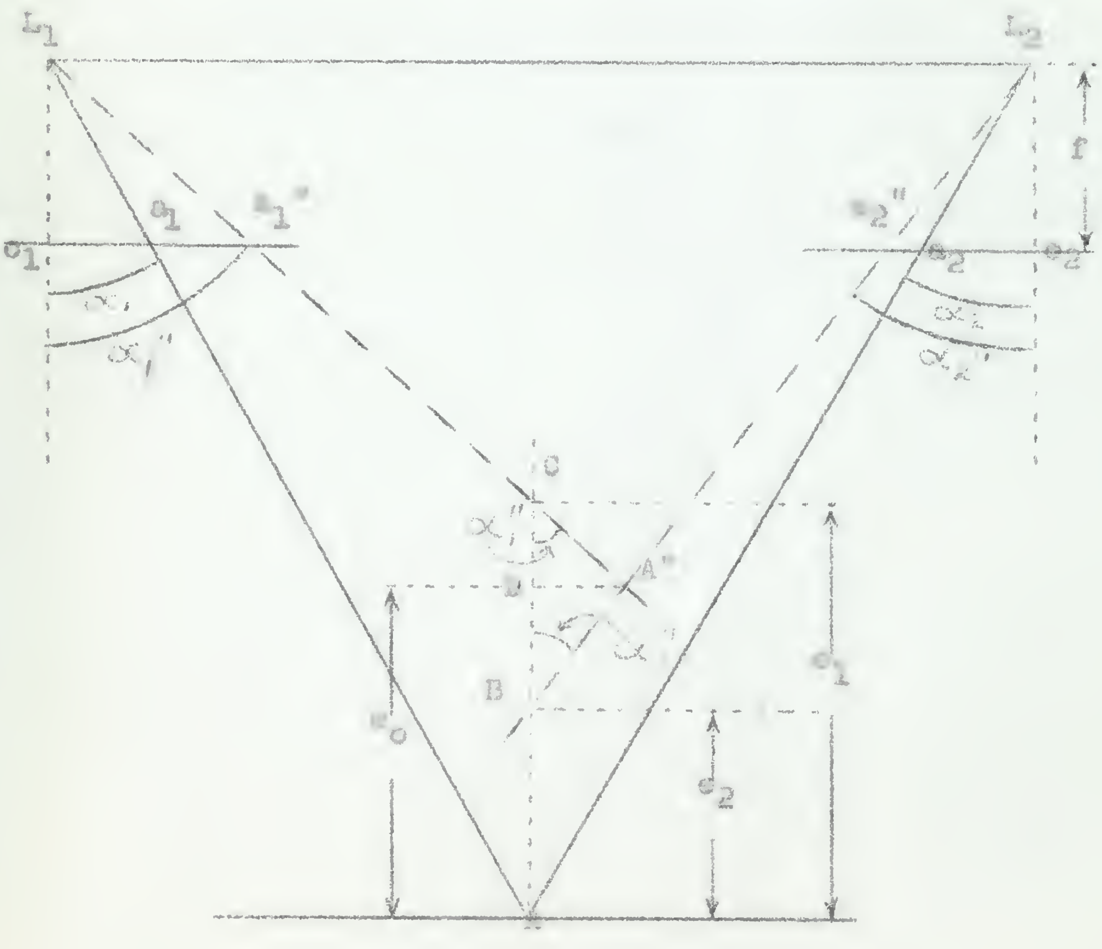

Figure 3

Let: $x_{a_1} = O_1a_1"$ $\quad x_{a_2} = O_2a_2"$ $\quad dX" = DA"$

Then:

$$\tan\alpha_1" = \frac{x_{a_1}}{f} = \frac{dX"}{CD} \qquad \tan\alpha_2" = \frac{x_{a_2}}{f} = \frac{dX"}{DB}$$

$$dX" = \frac{CDx_{a_1}}{f} = \frac{-BDx_{a_2}}{f} \text{ or } -BD = \frac{CDx_{a_1}}{x_{a_2}}$$

$$CD + BD = e_1 - e_2 \qquad CD = e_1 - e_2 - BD$$

$$x_{a_1}(e_1-e_2-BD) = -BDx_{a_2} \qquad BD(x_{a_1}-x_{a_2}) = x_{a_1}(e_1-e_2)$$

$$BD = \frac{x_{a_1}(e_1-e_2)}{x_{a_1} - x_{a_2}} \qquad dX" = \frac{-BDx_{a_2}}{f} = \frac{-x_{a_1}x_{a_2}(e_1-e_2)}{f(x_{a_1} - x_{a_2})}$$

A plus sign in dX" indicates displacement toward L_2.

The range of possible y displacements can be shown by drawing a vertical view of the scheme displayed in Figure 3.

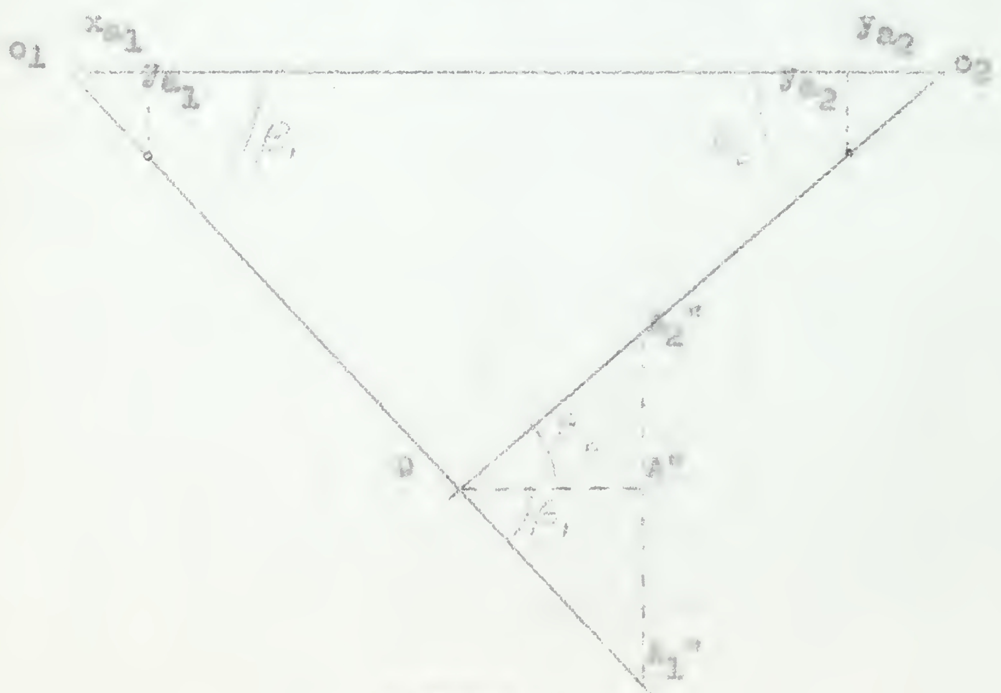

Figure 4

$DA'' = dX''$ (as shown in Figure 3)

$$A''A_2'' = dX'' \tan\beta_2 = \frac{y_{a_2} dX''}{-x_{a_2}} \qquad A''A_1'' = dX'' \tan\beta_1 = \frac{y_{a_1} dX''}{x_{a_1}}$$

$$A''A_2'' = \frac{y_{a_2}}{-x_{a_2}} \left[\frac{-x_{a_1} x_{a_2}(e_1 - e_2)}{f(x_{a_1} - x_{a_2})}\right] = \frac{x_{a_1} y_{a_2}(e_1 - e_2)}{f(x_{a_1} - x_{a_2})}$$

$$A''A_1'' = \frac{y_{a_1}}{x_{a_1}} \left(\frac{-x_{a_1} x_{a_2}(e_1 - e_2)}{f(x_{a_1} - x_{a_2})}\right) = \frac{-x_{a_2} y_{a_1}(e_1 - e_2)}{f(x_{a_1} - x_{a_2})}$$

Thus:

$$\text{total parallax } A_1''A_2'' = \frac{x_{a_1} y_{a_2}(e_1 - e_2)}{f(x_{a_1} - x_{a_2})} - \frac{x_{a_2} y_{a_1}(e_1 - e_2)}{f(x_{a_1} - x_{a_2})}$$

$$A_1''A_2'' = \frac{(e_1 - e_2)(x_{a_1} y_{a_2} - x_{a_2} y_{a_1})}{f(x_{a_1} - x_{a_2})} \text{ (at ground scale)}$$

$$\text{at photo scale } py = \frac{f}{H-h} A_1''A_2'' = \frac{(e_1 - e_2)(x_{a_1} y_{a_2} - x_{a_2} y_{a_1})}{(H - h)(x_{a_1} - x_{a_2})}$$

A plus sign in py indicates that A_2'' is in a positive Y direction from A_1''.

An example using lens number 25 and assuming a 100 mm base length, with the point of detail 40 mm from station 1 and 60 mm from station 2 along the line between principal points, is presented. In the case of points not on this line, bear in mind that true radial distance from the principal point must be used to determine elevation error, and this distance will differ from the values of x_{a_1} and x_{a_2}.

$BQ' = AQ'$ (as shown in Figure 8)

$$\delta' Y_A{}' = AQ' \tan \theta_A = \frac{-x_A{}' \, AQ'}{f} \qquad \delta' Y_B{}' = BQ' \tan \theta_B = \frac{-x_B{}' \, BQ'}{f}$$

$$\delta' Y_1{}' = \frac{-x_1{}'}{f} \left[\frac{d_1 \, d_2 \, (x_1 - x_2)}{f \, (d_1{}^2 - d_2{}^2)} \right] = \frac{-x_1{}' \, d_1 d_2 (x_1 - x_2)}{f^2 (d_1{}^2 - d_2{}^2)}$$

$$\delta' Y_2{}' = \frac{-x_2{}'}{f} \left[\frac{d_1 \, d_2 \, (x_1 - x_2)}{f \, (d_1{}^2 - d_2{}^2)} \right] = \frac{-x_2{}' \, d_1 d_2 (x_1 - x_2)}{f^2 (d_1{}^2 - d_2{}^2)}$$

Thus

total parallax $Y_1{}' Y_2{}' = \frac{d_1 d_2 (x_1 - x_2)}{f^2 (d_1{}^2 - d_2{}^2)} - \frac{d_1 d_2 (x_1 - x_2)}{f^2 (d_1{}^2 - d_2{}^2)}$

$$Y_1{}' Y_2{}' = \frac{(x_1 - x_2)(x_2 \, d_1 d_2 - x_1 \, d_1 d_2)}{f^2 (d_1{}^2 - d_2{}^2)} \text{ (plus for positive)}$$

so parallax $p_y = Y_2{}' - Y_1{}' = \frac{(x_1 - x_2)(x_2 d_1 d_2 - x_1 d_1 d_2)}{f^2 (d_1{}^2 - d_2{}^2)}$

A plus sign in p_y indicates that $Y_2{}'$ is in a positive Y direction from $Y_1{}'$.

An infinite series of points assuming a 500 mm base length, with the point of origin on the left station 1 and on the right station 2 along the line between principal points, is presented. In the case of points not on this line, bear in mind that the radial distance from the principal point must be used in determining distortion errors, and this distance will differ from the values of $x_1{}'$ and $x_2{}'$.

$x_{a_1} = 40$ mm $\quad x_{a_2} = 60$ mm $\quad e_1 = 1.3$ m $\quad e_2 = 0.48$ m

$f = 153.80$ mm

$py = \frac{(1.3 - 0.48)(40 \times 0 - 60 \times 0)}{4000\ (40 - 60)} = 0$ as the point is along the line between principal points.

$dX" = \frac{(40)(60)(1.3 - 0.48)}{(153.80)(40 + 60)} = 0.128$ m at natural scale.

The magnitude of the resultant elevation error can also be computed using Figure 3 as a reference.

$AD = e_o$ (resultant elevation error) $= AB + BD$

$AB = e_2 \qquad\qquad BD = dX" \cot \alpha_2"$

$\cot \alpha_2" = f/-x_{a_2}$

$BD = \frac{f dX"}{-x_{a_2}}$

Thus: $\quad e_o = e_2 - \frac{f dX"}{x_{a_2}}$

Using the example of lens number 25:

$e_o = 0.48 - \frac{153.80 \times 0.128}{-60} = 0.81$ m

The signs of x_{a_1}, x_{a_2}, y_{a_1}, y_{a_2} are as measured in a photo scale model (positive print) for the above derivations. The above computational procedures are applicable to all types of photography once the curve of elevation errors due to distortion has been determined. Thus the elevation error and the X displacement caused by lens distortion can be computed for any given point in the stereo model. This condition, of course, will only be the true situation

if the relative orientation has been completed so that a true spatial model has been developed.

In the above example, presume that the elevation variation of the terrain is 10% of the flying height above the terrain. Because the values of e_1 and e_2 are directly proportional to the flying heights, and e_o and dX'' are directly proportional to first order equations containing e_1 and e_2, the values will vary 10% of the computed value, thus:

Qty	Computed Value	10% Variation
e_o	0.81 m	0.73 to 0.89 m
dX''	0.128 m	0.115 to 0.141 m

Therefore the accuracy of elevation computation would be one part in 50,000 of the flying height, and the accuracy of the X coordinate would be one part in 300,000 of the flying height.

TABLE I

FOCAL LENGTHS

Lens No.	Equivalent Focal Length	Calibrated Focal Length
	mm	mm
1	152.67	152.77
2	153.39	153.45
3	154.31	154.31
4	153.86	153.85
5	151.85	151.90
6	154.34	154.37
7	151.70	151.70
8	152.94	152.95
9	154.34	154.34
10	153.19	153.22
11	153.33	153.30
12	153.73	153.70
13	153.67	153.75
14	152.58	152.62
15	153.19	153.20
16	153.36	153.30
17	152.79	152.76
18	153.72	153.68
19	153.81	153.80
20	155.37	155.35
21	153.98	153.89
22	153.40	153.36
23	154.22	154.19
24	152.54	152.49
25	153.90	153.80
Ave.		153.44

The probable errors of these determinations of focal length do not exceed ± 0.10 mm.

TABLE II

DISTORTION REFERRED TO THE EQUIVALENT FOCAL LENGTH IN MICRONS

Lens No.	0°	5°	10°	15°	20°	25°	30°	35°	40°	45°
1	0	-2	1	13	38	76	126	173	172	9
2	0	-2	2	12	31	65	119	164	142	- 74
3	0	-1	1	10	30	60	96	119	81	-120
4	0	-2	1	12	31	62	92	108	62	-128
5	0	-2	2	16	34	70	107	140	113	- 63
6	0	-2	2	13	22	64	96	132	110	- 80
7	0	-2	2	12	34	65	96	115	70	-120
8	0	-2	2	14	34	64	100	130	100	-104
9	0	0	0	11	32	61	99	123	96	-120
10	0	-2	2	13	30	71	114	146	120	- 92
11	0	-2	2	6	33	73	112	146	116	- 89
12	0	-3	2	10	30	60	92	110	62	-150
13	0	-3	2	9	28	61	103	158	172	- 10
14	0	-2	1	14	36	72	109	140	115	- 82
15	0	-2	2	13	33	67	100	119	89	- 97
16	0	-1	0	10	28	50	74	86	34	-184
17	0	0	0	10	30	56	87	102	56	-153
18	0	-1	1	11	26	52	77	95	35	-163
19	0	-1	1	13	30	58	94	121	83	-135
20	0	-1	-2	10	28	57	97	119	77	-154
21	0	-3	2	12	28	49	74	77	11	-227
22	0	-4	3	10	29	52	80	94	49	-161
23	0	-2	2	12	34	63	94	110	62	-148
24	0	-1	1	8	36	66	88	94	40	-174
25	0	0	0	8	19	42	60	61	- 1	-220
Average	0	-2	1	11	31	62	95	119	83	-122

TABLE III

DISTORTION REFERRED TO THE CALIBRATED FOCAL LENGTH IN MICRONS

Lens No.	0°	5°	10°	15°	20°	25°	30°	35°	40°	45°
1	0	-11	-18	-15	0	27	65	98	84	- 98
2	0	- 6	- 7	- 2	12	44	89	127	98	-127
3	0	- 1	1	10	30	60	96	119	81	-120
4	0	- 1	3	15	35	67	98	116	71	-116
5	0	- 6	- 6	4	18	49	81	108	75	-108
6	0	- 5	- 3	5	11	50	79	111	85	-110
7	0	- 2	3	13	36	67	99	116	74	-116
8	0	- 3	- 1	10	29	57	91	120	87	-119
9	0	0	0	11	32	61	99	123	96	-120
10	0	- 5	- 3	5	19	56	96	124	94	-124
11	0	- 5	- 4	- 2	21	58	93	123	88	-123
12	0	- 1	6	16	38	71	105	126	82	-126
13	0	-10	-13	-14	- 3	21	53	97	100	- 97
14	0	- 5	- 4	5	23	57	90	116	87	-116
15	0	- 3	0	10	29	61	93	110	79	-110
16	0	4	10	25	49	77	107	126	82	-126
17	0	3	5	18	41	70	104	123	81	-123
18	0	3	8	22	41	72	100	123	69	-123
19	0	0	3	15	33	62	99	128	89	-127
20	0	1	2	15	35	66	109	133	94	-134
21	0	4	17	35	59	89	123	137	82	-139
22	0	0	10	21	44	71	103	122	83	-122
23	0	0	6	18	42	73	107	125	80	-125
24	0	3	9	20	52	87	114	125	79	-125
25	0	8	16	32	52	85	114	126	79	-126
Average	0	- 2	2	12	31	62	96	120	84	-120

The values of the distortion are measured in microns and indicate the displacement of the image from its distortion-free position. A positive value indicates a displacement from the center of the plate. The probable error does not exceed ± 10 microns.

TABLE IV

RADIAL DISTANCES BASED ON FOCAL LENGTHS IN MM

Lens	f	5°	10°	15°	20°	25°	30°	35°	40°	42.5°
1	152.77	13.37	26.94	40.93	55.60	71.24	88.20	106.97	128.19	139.99
2	153.45	13.43	27.06	41.12	55.85	71.55	88.59	107.45	128.76	140.61
3	154.31	13.50	27.21	41.35	56.16	71.96	89.09	108.05	129.48	141.40
4	153.85	13.46	27.13	41.22	56.00	71.74	88.83	107.73	129.10	140.98
5	151.90	13.29	26.78	40.70	55.29	70.83	87.70	106.36	127.46	139.19
6	154.37	13.51	27.22	41.36	56.19	71.98	89.13	108.09	129.53	141.45
7	151.70	13.27	26.75	40.65	55.21	70.74	87.58	106.22	127.29	139.01
8	152.95	13.38	26.97	40.98	55.67	71.32	88.31	107.10	128.34	140.15
9	154.34	13.50	27.21	41.36	56.18	71.97	89.11	108.07	129.51	141.43
10	153.22	13.41	27.02	41.06	55.77	71.45	88.46	107.29	128.57	140.40
11	153.30	13.41	27.03	41.08	55.80	71.49	88.51	107.34	128.63	140.47
12	153.70	13.45	27.10	41.18	55.94	71.67	88.74	107.62	128.97	140.84
13	153.75	13.45	27.11	41.20	55.96	71.69	88.77	107.66	129.01	140.89
14	152.62	13.35	26.91	40.89	55.55	71.17	88.12	106.87	128.06	139.85
15	153.20	13.40	27.01	41.05	55.76	71.44	88.45	107.27	128.55	140.38
16	153.30	13.41	27.03	41.08	55.80	71.49	88.51	107.34	128.63	140.47
17	152.76	13.36	26.94	40.93	55.60	71.23	88.20	106.96	128.18	139.96
18	153.68	13.45	27.10	41.18	55.93	71.66	88.73	107.61	128.95	140.82
19	153.80	13.46	27.12	41.21	55.98	71.72	88.80	107.69	129.05	140.93
20	155.35	13.59	27.39	41.63	56.54	72.44	89.69	108.78	130.35	142.35
21	153.89	13.46	27.13	41.23	56.01	71.76	88.85	107.76	129.13	141.01
22	153.36	13.42	27.04	41.09	55.82	71.51	88.54	107.38	128.68	140.53
23	154.19	13.49	27.19	41.32	56.12	71.90	89.02	107.97	129.38	141.29
24	152.49	13.34	26.89	40.86	55.50	71.11	88.04	106.77	127.95	139.73
25	153.80	13.46	27.12	41.21	55.98	71.72	88.80	107.69	129.05	140.93
Ave.	153.44	13.43	27.06	41.12	55.85	71.55	88.58	107.45	128.75	140.60

TABLE V

TABLE OF LENS DISTORTIONS IN MICRONS TAKEN FROM RECONSTRUCTED CURVES

Lens	20 mm	40 mm	60 mm	80 mm	100 mm	120 mm	140 mm	150 mm
1	-14.4	-15.5	+ 6.0	+ 46.0	+ 89.2	+100.0	0	- 77.0
2	- 6.8	- 2.8	+16.2	+ 66.3	+117.1	+120.7	+ 5.0	- 93.3
3	- 0.4	+ 8.6	+36.5	+ 78.2	+112.2	+109.8	+13.2	- 78.8
4	+ 0.1	+13.7	+42.0	+ 83.1	+113.6	+101.0	+ 3.0	- 84.0
5	- 6.8	+ 3.7	+25.9	+ 66.7	+103.0	+ 94.6	- 7.0	- 93.0
6	- 4.7	+ 4.1	+15.0	+ 66.0	+102.0	+105.0	+13.0	- 72.0
7	- 0.2	+12.6	+46.0	+ 85.0	+113.2	+102.3	- 9.6	-100.0
8	- 3.0	+ 8.4	+36.6	+ 73.4	+114.5	+110.6	+ 3.5	- 91.2
9	0	+ 9.0	+38.4	+ 78.0	+118.0	+117.8	+13.0	- 80.0
10	- 4.8	+ 4.1	+28.5	+ 76.4	+118.3	+116.0	+ 4.0	- 92.0
11	- 4.8	- 2.2	+30.7	+ 76.5	+114.0	+113.0	+ 4.3	- 91.0
12	+ 1.5	+14.8	+46.4	+ 87.5	+122.2	+114.5	+ 7.0	- 93.0
13	-12.2	-14.3	+ 1.8	+ 36.4	+ 77.5	+117.3	- 6.7	- 69.0
14	- 5.2	+ 3.8	+31.2	+ 74.5	+110.0	+107.5	- 2.3	- 93.0
15	- 2.8	+ 9.3	+36.2	+ 78.0	+107.0	+100.4	+ 3.0	- 81.7
16	+ 5.7	+23.3	+54.5	+ 92.8	+122.2	+112.5	+ 3.3	- 92.3
17	+ 3.0	+16.6	+49.5	+ 86.0	+120.0	+110.4	- 0.5	- 98.2
18	+ 4.8	+20.3	+48.0	+ 86.0	+116.0	+101.0	+ 4.8	- 85.0
19	+ 0.4	+13.3	+40.9	+ 79.4	+122.5	+119.0	+ 8.0	- 90.0
20	0	+12.9	+41.0	+ 83.0	+128.0	+125.0	+24.0	- 79.0
21	+ 9.7	+33.0	+66.2	+106.3	+135.4	+122.0	+ 8.0	- 98.0
22	+ 4.2	+19.7	+51.0	+ 86.4	+118.2	+111.3	+ 4.0	- 82.3
23	+ 2.0	+16.5	+48.8	+ 89.5	+121.5	+113.5	+11.0	- 83.2
24	+ 5.6	+19.0	+64.0	+102.2	+125.3	+105.0	- 3.0	-100.0
25	+11.9	+30.0	+58.2	+101.5	+123.8	+111.5	+ 6.7	- 89.5
Ave.	- 0.7	+11.2	+39.0	+ 79.0	+115.6	+109.0	+ 5.8	- 88.0

TABLE VI

TABLE OF DISTORTION, IN MICRONS, REMAINING UNCOMPENSATED BY PLATES

Lens	20 mm	40 mm	60 mm	80 mm	100 mm	120 mm	140 mm	150 mm
1	−16.4	−32.5	−45.0	−44.0	−26.8	− 1.0	−10.0	− 1.0
2	− 8.8	−19.8	−34.8	−23.7	+ 1.1	+19.7	− 5.0	−17.0
3	− 2.4	− 8.4	−14.5	−11.8	− 3.8	+ 8.8	+ 3.2	− 2.8
4	− 1.9	− 3.3	− 9.0	− 6.9	− 2.4	0	− 7.0	− 8.0
5	− 8.8	−13.3	−25.1	−23.3	−13.0	− 6.4	−17.0	−17.0
6	− 6.7	−12.9	−36.0	−24.0	−14.0	+ 4.0	+ 3.0	+ 4.0
7	−2.2	− 4.4	− 5.0	− 5.0	− 2.8	+ 1.3	−19.6	−24.0
8	− 5.0	− 8.6	−14.4	−16.6	− 1.5	+ 9.6	− 6.5	−15.2
9	− 2.0	− 8.0	−12.6	−12.0	+ 2.0	+16.8	+ 3.0	− 4.0
10	− 6.8	−12.9	−22.5	−13.6	+ 2.3	+15.0	− 6.0	−16.0
11	− 6.8	−19.2	−20.3	−13.5	− 2.0	+12.0	− 5.7	−15.0
12	− 0.5	− 2.2	− 4.6	− 2.5	+ 6.2	+13.5	− 3.0	−17.0
13	−14.2	−31.3	−49.2	−53.6	−38.5	+16.3	− 3.3	+ 7.0
14	− 7.2	−13.2	−19.8	−15.5	− 6.0	+ 6.5	−12.3	−17.0
15	− 4.8	− 6.7	−14.8	−12.0	− 9.0	− 0.6	− 7.0	− 5.7
16	+ 3.7	+ 6.3	+ 3.5	+ 2.8	+ 6.2	+11.5	− 6.7	−16.3
17	+ 1.0	− 0.4	− 1.5	− 4.0	+ 4.0	+ 9.4	−10.5	−22.2
18	+ 2.8	+ 3.3	− 3.0	− 4.0	0	0	− 5.2	− 9.0
19	− 1.6	− 3.7	−10.1	−10.6	+ 6.5	+18.0	− 2.0	−14.0
20	− 2.0	− 4.1	−10.0	− 7.0	+12.0	+24.0	+14.0	− 3.0
21	+ 7.7	+16.0	+15.2	+16.3	+19.4	+21.0	− 2.0	−22.0
22	+ 2.2	+ 2.7	0	− 3.6	+ 2.2	+10.3	− 6.0	− 6.3
23	0	− 0.5	− 2.2	− 0.5	+ 5.5	+12.5	+ 1.0	− 7.2
24	+ 3.6	+ 2.0	+13.0	+12.2	+ 9.3	+ 4.0	−13.0	−24.0
25	+ 9.9	+13.0	+ 7.2	+11.5	+ 7.8	+10.5	− 3.3	−13.5
Ave.	− 2.7	− 5.8	−12.0	−11.0	− 0.4	+ 8.0	− 4.2	−12.0

TABLE VII

TABLE OF ELEVATION ERRORS IN METERS

Lens	20 mm	40 mm	60 mm	80 mm	100 mm	120 mm	140 mm	150 mm
1	-3.28	-3.25	-3.00	-2.20	-1.07	-0.03	-0.29	-0.03
2	-1.76	-1.98	-2.32	-1.18	+0.04	+0.66	-0.14	-0.45
3	-0.48	-0.84	-0.97	-0.59	-0.15	+0.29	+0.09	-0.07
4	-0.38	-0.33	-0.60	-0.35	-0.10	0	-0.20	-0.21
5	-1.76	-1.33	-1.67	-1.16	-0.52	-0.21	-0.49	-0.45
6	-1.34	-1.29	-2.40	-1.20	-0.56	+0.13	+0.09	+0.11
7	-0.44	-0.44	-0.33	-0.25	-0.11	+0.04	-0.56	-0.64
8	-1.00	-0.86	-0.96	-0.83	-0.06	+0.32	-0.19	-0.41
9	-0.40	-0.80	-0.84	-0.60	+0.08	+0.56	+0.09	-0.11
10	-1.36	-1.29	-1.50	-0.68	-0.09	+0.50	-0.17	-0.43
11	-1.36	-1.92	-1.35	-0.68	-0.08	+0.40	-0.16	-0.40
12	-0.10	-0.22	-0.31	-0.12	-0.25	+0.45	-0.09	-0.45
13	-2.84	-3.13	-3.28	-2.68	-1.54	+0.55	-0.09	+0.19
14	-1.44	-1.32	-1.32	-0.78	-0.24	+0.22	-0.35	-0.45
15	-0.96	-0.67	-0.98	-0.60	-0.36	-0.02	-0.20	-0.15
16	+0.74	+0.63	+0.23	+0.14	+0.25	+0.35	-0.19	-0.43
17	+0.20	-0.04	-0.10	-0.20	+0.16	+0.31	-0.30	-0.59
18	+0.56	+0.33	-0.20	-0.20	0	0	-0.15	-0.24
19	-0.32	-0.37	-0.67	-0.53	+0.26	+0.60	-0.06	-0.37
20	-0.40	-0.41	-0.67	-0.35	+0.48	+0.80	+0.40	-0.08
21	+1.54	+1.60	-1.01	+0.82	+0.78	+0.70	-0.06	-0.59
22	+0.44	+0.27	0	-0.18	+0.09	+0.34	-0.17	-0.17
23	0	-0.05	-0.14	-0.03	+0.22	+0.42	+0.03	-0.19
24	+0.72	+0.20	+0.87	+0.61	+0.38	+0.13	-0.37	-0.64
25	+1.98	+1.30	+0.48	+0.58	+0.31	+0.35	-0.09	-0.36
Ave.	-0.54	-0.58	-0.80	-0.55	-0.02	+0.27	-0.12	-0.32

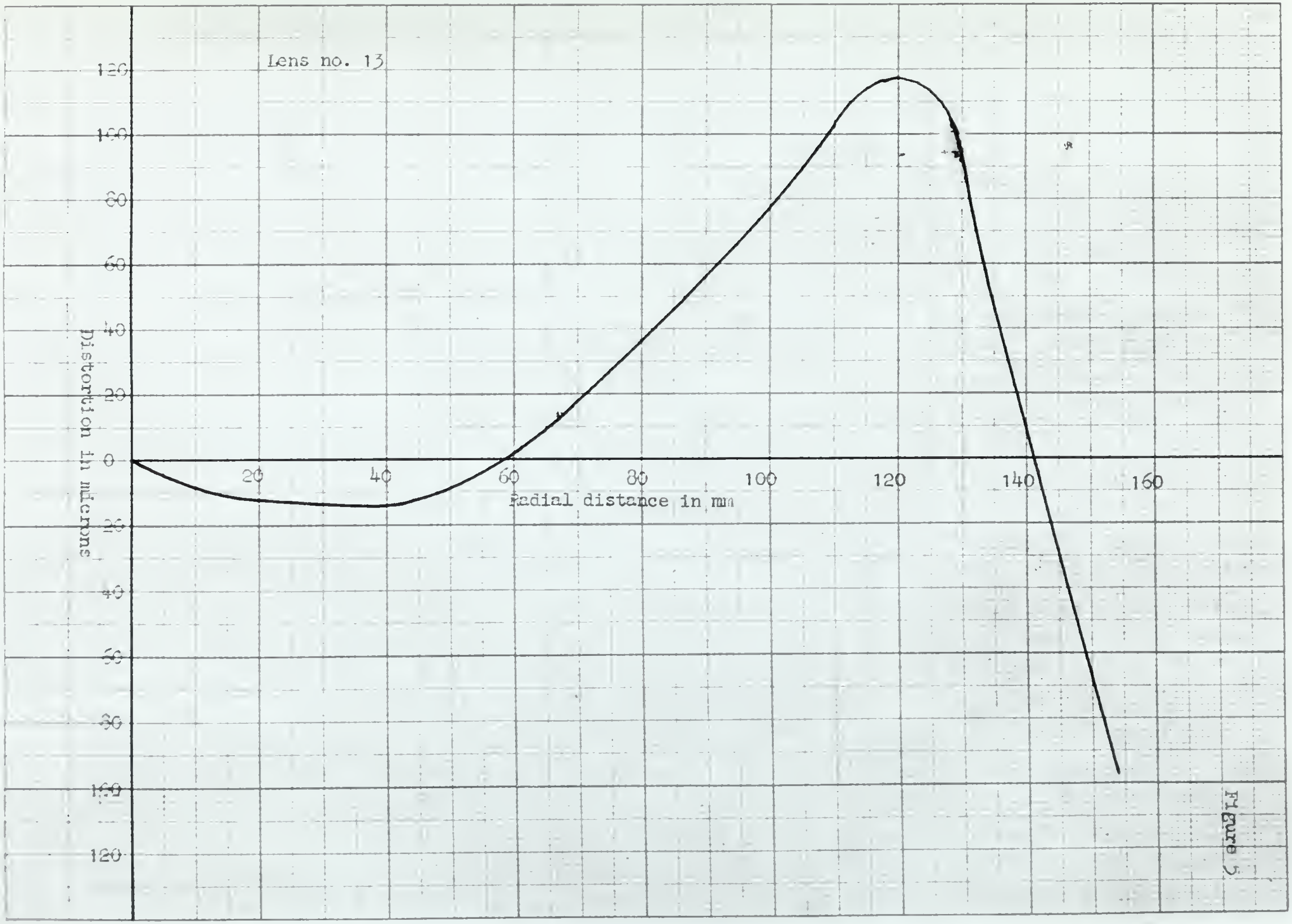
Lens no. 13
Distortion in microns
Radial distance in mm
120
100
80
60
40
20
0
20
40
60
80
100
120
140
160
Figure 5

Figure 7

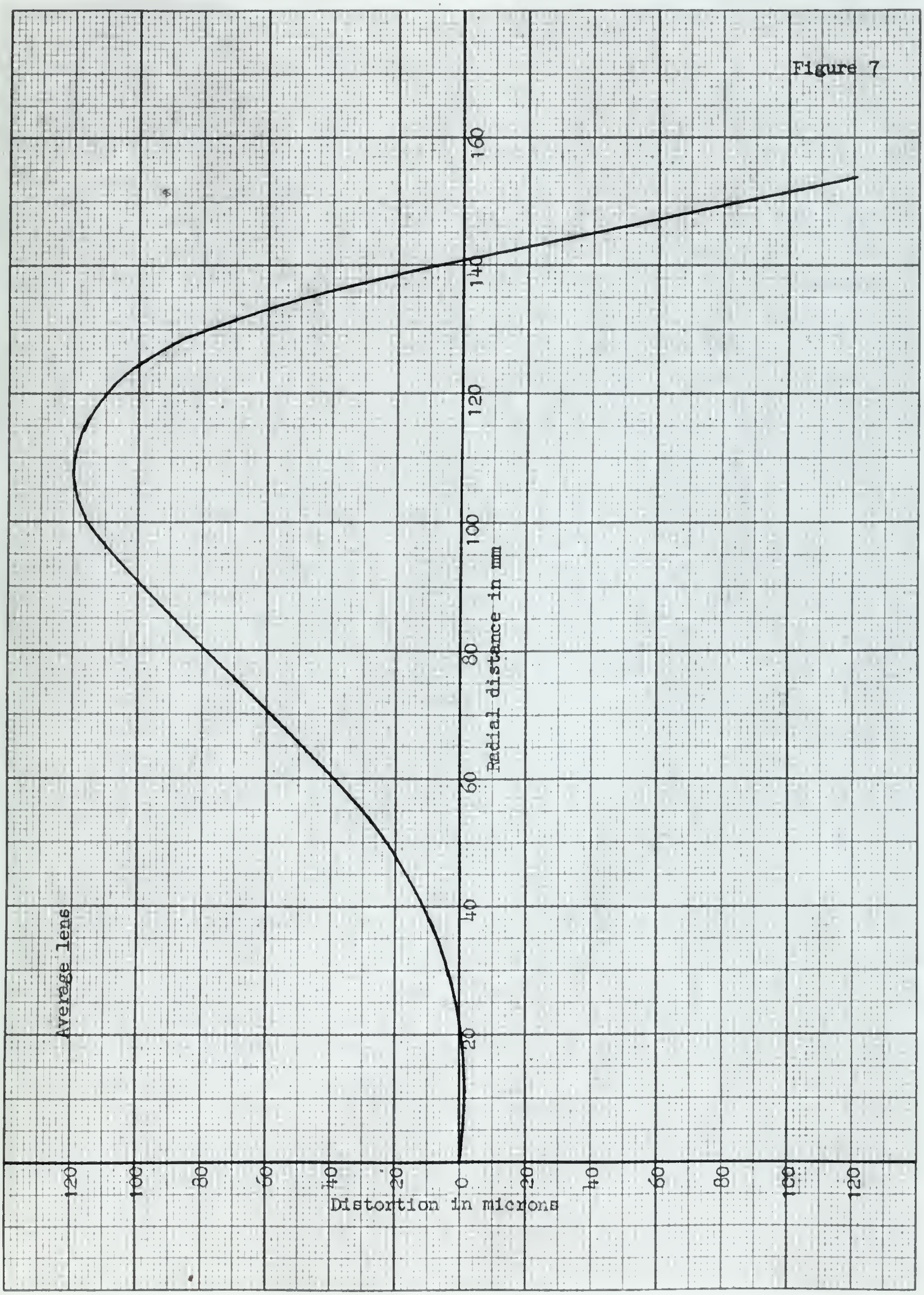

Average lens
Radial distance in mm
Distortion in microns
20 40 60 80 100 120 140 160
120 100 80 60 40 20 0 20 40 60 80 100 120

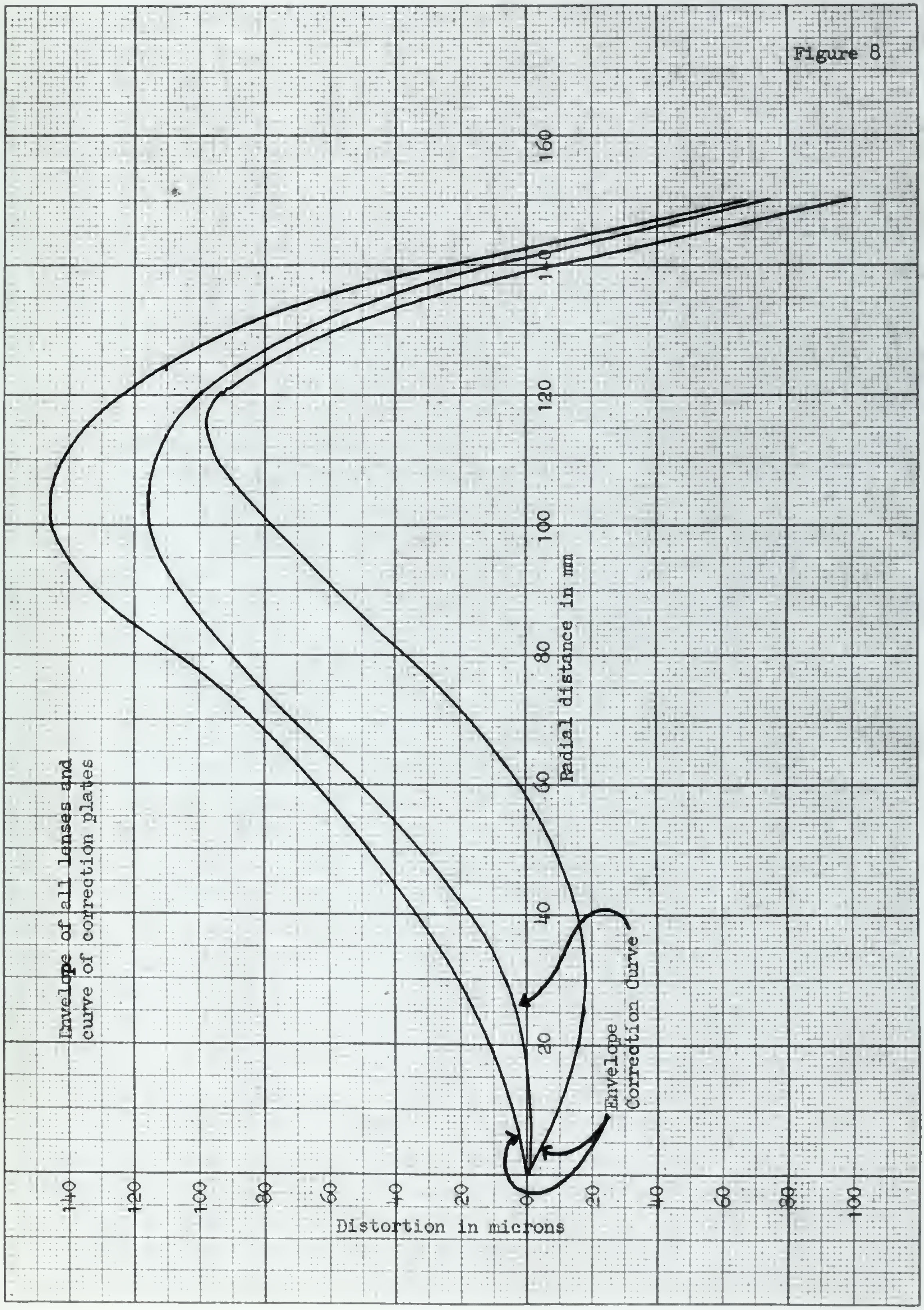
Envelope of all lenses and
curve of correction plates
Envelope
Correction Curve
Radial distance in mm
20
40
60
80
100
120
140
160
Distortion in microns
140
120
100
80
60
40
20
0
20
40
60
80
100

Figure 8

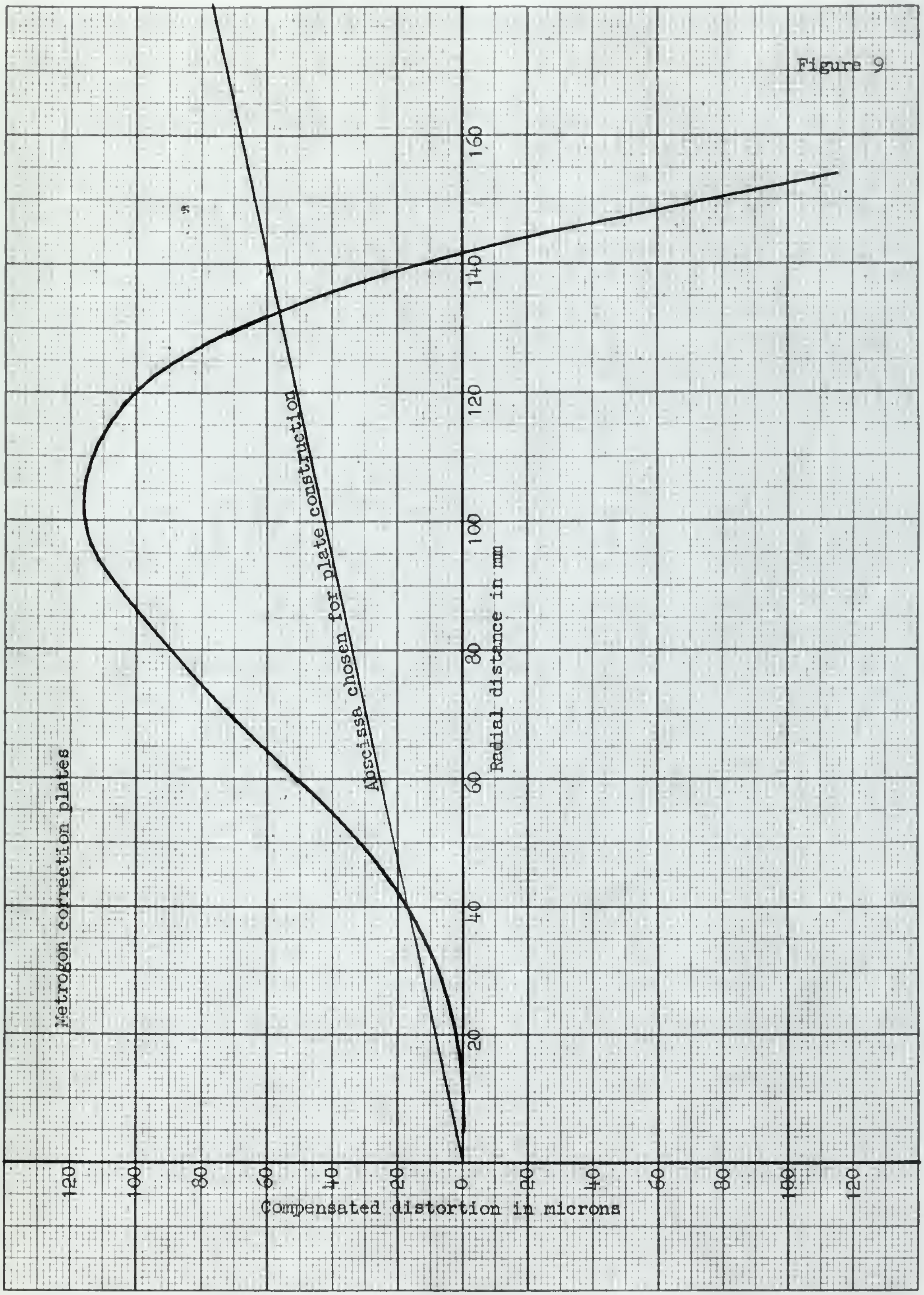
Metrogon correction plates
Abscissa chosen for plate construction
Radial distance in mm
Compensated distortion in microns
20 40 60 80 100 120 140 160
120 100 80 60 40 20 0 20 40 60 80 100 120

Figure 9

VERIFYING THE CURVE OF THE METROGON CORRECTION PLATES

The metrogon correction plates, serials 49 and 50, which were manufactured for The Ohio State University by Wild Instruments were used with grid test plates 377 and 378 to determine the actual displacement caused by the correction plates. These observations were made in the Wild A7 Autograph, using monocular vision and observing each grid plate through each correction plate. The instrument adjustments were all zeroed except focal length, set at 125 mm, and z, set at 300 mm. The measurements are contained in Tables VIII through XI. The numbering system used is consistent for all measurements. The first number refers to rows parallel to the X axis, starting on the Y positive (upper) side of the plate. The second number refers to rows parallel to the Y axis, starting at the X negative (left) side of the plate. The average distance of the projection of each grid intersection from the center is tabulated in Tables XII through XV.

These measurements were then compared with the true positions of the grid intersections. The distortions were then graphically converted to radial and tangential distortion and tabulated in Tables XVI through XIX. Then the distortion figures were reduced to photo scale, averaged for each correction plate and tabulated in Tables XX and XXI. The sign conventions used in Table XVI and subsequently are positive away from center in the case of radial, and

positive clockwise when viewed from above in the case of tangential distortion.

As is obvious from the tangential distortion figures, there is apparently some rotation error in the alignment of the grid plates in the autograph. In order to eliminate any effect of this error, the summation of the tangential distortions divided by the radial distance from center was set equal to zero and corrections applied accordingly. The results of these computations appear in Tables XXII and XXIII. Plots of these values do not indicate any systematic error except that the lower left half (as viewed from the top) is predominately negative and the upper right half is predominately positive. The magnitudes of distortion within these areas are completely random. The positive and negative patterns being similar indicates a systematic error either in the autograph optics or in the manufacture of the correction plates. There is not sufficient information or specialized equipment available to this writer to determine which source caused the error.

The radial distortions contained in Tables XX and XXI are plotted in relation to the curve provided Wild for the manufacture of the correction plates in Figures 10 and 11. As can be seen, the same range of random errors is present in radial distortion as is present in tangential distortion. However, the radial figures indicate a displacement toward the lower right of approximately the same magnitude as is evidenced by the tangential distortion.

If the above displacement were compensated, the tangential distortion figures would show no definite pattern and the radial

distortion would approximate, within ± 10 microns, the curve provided for the construction of the plates. The errors resulting can be disregarded in any computation, without resulting in any appreciable error.

TABLE VIII

GRID 377 PLATE 49, GRID INTERSECTION COORDINATES

Point	X	Y	Point	X	Y
1-1	5627.53	1071.21	2-1	5627.42	1023.10
	53	22		42	11
	52	22		42	10
	53	21		42	10
2	5579.43	1071.09	2	5579.39	1023.03
	44	09		39	03
	44	10		39	03
	43	11		39	03
3	5531.41	1071.02	3	5531.39	1023.00
	40	02		39	01
	40	01		39	00
	41	03		39	01
4	5483.41	1070.99	4	5483.43	1023.00
	41	98		43	00
	41	99		43	01
	42	00		43	22.99
5	5435.46	1070.99	5	5435.49	1023.01
	46	99		50	01
	45	98		49	01
	46	98		49	01
6	5387.50	1070.98	6	5387.52	1023.03
	49	99		52	03
	49	99		52	03
	50	99		52	03
7	5339.54	1070.99	7	5339.55	1023.03
	54	99		55	03
	53	99		55	03
	53	98		55	02
8	5291.57	1071.01	8	5291.60	1023.02
	57	01		60	03
	57	70.99		60	02
	57	99		59	01
9	5243.58	1071.03	9	5243.63	1023.02
	59	04		64	02
	59	03		64	02
	60	03		63	02
10	5195.55	1071.11	10	5195.65	1023.07
	56	12		64	07
	57	11		64	06
	56	11		64	06
11	5147.42	1071.24	11	5147.56	1023.14
	42	23		57	13
	42	25		56	13
	42	25		56	13

TABLE VIII—Continued

Point	X	Y	Point	X	Y
3-1	5627.37	975.09	4-1	5627.34	927.09
	36	09		33	09
	37	10		33	09
	36	09		33	09
2	5579.36	975.05	2	5579.36	927.06
	36	05		35	07
	36	05		35	07
	36	04		35	07
3	5531.40	975.05	3	5531.43	927.08
	40	05		43	09
	40	05		43	09
	40	05		43	09
4	5483.47	975.08	4	5483.49	927.12
	47	08		49	12
	46	08		49	13
	47	08		49	12
5	5435.50	975.10	5	5435.51	927.13
	50	10		52	13
	49	10		52	13
	49	10		52	14
6	5387.53	975.12	6	5387.52	927.15
	53	12		52	15
	53	12		51	15
	52	12		51	15
7	5339.54	975.12	7	5339.52	927.16
	54	12		52	16
	54	12		51	16
	54	12		51	16
8	5291.59	975.09	8	5291.55	927.13
	58	09		54	13
	58	08		54	13
	58	08		54	14
9	5243.63	975.06	9	5243.60	927.10
	63	07		59	11
	63	06		59	11
	63	06		60	10
10	5195.68	975.06	10	5195.67	927.09
	68	06		67	10
	68	06		67	09
	67	05		66	09
11	5147.64	975.09	11	5147.67	927.08
	64	10		67	09
	65	10		67	09
	64	10		66	08

TABLE VIII—Continued

Point	X	Y	Point	X	Y
5-1	5627.34	879.12	6-1	5627.32	831.15
	34	13		32	16
	34	13		32	16
	34	12		31	16
2	5579.40	879.11	2	5579.38	831.15
	39	12		38	16
	39	12		38	16
	39	11		38	15
3	5531.47	879.13	3	5531.47	831.15
	47	13		46	16
	47	13		47	16
	47	13		47	16
4	5483.53	879.15	4	5483.53	831.16
	53	16		53	17
	53	16		54	17
	53	15		54	17
5	5435.55	879.16	5	5435.56	831.16
	56	17		56	17
	56	17		56	16
	55	17		57	16
6	5387.53	879.19	6	5387.53	831.19
	53	20		53	19
	52	20		53	18
	53	20		53	18
7	5339.51	879.19	7	5339.49	831.20
	51	19		49	20
	50	18		49	19
	50	19		49	20
8	5291.54	879.16	8	5291.52	831.17
	53	16		52	17
	53	16		52	18
	53	15		53	17
9	5243.59	879.14	9	5243.58	831.18
	59	14		58	18
	59	15		57	18
	59	14		57	18
10	5195.67	879.13	10	5195.67	831.19
	67	13		66	19
	67	14		66	19
	67	13		66	19
11	5147.70	879.12	11	5147.70	831.18
	70	13		70	17
	70	13		69	17
	70	13		70	18

TABLE VIII—Continued

Point	X	Y	Point	X	Y
7-1	5627.33	783.19	8-1	5627.35	735.22
	33	20		34	23
	32	20		34	24
	33	19		35	23
2	5579.37	783.18	2	5579.36	735.23
	37	18		36	23
	37	18		36	23
	37	18		36	23
3	5531.45	783.17	3	5531.43	735.21
	45	17		43	21
	46	17		44	21
	46	17		43	21
4	5483.51	783.16	4	5483.49	735.19
	50	16		49	19
	51	16		49	19
	51	16		50	19
5	5435.54	783.13	5	5435.52	735.15
	54	13		52	15
	54	13		53	15
	55	14		53	15
6	5387.53	783.13	6	5387.51	735.15
	53	13		51	16
	53	13		51	16
	52	13		52	16
7	5339.50	783.15	7	5339.51	735.18
	49	16		51	18
	50	16		51	18
	49	15		51	19
8	5291.51	783.14	8	5291.54	735.19
	51	15		54	19
	51	14		54	19
	51	15		55	19
9	5243.57	783.17	9	5243.60	735.23
	57	17		60	23
	57	17		59	23
	57	17		60	22
10	5195.65	783.18	10	5195.66	735.24
	64	19		67	25
	65	20		66	25
	65	19		66	25
11	5147.68	783.18	11	5147.66	735.22
	68	18		66	22
	68	19		66	23
	68	17		67	22

TABLE VIII—Continued

Point	X	Y	Point	X	Y
9-1	5627.37	687.25	10-1	5627.43	639.19
	36	25		42	20
	36	25		42	21
	36	25		42	20
2	5579.35	687.27	2	5579.40	639.27
	35	28		39	26
	35	28		40	27
	35	28		39	26
3	5531.40	687.28	3	5531.40	639.29
	41	28		40	30
	41	29		40	30
	40	28		40	29
4	5483.45	687.27	4	5483.43	639.31
	45	27		43	32
	46	28		44	32
	45	28		44	32
5	5435.50	687.24	5	5435.48	639.28
	50	23		48	28
	50	24		48	28
	50	24		48	28
6	5387.51	687.24	6	5387.50	639.29
	51	23		50	29
	51	24		50	29
	51	23		50	29
7	5339.53	687.26	7	5339.53	639.32
	53	26		53	31
	52	27		52	37
	53	26		52	36
8	5291.57	687.25	8	5291.57	639.29
	57	26		57	29
	57	26		57	30
	56	25		57	30
9	5243.62	687.27	9	5243.61	639.29
	61	28		60	29
	61	28		60	29
	61	28		60	29
10	5195.66	687.29	10	5195.63	639.26
	66	28		63	27
	66	28		63	27
	66	28		62	26
11	5147.63	687.23	11	5147.53	639.18
	64	23		53	18
	63	24		53	19
	63	23		53	17

TABLE VIII—Continued

Point	X	Y
11-1	5627.58	591.07
	57	08
	57	08
	56	08
2	5579.45	591.21
	45	22
	45	22
	45	21
3	5531.43	591.29
	41	30
	42	30
	41	31
4	5483.43	591.34
	43	34
	44	35
	43	34
5	5435.46	591.34
	47	34
	46	35
	47	34
6	5387.50	591.35
	49	36
	50	36
	49	35
7	5339.52	591.37
	52	37
	52	37
	52	36
8	5291.54	591.30
	55	31
	55	31
	54	31
9	5243.56	591.27
	55	29
	56	29
	55	29
10	5195.52	591.22
	52	22
	52	23
	52	22
11	5147.38	591.05
	38	06
	37	05
	38	06

TABLE IX

GRID 378 PLATE 49, GRID INTERSECTION COORDINATES

Point	X	Y	Point	X	Y
1-1	5029.59	1060.01	2-1	5029.48	1011.91
	59	02		48	92
	59	01		48	92
	60	01		48	91
2	4981.49	1059.91	2	4981.45	1011.84
	49	91		44	84
	49	90		45	85
	50	91		45	84
3	4933.46	1059.84	3	4933.46	1011.82
	45	84		45	82
	46	85		45	82
	46	84		46	83
4	4885.48	1059.79	4	4885.51	1011.81
	47	81		50	82
	47	80		50	82
	47	81		50	81
5	4837.52	1059.79	5	4837.56	1011.82
	52	79		55	82
	51	79		55	83
	51	80		55	82
6	4789.56	1059.79	6	4789.59	1011.85
	57	80		58	84
	56	80		58	84
	56	79		58	84
7	4741.61	1059.80	7	4741.61	1011.85
	61	81		62	84
	60	81		62	85
	60	80		61	85
8	4693.63	1059.81	8	4693.66	1011.83
	64	83		66	83
	63	82		65	84
	63	82		65	83
9	4645.65	1059.84	9	4645.70	1011.84
	65	85		70	84
	66	86		70	85
	65	86		69	85
10	4597.61	1059.94	10	4597.71	1011.88
	61	95		70	89
	61	95		70	89
	61	94		70	88
11	4549.48	1060.07	11	4549.62	1011.95
	49	06		61	95
	48	06		62	95
	48	06		61	95

TABLE IX—Continued

Point	X	Y	Point	X	Y
3-1	5029.43	963.90	4-1	5029.40	915.89
	43	91		39	90
	42	91		39	90
	42	90		40	89
2	4981.42	963.86	2	4981.41	915.87
	42	87		40	88
	41	86		40	89
	42	86		41	88
3	4933.46	963.86	3	4933.48	915.90
	46	85		48	91
	46	85		47	90
	46	86		47	91
4	4885.52	963.89	4	4885.54	915.93
	52	90		55	93
	51	90		54	94
	52	90		54	94
5	4837.56	963.91	5	4837.58	915.95
	56	91		59	94
	55	92		57	94
	55	92		57	95
6	4789.59	963.92	6	4789.58	915.97
	59	93		58	97
	58	92		58	97
	58	92		58	97
7	4741.61	963.93	7	4741.57	915.97
	60	93		58	98
	60	93		57	97
	60	93		57	98
8	4693.64	963.90	8	4693.61	915.94
	63	91		60	95
	63	91		60	95
	63	90		60	94
9	4645.69	963.88	9	4645.66	915.93
	70	89		66	93
	69	88		66	93
	69	89		66	92
10	4597.74	963.89	10	4597.73	915.91
	74	90		73	92
	74	90		73	91
	74	89		72	91
11	4549.70	963.94	11	4549.73	915.92
	71	95		73	92
	70	95		73	93
	71	94		73	92

TABLE IX—Continued

Point	X	Y	Point	X	Y
5-1	5029.39	867.93	6-1	5029.37	819.97
	39	94		36	97
	38	94		36	98
	38	94		37	98
2	4981.44	867.93	2	4981.43	819.96
	44	93		43	97
	44	93		43	97
	44	93		42	97
3	4933.51	867.94	3	4933.52	819.97
	52	94		51	98
	51	94		51	98
	52	94		51	98
4	4885.59	867.96	4	4885.58	819.98
	58	96		58	97
	58	97		58	98
	58	97		58	98
5	4837.61	867.98	5	4837.62	819.97
	61	98		61	97
	61	98		62	98
	60	98		62	97
6	4789.60	868.01	6	4789.58	820.00
	59	01		58	00
	58	01		58	00
	59	01		58	00
7	4741.57	868.01	7	4741.55	820.01
	57	01		54	01
	57	02		54	01
	57	01		55	01
8	4693.59	867.97	8	4693.57	819.98
	58	97		57	99
	58	98		56	98
	58	97		56	98
9	4645.65	867.96	9	4645.64	820.01
	65	96		64	01
	64	97		63	00
	64	96		63	00
10	4597.73	867.96	10	4597.72	820.00
	72	96		71	02
	73	96		71	01
	72	95		71	01
11	4549.76	867.96	11	4549.75	820.00
	75	96		75	00
	75	96		74	00
	75	95		75	00

TABLE IX—Continued

Point	X	Y	Point	X	Y
7-1	5029.37	772.00	8-1	5029.39	724.04
	37	01		39	04
	37	01		39	05
	36	00		39	05
2	4981.41	771.99	2	4981.40	724.04
	41	99		41	05
	41	72.00		40	05
	41	99		41	05
3	4933.50	771.98	3	4933.48	724.03
	50	98		48	03
	50	98		48	03
	50	97		48	03
4	4885.56	771.97	4	4885.54	724.00
	56	97		54	01
	56	97		54	01
	56	98		54	01
5	4837.59	771.95	5	4837.57	723.97
	59	95		56	97
	59	95		57	97
	59	94		56	97
6	4789.58	771.96	6	4789.56	723.97
	57	95		56	98
	56	95		56	97
	57	96		56	97
7	4741.55	771.96	7	4741.56	724.00
	55	96		57	00
	54	97		57	00
	54	96		57	00
8	4693.56	771.95	8	4693.59	724.01
	55	96		59	01
	56	96		59	01
	56	96		60	01
9	4645.62	771.98	9	4645.65	724.06
	61	99		64	05
	61	99		64	05
	61	99		65	05
10	4597.69	772.01	10	4597.71	724.08
	69	02		71	08
	70	01		71	08
	69	01		71	07
11	4549.73	772.00	11	4549.71	724.06
	73	01		72	07
	72	01		71	05
	73	00		72	05

TABLE IX—Continued

Point	X	Y	Point	X	Y
9-1	5029.40	676.08	10-1	5029.48	628.02
	41	08		48	01
	40	08		47	03
	40	08		47	03
2	4981.41	676.10	2	4981.44	628.08
	40	10		44	08
	40	10		43	09
	40	10		43	09
3	4933.45	676.09	3	4933.45	628.11
	46	08		45	11
	46	09		45	11
	45	09		44	11
4	4885.50	676.09	4	4885.48	628.13
	50	09		48	13
	50	09		48	13
	50	09		48	12
5	4837.54	676.05	5	4837.53	628.10
	55	05		53	10
	54	05		53	10
	54	06		53	10
6	4789.56	676.05	6	4789.55	628.10
	56	06		56	10
	55	06		56	10
	56	06		55	10
7	4741.58	676.07	7	4741.58	628.12
	58	07		58	13
	57	08		58	13
	57	07		58	13
8	4693.61	676.07	8	4693.62	628.11
	61	07		61	11
	61	07		61	11
	61	07		62	11
9	4645.67	676.09	9	4645.66	628.11
	67	09		65	11
	67	09		65	11
	67	09		65	12
10	4597.71	676.10	10	4597.66	628.11
	70	12		67	10
	70	11		67	10
	70	11		66	10
11	4549.69	676.06	11	4549.58	628.01
	68	07		57	00
	68	07		57	01
	69	07		57	01

TABLE IX—Continued

Point	X	Y
11-1	5029.62	579.89
	63	90
	62	90
	61	89
2	4981.49	580.04
	50	04
	50	04
	49	03
3	4933.47	580.10
	47	10
	47	11
	47	10
4	4885.48	580.16
	48	15
	48	16
	48	16
5	4837.52	580.16
	51	16
	51	16
	50	16
6	4789.55	580.17
	55	17
	54	17
	54	18
7	4741.57	580.18
	57	18
	57	18
	56	18
8	4693.59	580.12
	59	13
	59	13
	59	13
9	4645.60	580.09
	61	10
	61	10
	60	09
10	4597.56	580.02
	56	02
	56	03
	56	03
11	4549.42	579.86
	43	85
	42	86
	43	85

TABLE X

GRID 377 PLATE 50, GRID INTERSECTION COORDINATES

Point	X	Y	Point	X	Y
1-1	231.93	240.06	2-1	231.85	191.95
	93	04		86	94
	94	04		84	94
	94	05		85	96
2	183.86	239.95	2	183.81	191.88
	86	94		81	89
	86	94		80	88
	86	95		81	88
3	135.84	239.86	3	135.82	191.86
	83	87		81	86
	84	87		82	86
	84	88		82	86
4	87.85	239.84	4	87.85	191.87
	84	83		86	87
	84	84		86	87
	84	84		86	87
5	39.89	239.82	5	39.90	191.87
	88	81		90	88
	90	82		89	87
	90	83		90	87
6	9991.94	239.83	6	9991.95	191.89
	93	83		95	89
	93	83		95	89
	94	83		95	89
7	9943.97	239.83	7	9943.98	191.88
	96	83		98	88
	97	83		98	88
	97	84		98	88
8	9896.01	239.85	8	9896.02	191.87
	01	85		02	86
	00	84		02	86
	01	85		02	86
9	9848.02	239.87	9	9848.06	191.86
	02	89		07	87
	01	88		06	86
	02	88		06	86
10	9799.99	239.95	10	9800.07	191.89
	99	95		06	89
	98	94		06	89
	98	95		06	90
11	9751.85	240.09	11	9751.98	191.95
	85	10		98	95
	84	09		98	95
	85	08		98	95

TABLE X—Continued

Point	X	Y	Point	X	Y
3-1	231.79	143.93	4-1	231.75	95.94
	80	93		76	93
	79	93		76	93
	79	93		76	92
2	183.79	143.88	2	183.78	95.92
	79	88		78	92
	79	88		79	92
	79	88		79	92
3	135.83	143.89	3	135.85	95.95
	83	90		85	95
	83	89		85	95
	83	90		85	95
4	87.90	143.93	4	87.92	95.98
	90	93		92	98
	90	92		92	99
	90	93		92	98
5	39.93	143.94	5	39.95	96.00
	94	94		95	00
	93	94		94	00
	93	95		95	00
6	9991.95	143.96	6	9991.95	96.02
	96	96		95	02
	95	96		95	01
	95	96		95	01
7	9943.98	143.97	7	9943.96	96.01
	97	96		95	01
	98	96		94	01
	97	96		95	01
8	9896.01	143.94	8	9895.99	95.97
	01	93		98	97
	01	93		98	97
	01	94		98	96
9	9848.07	143.91	9	9848.04	95.96
	06	91		03	95
	06	91		03	96
	06	91		03	95
10	9800.11	143.90	10	9800.10	95.93
	11	90		09	93
	11	90		09	93
	10	90		10	92
11	9752.07	143.96	11	9752.11	95.93
	07	95		10	93
	07	95		11	93
	07	95		11	92

TABLE X—Continued

Point	X	Y	Point	X	Y
5-1	231.76	47.98	6-1	231.74	0.02
	76	97		74	02
	76	97		75	02
	76	98		75	02
2	183.81	47.97	2	183.81	0.01
	81	97		81	01
	81	96		81	01
	81	96		81	02
3	135.89	47.98	3	135.90	0.02
	89	98		90	02
	90	98		90	01
	89	98		90	01
4	87.97	48.02	4	87.97	0.03
	97	01		97	04
	97	01		97	03
	96	01		97	03
5	39.98	48.02	5	40.01	0.01
	98	02		01	01
	99	02		01	01
	98	02		00	01
6	9991.97	48.05	6	9991.97	0.02
	97	06		97	02
	96	05		97	03
	96	04		97	03
7	9943.93	48.05	7	9943.93	0.03
	93	04		93	03
	93	06		93	03
	93	05		92	03
8	9895.97	48.01	8	9895.95	0.02
	96	00		94	01
	97	01		95	02
	97	00		95	01
9	9848.03	47.98	9	9848.01	0.01
	02	99		01	01
	02	99		02	01
	01	98		01	01
10	9800.10	47.97	10	9800.07	0.01
	09	98		08	02
	10	98		08	01
	09	97		08	02
11	9752.13	47.96	11	9752.13	0.00
	12	97		12	00
	13	96		11	01
	13	96		12	01

TABLE X—Continued

Point	X	Y	Point	X	Y
7-1	231.75	9952.03	8-1	231.78	9904.07
	76	04		78	08
	76	04		78	08
	76	04		78	08
2	183.79	9952.02	2	183.79	9904.09
	79	02		80	09
	79	02		80	09
	79	03		80	08
3	135.88	9952.01	3	135.88	9904.08
	87	02		87	07
	89	01		88	07
	88	01		88	07
4	87.94	9952.00	4	87.93	9904.06
	94	00		93	06
	95	00		93	05
	95	01		94	05
5	39.97	9951.99	5	39.97	9904.01
	96	98		96	01
	96	98		97	00
	97	98		97	01
6	9991.95	9951.99	6	9991.97	9904.01
	94	99		96	01
	94	99		97	00
	94	98		97	00
7	9943.90	9952.00	7	9943.95	9904.03
	91	00		96	04
	91	00		96	03
	91	00		95	03
8	9895.94	9952.00	8	9895.98	9904.02
	94	00		98	02
	93	00		99	03
	93	9951.99		98	02
9	9847.99	9952.02	9	9848.03	9904.06
	99	02		02	06
	9848.00	02		03	06
	00	02		02	06
10	9800.07	9952.03	10	9800.09	9904.07
	07	03		09	07
	07	03		09	08
	07	02		08	07
11	9752.10	9952.02	11	9752.10	9904.04
	09	02		08	05
	10	01		09	05
	09	01		08	06

TABLE X—Continued

Point	X	Y	Point	X	Y
9-1	231.80	9856.09	10-1	231.86	9808.04
	80	09		87	05
	80	10		86	05
	80	09		86	04
2	183.79	9856.12	2	183.82	9808.11
	79	12		83	11
	80	12		83	11
	79	12		82	11
3	135.82	9856.13	3	135.83	9808.14
	83	12		83	13
	83	12		83	13
	83	13		83	12
4	87.88	9856.12	4	87.85	9808.16
	88	12		86	16
	89	12		86	16
	88	11		86	16
5	39.93	9856.08	5	39.90	9808.13
	92	07		90	12
	92	08		90	13
	93	07		90	12
6	9991.94	9856.08	6	9991.94	9808.13
	95	08		93	12
	94	08		93	13
	94	08		93	12
7	9943.95	9856.11	7	9943.96	9808.14
	94	11		96	14
	94	11		96	14
	94	11		96	14
8	9895.99	9856.09	8	9896.00	9808.12
	99	09		00	12
	99	10		9895.99	13
	98	10		99	12
9	9848.03	9856.13	9	9848.02	9808.11
	03	11		02	11
	03	12		02	12
	03	11		01	12
10	9800.08	9856.12	10	9800.01	9808.08
	08	12		02	09
	07	12		01	09
	07	12		02	08
11	9752.05	9856.07	11	9751.94	9808.00
	05	08		95	00
	06	07		96	00
	04	06		94	00

TABLE X—Continued

Point	X	Y
11-1	232.02	9759.93
	01	93
	01	94
	01	94
2	183.89	9760.07
	90	07
	90	07
	90	06
3	135.86	9760.11
	86	12
	86	12
	86	12
4	87.88	9760.19
	87	19
	88	20
	88	19
5	39.92	9760.17
	91	18
	92	19
	91	19
6	9991.94	9760.19
	94	19
	94	19
	94	19
7	9943.96	9760.19
	96	20
	96	20
	95	20
8	9895.99	9760.16
	98	15
	98	15
	98	15
9	9847.99	9760.11
	9848.00	12
	00	12
	00	11
10	9799.96	9760.06
	97	06
	97	05
	97	06
11	9751.81	9759.88
	82	87
	82	87
	81	87

TABLE XI

GRID 378 PLATE 50, GRID INTERSECTION COORDINATES

Point	X	Y	Point	X	Y
1-1	5673.43	1016.29	2-1	5673.33	968.21
	43	29		34	21
	43	29		33	21
	43	29		33	21
2	5625.35	1016.21	2	5625.28	968.15
	35	20		28	14
	34	20		28	14
	35	20		28	14
3	5577.32	1016.12	3	5577.30	968.14
	33	13		31	13
	32	13		31	13
	32	14		30	13
4	5529.34	1016.10	4	5529.35	968.15
	35	10		35	15
	34	10		34	15
	34	10		34	16
5	5481.39	1016.10	5	5481.39	968.16
	40	09		40	16
	38	09		39	16
	39	10		39	15
6	5433.43	1016.12	6	5433.44	968.18
	44	11		44	17
	43	11		45	18
	43	12		44	18
7	5385.47	1016.12	7	5385.47	968.17
	47	11		48	17
	46	12		48	17
	47	11		47	17
8	5337.52	1016.12	8	5337.51	968.16
	51	13		52	16
	51	13		51	15
	51	12		51	15
9	5289.53	1016.17	9	5289.56	968.16
	53	16		56	16
	53	16		56	15
	52	17		55	15
10	5241.50	1016.23	10	5241.56	968.19
	49	23		55	19
	49	23		55	18
	49	24		55	18
11	5193.36	1016.36	11	5193.48	968.25
	36	36		48	24
	36	37		48	24
	36	37		47	25

TABLE XI--Continued

Point	X	Y	Point	X	Y
3-1	5673.26	920.19	4-1	5673.23	872.20
	26	19		23	20
	25	19		23	20
	25	19		22	20
2	5625.26	920.17	2	5625.25	872.21
	26	17		26	21
	25	16		25	20
	26	17		26	21
3	5577.30	920.18	3	5577.33	872.24
	31	18		33	23
	31	18		33	23
	31	18		33	23
4	5529.38	920.23	4	5529.39	872.29
	38	23		39	28
	37	22		40	28
	37	23		39	28
5	5481.42	920.24	5	5481.42	872.30
	41	24		43	30
	42	25		43	31
	41	24		42	31
6	5433.43	920.26	6	5433.43	872.33
	43	26		43	32
	43	26		44	33
	42	26		43	33
7	5385.46	920.26	7	5385.44	872.32
	46	27		43	32
	45	27		43	33
	46	27		43	33
8	5337.49	920.24	8	5337.45	972.28
	50	24		46	29
	50	24		46	28
	49	23		45	28
9	5289.55	920.21	9	5289.51	872.26
	55	21		51	26
	55	21		50	27
	55	21		51	26
10	5241.60	920.20	10	5241.58	872.24
	60	19		58	24
	59	20		58	24
	59	20		57	24
11	5193.56	920.24	11	5193.60	872.22
	57	23		59	23
	56	23		59	23
	57	23		59	23

TABLE XI—Continued

Point	X	Y	Point	X	Y
5-1	5673.23	824.24	6-1	5673.21	776.29
	23	24		22	28
	22	23		21	28
	22	24		22	28
2	5625.28	824.25	2	5625.28	776.29
	29	25		27	28
	28	25		28	29
	28	25		28	30
3	5577.37	824.27	3	5577.37	776.31
	37	27		38	30
	38	26		38	29
	37	27		37	31
4	5529.44	824.31	4	5529.44	776.32
	44	31		44	32
	45	31		44	32
	44	31		43	33
5	5481.46	824.33	5	5481.48	776.31
	46	32		47	31
	46	32		47	31
	46	33		47	31
6	5433.44	824.35	6	5433.46	776.32
	43	35		45	32
	44	35		45	32
	44	35		45	32
7	5385.42	824.36	7	5385.41	776.33
	42	36		40	34
	41	35		40	34
	41	36		40	33
8	5337.44	824.32	8	5337.41	776.32
	43	32		42	33
	43	32		42	32
	43	32		41	33
9	5289.50	824.30	9	5289.48	776.32
	50	30		48	33
	49	30		48	33
	49	30		48	33
10	5241.57	824.28	10	5241.56	776.33
	57	29		55	33
	57	28		56	32
	56	29		55	33
11	5193.59	824.26	11	5193.58	776.31
	59	25		59	31
	60	25		59	31
	59	26		59	31

TABLE XI—Continued

Point	X	Y	Point	X	Y
7-1	5673.20	728.31	8-1	5673.23	680.35
	21	30		23	36
	21	31		22	35
	21	31		23	36
2	5625.24	728.31	2	5625.25	680.36
	25	30		25	36
	25	31		25	35
	25	31		25	37
3	5577.34	728.31	3	5577.32	680.36
	34	31		32	36
	34	31		32	35
	34	30		32	37
4	5529.40	728.30	4	5529.38	680.35
	40	30		39	35
	40	30		39	34
	40	30		39	35
5	5481.43	728.29	5	5481.42	680.32
	44	27		42	31
	45	28		42	31
	44	28		42	32
6	5433.41	728.29	6	5433.42	680.30
	41	28		42	30
	40	29		43	31
	41	28		42	31
7	5385.37	728.30	7	5385.42	680.34
	37	30		42	33
	37	30		42	34
	38	30		41	34
8	5337.40	728.31	8	5337.45	680.33
	40	31		44	32
	40	31		45	32
	39	31		44	33
9	5289.47	728.34	9	5289.50	680.36
	47	33		50	36
	47	33		49	36
	48	34		49	36
10	5241.53	728.35	10	5241.56	680.38
	54	34		56	38
	54	34		55	38
	54	35		55	38
11	5193.56	728.31	11	5193.56	680.36
	57	31		55	34
	57	32		56	35
	57	32		55	34

TABLE XI—Continued

Point	X	Y	Point	X	Y
9-1	5673.25	632.36	10-1	5673.33	584.31
	26	35		33	30
	25	36		33	31
	26	36		33	31
2	5625.23	632.39	2	5625.28	584.37
	24	39		29	37
	23	39		28	37
	24	39		29	37
3	5577.28	632.40	3	5577.28	584.40
	28	41		29	40
	28	40		28	40
	29	41		28	41
4	5529.34	632.40	4	5529.32	584.43
	34	40		32	42
	34	40		32	43
	34	41		32	44
5	5481.39	632.37	5	5481.35	584.41
	38	36		36	41
	39	37		36	41
	38	37		36	42
6	5433.41	632.38	6	5433.38	584.41
	40	38		39	42
	40	38		39	42
	39	39		38	43
7	5385.42	632.40	7	5385.42	584.43
	42	39		42	43
	42	40		41	43
	41	40		42	44
8	5337.44	632.39	8	5337.46	584.41
	45	38		45	41
	45	38		45	41
	44	39		45	41
9	5289.50	632.41	9	5289.48	584.41
	50	41		48	40
	50	41		48	40
	50	41		48	41
10	5241.54	632.41	10	5241.47	584.37
	54	41		48	37
	54	41		48	37
	54	41		48	37
11	5193.51	632.34	11	5193.41	584.28
	51	34		41	28
	51	34		41	28
	51	34		42	27

TABLE XI—Continued

Point	X	Y
11-1	5673.46	536.19
	46	19
	45	20
	46	19
2	5625.36	536.32
	36	31
	35	32
	35	32
3	5577.34	536.39
	34	39
	34	39
	34	39
4	5529.34	536.43
	34	44
	35	44
	35	44
5	5481.37	536.45
	37	44
	37	45
	37	45
6	5433.40	536.47
	41	46
	40	47
	40	47
7	5385.43	536.48
	42	48
	42	48
	42	48
8	5337.45	536.43
	43	42
	45	43
	44	42
9	5289.46	536.39
	47	39
	46	39
	47	40
10	5241.43	536.32
	43	33
	43	33
	44	32
11	5193.27	536.17
	28	16
	28	16
	28	16

TABLE XII

GRID 377 PLATE 49, AVERAGE DISTANCES FROM CENTER IN MM AT MODEL SCALE

Point	X	Y	Point	X	Y
1-1	-239.998	240.030	5-1	-239.810	47.940
2	-191.905	239.912	2	-191.862	47.930
3	-143.875	239.835	3	-143.940	47.945
4	- 95.882	239.805	4	- 96.000	47.970
5	- 47.928	239.800	5	- 48.015	47.982
6	0.035	239.802	6	0.002	48.012
7	47.995	239.802	7	48.025	48.002
8	95.960	239.815	8	95.998	47.972
9	143.940	239.848	9	143.940	47.958
10	191.970	239.928	10	191.860	47.948
11	240.110	240.058	11	239.830	47.942
2-1	-239.890	191.918	6-1	-239.788	- 0.028
2	-191.860	191.845	2	-191.850	- 0.030
3	-143.860	191.820	3	-143.938	- 0.028
4	- 95.900	191.815	4	- 96.005	- 0.018
5	- 47.962	191.825	5	- 48.032	- 0.012
6	0.010	191.845	6	0	0
7	47.980	191.842	7	48.040	0.012
8	95.932	191.835	8	96.008	- 0.002
9	143.895	191.835	9	143.955	- 0.005
10	191.888	191.880	10	191.868	0.005
11	239.968	191.948	11	239.832	- 0.010
3-1	-239.835	143.9075	7-1	-239.798	- 47.990
2	-191.830	143.862	2	-191.840	- 48.005
3	-143.870	143.865	3	-143.925	- 48.015
4	- 95.938	143.895	4	- 95.978	- 48.025
5	- 47.965	143.915	5	- 48.012	- 48.052
6	0.002	143.935	6	0.008	- 48.055
7	47.990	143.935	7	48.035	- 48.030
8	95.948	143.900	8	96.020	- 48.040
9	143.900	143.878	9	143.960	- 48.015
10	191.852	143.872	10	191.882	- 47.995
11	239.888	143.912	11	239.850	- 48.005
4-1	-239.802	95.905	8-1	-239.815	- 95.955
2	-191.822	95.882	2	-191.830	- 95.955
3	-143.900	95.902	3	-143.902	- 95.975
4	- 95.960	95.940	4	- 95.962	- 95.995
5	- 47.988	95.948	5	- 47.995	- 96.035
6	0.015	95.965	6	0.018	- 96.028
7	48.015	95.975	7	48.020	- 96.002
8	95.988	95.948	8	95.988	- 95.995
9	143.935	95.920	9	143.932	- 95.958
10	191.862	95.908	10	191.868	- 95.938
11	239.862	95.900	11	239.868	- 95.962

TABLE XII—Continued

Point	X	Y	Point	X	Y
9-1	-239.832	-143.935	11-1	-240.040	-240.108
2	-191.820	-143.908	2	-191.920	-239.970
3	-143.875	-143.902	3	-143.888	-239.885
4	- 95.922	-143.910	4	- 95.902	-239.842
5	- 47.970	-143.948	5	- 47.935	-239.842
6	0.020	-143.950	6	0.035	-239.830
7	48.002	-143.922	7	48.010	-239.818
8	95.962	-143.930	8	95.985	-239.878
9	143.918	-143.908	9	143.975	-239.900
10	191.870	-143.902	10	192.010	-239.962
11	239.898	-143.952	11	240.152	-240.130
10-1	-239.892	-191.985			
2	-191.865	-191.920			
3	-143.870	-191.890			
4	- 96.905	-191.872			
5	- 47.950	-191.905			
6	0.030	-191.895			
7	48.005	-191.870			
8	95.960	-191.890			
9	143.928	-191.895			
10	191.902	-191.920			
11	240.000	-192.005			

TABLE XIII

GRID 378 PLATE 49, AVERAGE DISTANCES FROM CENTER IN MM AT MODEL SCALE

Point	X	Y	Point	X	Y
1-1	-240.012	240.012	5-1	-239.805	47.938
2	-191.912	239.908	2	-191.860	47.930
3	-143.878	239.842	3	-143.935	47.940
4	- 95.892	239.802	4	- 96.002	47.965
5	- 47.935	239.792	5	- 48.028	47.980
6	0.018	239.795	6	- 0.010	48.010
7	47.975	239.805	7	48.010	48.012
8	95.948	239.820	8	95.998	47.972
9	143.928	239.852	9	143.835	47.962
10	191.970	239.945	10	191.855	47.958
11	240.098	240.062	11	239.828	47.958
2-1	-239.900	191.915	6-1	-239.782	- 0.025
2	-191.868	191.842	2	-191.848	- 0.032
3	-143.875	191.822	3	-143.932	- 0.022
4	- 95.922	191.815	4	- 96.000	- 0.022
5	- 47.972	191.822	5	- 48.038	- 0.028
6	- 0.002	191.842	6	0	0
7	47.965	191.848	7	48.035	0.010
8	95.925	191.832	8	96.035	- 0.018
9	143.882	191.845	9	143.945	0.005
10	191.878	191.885	10	191.868	0.010
11	239.965	191.950	11	239.832	0
3-1	-239.845	143.908	7-1	-239.782	- 47.995
2	-191.838	143.862	2	-191.830	- 48.008
3	-143.880	143.855	3	-143.920	- 48.022
4	- 95.938	143.898	4	- 95.980	- 48.028
5	- 47.975	143.915	5	- 48.010	- 48.052
6	- 0.005	143.922	6	0.010	- 48.045
7	47.978	143.930	7	48.035	- 48.038
8	95.948	143.905	8	96.022	- 48.042
9	143.888	143.885	9	143.968	- 48.012
10	191.840	143.895	10	191.892	- 47.988
11	239.875	143.945	11	239.852	- 47.995
4-1	-239.815	95.895	8-1	-239.810	- 95.955
2	-191.825	95.880	2	-191.825	- 95.952
3	-143.895	95.905	3	-143.900	- 95.970
4	- 95.962	95.935	4	- 95.960	- 95.992
5	- 47.998	95.945	5	- 47.985	- 96.030
6	0	95.970	6	0.020	- 96.038
7	48.008	95.975	7	48.012	- 96.000
8	95.978	95.945	8	95.988	- 95.990
9	143.920	95.928	9	143.935	- 95.948
10	191.852	95.912	10	191.870	- 95.922
11	239.850	95.922	11	239.862	- 95.942

TABLE XIII—Continued

Point	X	Y	Point	X	Y
9-1	-239.822	-143.920	11-1	-240.040	-240.105
2	-191.822	-143.900	2	-191.915	-239.962
3	-143.875	-143.912	3	-143.890	-239.898
4	- 95.920	-143.910	4	- 95.900	-239.842
5	- 47.962	-143.948	5	- 47.930	-239.840
6	- 0.008	-143.942	6	0.035	-239.828
7	48.005	-143.928	7	48.012	-239.820
8	95.970	-143.930	8	95.990	-239.872
9	143.910	-143.910	9	143.975	-239.905
10	191.878	-143.890	10	192.020	-239.975
11	239.895	-143.938	11	240.155	-240.145
10-1	-239.895	-191.978			
2	-191.855	-191.915			
3	-143.868	-191.890			
4	- 95.900	-191.872			
5	- 47.950	-191.900			
6	0.025	-191.900			
7	48.000	-191.872			
8	95.965	-191.890			
9	143.928	-191.888			
10	191.915	-191.898			
11	240.008	-191.992			

TABLE XIV

GRID 377 PLATE 50, AVERAGE DISTANCES FROM CENTER IN MM AT MODEL SCALE

Point	X	Y	Point	X	Y
1-1	-239.965	240.022	5-1	-239.990	47.950
2	-191.890	239.920	2	-191.840	47.940
3	-143.868	239.848	3	-143.922	47.955
4	- 95.878	239.812	4	- 95.998	47.968
5	- 47.922	239.798	5	- 48.012	48.045
6	0.035	239.805	6	0.005	48.025
7	48.002	239.858	7	48.040	48.025
8	95.962	239.822	8	96.002	47.980
9	143.952	239.905	9	143.950	47.960
10	191.985	239.972	10	191.885	47.950
11	240.122	240.065	11	239.852	47.938
2-1	-239.880	191.922	6-1	-239.775	- 0.005
2	-191.838	191.858	2	-191.840	- 0.012
3	-143.848	191.835	3	-143.930	- 0.010
4	- 95.888	191.895	4	- 96.000	0.008
5	- 47.928	191.848	5	- 48.038	- 0.015
6	0.020	191.868	6	0	0
7	47.990	191.855	7	48.042	0.005
8	95.950	191.838	8	96.022	- 0.010
9	143.908	191.838	9	143.958	- 0.015
10	191.908	191.868	10	191.892	- 0.010
11	239.990	191.925	11	239.850	- 0.020
3-1	-239.822	143.905	7-1	-239.788	- 47.988
2	-191.820	143.855	2	-191.820	- 47.952
3	-143.860	143.870	3	-143.910	- 48.012
4	- 95.930	143.906	4	- 95.975	- 48.022
5	- 47.962	143.918	5	- 47.995	- 48.042
6	0.018	143.935	6	0.028	- 48.038
7	47.995	143.988	7	48.072	- 48.025
8	95.960	143.910	8	96.035	- 48.032
9	143.908	143.885	9	143.975	- 48.005
10	191.862	143.875	10	191.900	- 47.998
11	239.900	143.978	11	239.875	- 48.010
4-1	-239.788	95.905	8-1	-239.810	- 95.948
2	-191.815	95.895	2	-191.828	- 95.938
3	-143.880	95.925	3	-143.908	- 95.948
4	- 95.950	95.958	4	- 95.962	- 95.970
5	- 47.978	95.975	5	- 47.998	- 96.018
6	0.020	95.990	6	0.002	- 96.020
7	48.020	95.985	7	48.015	- 95.992
8	95.988	95.942	8	95.988	- 96.002
9	143.938	95.930	9	143.945	- 95.965
10	191.875	95.902	10	191.882	- 95.952
11	239.862	95.902	11	239.882	- 95.975

TABLE XIV—Continued

Point	X	Y	Point	X	Y
9-1	-239.830	-143.932	11-1	-240.042	-240.090
2	-191.822	-143.905	2	-191.928	-239.958
3	-143.858	-143.900	3	-143.890	-239.908
4	- 95.912	-143.908	4	- 95.908	-239.832
5	- 47.955	-143.950	5	- 47.945	-239.842
6	0.028	-143.945	6	0.030	-239.835
7	48.028	-143.915	7	48.012	-239.828
8	95.982	-143.930	8	95.988	-239.872
9	143.940	-143.908	9	143.972	-239.910
10	191.895	-143.905	10	192.002	-239.928
11	239.920	-143.955	11	240.155	-240.152
10-1	-238.892	-191.980			
2	-191.855	-191.915			
3	-143.860	-191.895			
4	- 95.888	-191.865			
5	- 47.930	-191.900			
6	0.038	-191.900			
7	48.010	-191.885			
8	95.975	-191.902			
9	143.952	-191.910			
10	191.955	-191.940			
11	240.022	-192.025			

TABLE XV

GRID 378 PLATE 50, AVERAGE DISTANCES FROM CENTER IN MM AT MODEL SCALE

Point	X	Y	Point	X	Y
1-1	-239.978	239.970	5-1	-239.772	47.918
2	-191.895	239.882	2	-191.830	47.930
3	-143.870	239.810	3	-143.920	47.948
4	- 95.890	239.780	4	- 95.990	47.990
5	- 47.938	239.775	5	- 48.008	48.005
6	0.020	239.795	6	0.020	48.030
7	47.938	239.795	7	48.038	48.032
8	95.940	239.805	8	96.020	48.000
9	143.925	239.845	9	143.958	47.980
10	191.960	239.912	10	191.885	47.965
11	240.092	240.045	11	239.860	47.935
2-1	-239.880	191.890	6-1	-239.762	- 0.038
2	-191.828	191.822	2	-191.825	- 0.030
3	-143.842	191.812	3	-143.922	- 0.018
4	- 96.892	191.832	4	- 95.985	0.002
5	- 47.940	191.838	5	- 48.020	- 0.010
6	0.010	191.858	6	0	0
7	47.978	191.850	7	48.050	0.015
8	195.940	191.835	8	96.038	0.005
9	143.895	191.835	9	143.972	0.008
10	191.900	191.865	10	191.898	0.008
11	239.975	191.925	11	239.865	- 0.010
3-1	-239.802	143.870	7-1	-239.755	- 48.012
2	-191.805	143.848	2	-191.795	- 48.012
3	-143.855	143.860	3	-143.888	- 48.012
4	- 95.922	143.908	4	- 95.948	- 48.020
5	- 47.962	143.922	5	- 47.988	- 48.040
6	0.025	143.940	6	0.045	- 48.035
7	47.995	143.948	7	48.075	- 48.020
8	95.958	143.918	8	96.055	- 48.010
9	143.902	143.890	9	143.980	- 47.985
10	191.858	143.878	10	191.915	- 47.975
11	239.888	143.912	11	239.885	- 48.005
4-1	-239.775	95.880	8-1	-239.775	- 95.965
2	-191.802	95.888	2	-191.808	- 95.960
3	-143.888	95.912	3	-143.868	- 95.960
4	- 95.940	95.962	4	- 95.935	- 95.972
5	- 47.972	95.985	5	- 47.968	- 96.005
6	0.020	96.008	6	0.030	- 96.015
7	48.020	96.005	7	48.035	- 95.982
8	95.998	95.962	8	96.008	- 95.995
9	143.945	95.942	9	143.958	- 95.960
10	192.875	95.920	10	191.898	- 95.940
11	239.860	95.908	11	239.898	- 95.972

TABLE XV--Continued

Point	X	Y	Point	X	Y
9-1	-239.802	-143.962	11-1	-240.005	-240.122
2	-191.782	-143.930	2	-191.902	-240.002
3	-143.830	-143.915	3	-143.888	-239.930
4	- 95.888	-143.918	4	- 95.892	-239.882
5	- 47.932	-143.952	5	- 47.918	-239.872
6	0.052	-143.938	6	0.050	-239.858
7	48.035	-143.922	7	48.030	-239.840
8	96.008	-143.935	8	96.010	-239.895
9	143.952	-143.910	9	143.988	-239.928
10	191.912	-143.910	10	192.020	-239.995
11	239.942	-143.980	11	240.175	-240.158
10-1	-239.878	-192.012			
2	-191.832	-191.950			
3	-143.830	-191.918			
4	- 95.878	-191.890			
5	- 47.905	-191.908			
6	0.068	-191.900			
7	48.035	-191.888			
8	96.000	-191.910			
9	143.972	-191.915			
10	191.975	-191.950			
11	240.040	-192.048			

TABLE XVI

GRID 377 PLATE 49, DISTORTION IN MICRONS AT MODEL SCALE

Point	Radial	Tang.	Point	Radial	Tang.	Point	Radial	Tang.
1-1	20	23	5-1	-198	-22	9-1	- 91	20
2	-128	18	2	-151	-35	2	-198	-36
3	-205	22	3	- 74	-33	3	-158	-19
4	-225	37	4	- 13	-27	4	-118	-15
5	-210	30	5	- 2	-23	5	- 59	-13
6	-192	35	6	12	2	6	- 50	-21
7	-189	32	7	19	17	7	- 73	-26
8	-186	31	8	- 13	25	8	- 80	- 6
9	-189	43	9	- 70	21	9	-123	- 7
10	- 74	22	10	-148	16	10	-162	0
11	+118	37	11	-178	24	11	-111	12
2-1	-136	5	6-1	-212	-28	10-1	- 94	-56
2	-207	-11	2	-150	-30	2	-152	-39
3	-208	19	3	- 62	-28	3	-166	-38
4	-201	55	4	5	-18	4	-157	-28
5	-178	- 6	5	- 32	-12	5	-107	- 3
6	-155	10	6	0	0	6	-105	-30
7	-158	19	7	40	-12	7	-125	-25
8	-178	13	8	- 8	2	8	-116	-12
9	-195	15	9	- 45	5	9	-127	- 5
10	-164	6	10	-132	10	10	-125	12
11	- 58	21	11	-168	10	11	4	4
3-1	-187	6	7-1	-199	-30	11-1	105	-47
2	-219	- 8	2	-153	-44	2	- 73	-44
3	-188	- 4	3	- 66	-38	3	-156	-37
4	-122	- 7	4	- 8	-33	4	-183	-33
5	- 76	7	5	46	-28	5	- 78	-39
6	- 65	2	6	55	- 8	6	-170	-35
7	- 65	11	7	46	- 4	7	-176	-44
8	-112	12	8	36	27	8	-118	-31
9	-156	15	9	33	26	9	- 98	-30
10	-195	13	10	-115	24	10	35	15
11	-141	18	11	-146	35	11	198	-15
4-1	-219	-15	8-1	-188	-17			
2	-212	-26	2	-172	-36			
3	-137	-26	3	- 95	-34			
4	- 71	-14	4	- 30	-23			
5	- 52	-12	5	29	-19			
6	- 25	15	6	28	-18			
7	- 17	25	7	10	-16			
8	-45	17	8	- 12	6			
9	- 99	30	9	- 79	3			
10	- 75	66	10	-146	26			
11	-166	42	11	- 44	-24			

TABLE XVII

GRID 378 PLATE 49, DISTORTION IN MICRONS AT MODEL SCALE

Point	Radial	Tang.	Point	Radial	Tang.	Point	Radial	Tang.
1-1	17	0	5-1	-203	-23	9-1	-193	-24
2	-127	12	2	-153	-35	2	-202	-27
3	-197	23	3	- 60	-38	3	-150	-26
4	-223	26	4	- 14	-33	4	-119	-17
5	-217	23	5	5	-32	5	- 65	- 3
6	-205	18	6	10	-10	6	- 58	8
7	-196	14	7	24	- 7	7	- 67	-26
8	-187	19	8	- 14	25	8	- 75	-14
9	-164	14	9	-169	-12	9	-128	0
10	- 62	12	10	-151	6	10	-164	-15
11	113	25	11	-177	8	11	-122	2
2-1	-130	- 4	6-1	-218	-25	10-1	- 96	-49
2	-204	-19	2	-152	-32	2	-162	-42
3	-217	- 8	3	- 68	-22	3	-167	-40
4	-200	-13	4	0	-22	4	-198	-32
5	-180	-16	5	38	-28	5	-109	-24
6	-158	- 2	6	0	0	6	-100	-25
7	-156	4	7	35	-10	7	-134	-32
8	-183	8	8	35	18	8	-113	-18
9	-195	- 2	9	- 55	- 5	9	-132	-10
10	-168	- 5	10	-132	-10	10	-132	-12
11	- 59	17	11	-188	0	11	- 6	-10
3-1	-180	2	7-1	-216	-38	11-1	102	-44
2	-212	-13	2	-163	-48	2	- 83	-43
3	-187	-18	3	- 69	-46	3	-144	-42
4	-105	5	4	- 11	-32	4	-184	-34
5	- 89	- 4	5	32	-40	5	-171	-37
6	- 78	- 5	6	45	-10	6	-172	-35
7	-74	2	7	51	2	7	-175	-47
8	-108	9	8	38	28	8	-123	-38
9	-161	2	9	- 25	12	9	- 94	-27
10	-190	-13	10	-107	15	10	- 8	-32
11	-136	-18	11	-119	24	11	212	- 7
4-1	-212	-28	8-1	-100	8			
2	-211	-30	2	-177	-36			
3	-140	-20	3	-100	-30			
4	- 72	-20	4	- 34	-23			
5	- 50	-23	5	20	-26			
6	- 30	0	6	38	-20			
7	-20	18	7	6	-11			
8	- 55	24	8	- 16	2			
9	-104	29	9	- 82	- 8			
10	-172	12	10	-151	-12			
11	-168	17	11	-150	- 3			

TABLE XVIII

GRID 377 PLATE 50, DISTORTION IN MICRONS AT MODEL SCALE

Point	Radial	Tang.	Point	Radial	Tang.	Point	Radial	Tang.
1-1	- 9	40	5-1	-215	- 9	9-1	-180	-30
2	-132	36	2	-170	-20	2	-199	-32
3	-199	35	3	- 88	-13	3	-171	-30
4	-223	42	4	- 9	-10	4	-126	-22
5	-213	36	5	- 40	24	5	- 61	-27
6	-195	35	6	25	5	6	- 55	-28
7	-139	30	7	44	12	7	- 72	-53
8	-180	31	8	- 7	19	8	- 68	-24
9	-107	8	9	- 60	23	9	-107	-23
10	76	- 7	10	-124	21	10	-142	-13
11	132	40	11	-157	32	11	- 91	4
2-1	-142	14	6-1	-225	- 5	10-1	- 96	- 52
2	-214	14	2	-160	-12	2	-163	-43
3	-222	22	3	- 70	-10	3	-168	-50
4	-144	53	4	0	8	4	-171	-40
5	-165	33	5	38	-15	5	-113	-44
6	-132	20	6	0	0	6	-100	-38
7	-143	26	7	42	- 5	7	-109	-37
8	-167	28	8	22	10	8	- 98	-22
9	-172	40	9	- 42	15	9	-100	-16
10	-145	42	10	-108	10	10	- 74	-11
11	- 55	52	11	-150	20	11	34	7
3-1	-200	10	7-1	-209	-30	11-1	94	-33
2	-231	- 7	2	-186	3	2	- 78	-30
3	-190	8	3	- 82	-40	3	-127	-53
4	-116	6	4	- 12	-30	4	-187	-14
5	- 95	39	5	26	-34	5	-166	-24
6	- 65	18	6	38	-28	6	-165	-30
7	-14	0	7	62	-46	7	-166	-46
8	- 97	17	8	46	12	8	-123	-36
9	-144	37	9	- 22	13	9	- 91	-22
10	-136	16	10	- 97	23	10	- 56	-46
11	- 97	-33	11	-120	34	11	217	- 3
4-1	-139	-47	8-1	-195	-21			
2	-220	- 7	2	-181	-22			
3	-140	5	3	-105	- 8			
4	- 64	6	4	- 48	- 6			
5	- 32	9	5	14	- 9			
6	- 10	20	6	20	- 2			
7	- 5	25	7	0	-16			
8	- 56	16	8	- 6	10			
9	- 90	14	9	- 65	2			
10	-153	26	10	-126	10			
11	-172	30	11	-118	21			

TABLE XIX

GRID 378 PLATE 50, DISTORTION IN MICRONS AT MODEL SCALE

Point	Radial	Tang.	Point	Radial	Tang.	Point	Radial	Tang.
1-1	- 36	6	5-1	-240	-36	9-1	-206	-42
2	-157	8	2	-182	-27	2	-216	-75
3	-229	14	3	- 92	-24	3	-180	-60
4	-245	20	4	- 13	- 5	4	-130	-48
5	-232	16	5	9	- 3	5	- 66	-50
6	-205	20	6	30	20	6	- 62	-52
7	-213	22	7	38	4	7	- 63	-57
8	-203	16	8	18	9	8	- 34	-57
9	-172	15	9	- 46	7	9	- 97	-30
10	- 94	24	10	-120	7	10	-124	-19
11	82	20	11	-150	37	11	- 60	16
2-1	-163	11	6-1	-238	-38	10-1	-102	-66
2	-247	18	2	-175	-30	2	-170	-72
3	-244	14	3	- 78	-18	3	-168	-87
4	-198	21	4	- 15	2	4	-153	-60
5	-171	18	5	20	-10	5	-112	-70
6	-142	10	6	0	0	6	-100	-32
7	-150	15	7	50	-15	7	-100	-60
8	-174	20	8	38	- 5	8	- 80	-40
9	-196	15	9	-28	- 88	9	- 84	-29
10	-166	24	10	-102	- 8	10	- 80	-40
11	- 66	43	11	-135	10	11	60	12
3-1	-225	-10	7-1	-237	-60	11-1	90	-80
2	-242	- 7	2	-195	-62	2	- 59	-78
3	-202	4	3	-102	-46	3	-118	-60
4	-125	22	4	- 37	-41	4	-150	-46
5	- 86	12	5	- 6	-12	5	-141	-46
6	-60	25	6	35	-45	6	-142	-50
7	- 51	12	7	67	-38	7	-152	-60
8	- 92	11	8	54	-16	8	- 93	-46
9	-140	15	9	-24	- 8	9	- 68	-26
10	-187	12	10	- 88	- 4	10	8	-19
11	-141	17	11	-111	28	11	237	-12
4-1	-253	-38	8-1	-222	-51			
2	-226	-12	2	-189	-51			
3	-141	17	3	-132	-40			
4	- 68	16	4	-72	-20			
5	- 26	19	5	- 9	-30			
6	8	20	6	15	-30			
7	14	16	7	0	-38			
8	- 28	26	8	49	-57			
9	- 77	18	9	- 57	-10			
10	-148	16	10	-117	- 7			
11	-164	34	11	-104	12			

TABLE XX

PLATE 49, AVERAGE DISTORTION IN MICRONS AT PHOTO SCALE

Point	Radial	Tang.	Point	Radial	Tang.	Point	Radial	Tang.
1-1	8	5	5-1	-84	- 9	9-1	-59	- 1
2	-53	6	2	-64	-15	2	-83	-13
3	-84	9	3	-32	-15	3	-64	- 9
4	-93	13	4	- 6	-13	4	-49	- 7
5	-89	11	5	1	-11	5	-26	- 3
6	-84	11	6	5	- 2	6	-23	- 3
7	-80	10	7	9	2	7	-29	-11
8	-78	10	8	- 6	10	8	-32	- 4
9	-74	12	9	-50	2	9	-52	- 2
10	-28	7	10	-62	5	10	-68	- 3
11	48	13	11	-74	7	11	-49	3
2-1	-55	0	6-1	-90	-11	10-1	-40	-22
2	-86	6	2	-63	-13	2	-65	-17
3	-89	2	3	-27	-10	3	-69	-16
4	-84	9	4	1	- 8	4	-74	-13
5	-75	- 5	5	1	- 8	5	-45	- 6
6	-65	2	6	0	0	6	-43	-11
7	-65	5	7	16	- 5	7	-54	-12
8	-75	4	8	-13	4	8	-48	- 6
9	-81	3	9	-21	0	9	-54	- 3
10	-69	0	10	-55	0	10	-54	0
11	-24	8	11	-70	2	11	0	- 1
3-1	-76	2	7-1	-86	-14	11-1	43	-19
2	-90	- 4	2	-66	-19	2	-33	-18
3	-78	- 5	3	-28	-18	3	-63	-16
4	-47	0	4	- 4	-14	4	-76	-14
5	-34	1	5	16	-14	5	-52	-16
6	-30	- 1	6	21	0	6	-71	-15
7	-29	3	7	20	6	7	-73	-19
8	-46	4	8	15	11	8	-50	-14
9	-66	3	9	1	8	9	-40	-12
10	-80	0	10	-46	8	10	6	- 4
11	-58	0	11	-55	12	11	85	- 5
4-1	-90	- 9	8-1	-60	- 2			
2	-88	-12	2	-73	-15			
3	-58	-10	3	-41	-13			
4	-30	- 7	4	-13	-10			
5	-21	- 7	5	10	-10			
6	-11	3	6	14	- 8			
7	- 8	9	7	3	- 6			
8	-21	9	8	- 8	2			
9	-42	12	9	-34	- 1			
10	-51	16	10	-62	3			
11	-70	12	11	-40	- 6			

TABLE XXI

PLATE 50, AVERAGE DISTORTION IN MICRONS AT PHOTO SCALE

Point	Radial	Tang.	Point	Radial	Tang.	Point	Radial	Tang.
1-1	-9	10	5-1	-93	-10	9-1	-80	-15
2	-60	9	2	-73	-10	2	-87	-22
3	-89	10	3	-38	-8	3	-73	-19
4	-98	13	4	-5	-3	4	-53	-15
5	-93	11	5	-6	4	5	-26	-16
6	-83	11	6	11	5	6	-24	-17
7	-73	11	7	17	3	7	-28	-23
8	-80	10	8	2	6	8	-21	-17
9	-58	5	9	-22	6	9	-43	-11
10	-4	4	10	-51	6	10	-41	-25
11	45	13	11	-64	14	11	-32	4
2-1	-64	5	6-1	-97	-9	10-1	-41	-25
2	-96	7	2	-70	-9	2	-69	-24
3	-97	8	3	-33	-6	3	-70	-29
4	-71	15	4	-3	2	4	-68	-21
5	-70	11	5	12	-5	5	-47	-24
6	-57	6	6	0	0	6	-42	-15
7	-61	9	7	19	-4	7	-44	-20
8	-71	10	8	13	1	8	-37	-13
9	-77	11	9	-15	2	9	-38	-9
10	-65	14	10	-44	0	10	-32	-11
11	-25	20	11	-59	6	11	20	4
3-1	-89	0	7-1	-93	-19	11-1	38	-24
2	-99	-3	2	-79	-12	2	-29	-23
3	-82	3	3	-38	-18	3	-51	-24
4	-50	6	4	-10	-15	4	-70	-13
5	-38	11	5	4	-10	5	-64	-15
6	-26	9	6	15	-15	6	-64	-17
7	-14	3	7	31	-18	7	-66	-22
8	-39	6	8	21	-1	8	-45	-17
9	-59	11	9	-10	1	9	-33	-10
10	-78	6	10	-39	4	10	-10	-14
11	-50	-3	11	-48	13	11	95	-3
4-1	-82	-18	8-1	-87	-15			
2	-93	-4	2	-77	-15			
3	-59	5	3	-49	-10			
4	-28	5	4	-25	-5			
5	-12	6	5	1	-8			
6	0	8	6	7	-7			
7	2	9	7	0	-11			
8	-18	9	8	9	-10			
9	-35	7	9	-25	-2			
10	-63	9	10	-51	1			
11	-70	13	11	-46	7			

TABLE XXII

PLATE 49, CORRECTED TANGENTIAL DISTORTION IN MICRONS

Pt.	Dist.	Pt.	Dist.	Pt.	Dist.
1-1	12	5-1	- 4	9-1	5
2	12	2	-11	2	- 8
3	15	3	-12	3	- 5
4	18	4	-11	4	- 3
5	16	5	-10	5	0
6	16	6	- 1	6	0
7	15	7	3	7	- 8
8	15	8	12	8	0
9	18	9	5	9	2
10	13	10	9	10	2
11	20	11	12	11	9
2-1	6	6-1	- 6	10-1	-16
2	12	2	- 9	2	-11
3	7	3	- 7	3	-11
4	13	4	- 6	4	- 9
5	- 1	5	- 7	5	- 2
6	6	6	0	6	- 7
7	9	7	- 4	7	- 8
8	8	8	6	8	- 2
9	8	9	3	9	2
10	6	10	4	10	6
11	14	11	7	11	5
3-1	8	7-1	- 9	11-1	-12
2	1	2	-15	2	-12
3	- 1	3	-15	3	-10
4	4	4	-12	4	- 9
5	4	5	-13	5	-11
6	2	6	1	6	-10
7	6	7	7	7	-14
8	8	8	13	8	- 9
9	7	9	11	9	- 6
10	5	10	12	10	2
11	6	11	17	11	2
4-1	- 4	8-1	3		
2	- 8	2	-11		
3	- 6	3	- 9		
4	- 4	4	- 7		
5	- 5	5	- 8		
6	5	6	- 6		
7	11	7	- 4		
8	12	8	5		
9	16	9	3		
10	20	10	7		
11	17	11	- 1		

TABLE XXIII

PLATE 50, CORRECTED TANGENTIAL DISTORTION IN MICRONS

Pt.	Dist.	Pt.	Dist.	Pt.	Dist.
1-1	16	5-1	- 6	9-1	-10
2	14	2	- 7	2	-18
3	15	3	- 5	3	-15
4	17	4	- 1	4	-12
5	15	5	5	5	-13
6	15	6	6	6	-14
7	15	7	4	7	-20
8	14	8	8	8	-14
9	10	9	9	9	- 7
10	9	10	9	10	-21
11	19	11	18	11	9
2-1	10	6-1	- 5	10-1	-20
2	12	2	- 6	2	-19
3	12	3	- 3	3	-25
4	19	4	4	4	-17
5	14	5	- 4	5	-21
6	9	6	0	6	-12
7	12	7	- 3	7	-17
8	14	8	3	8	- 9
9	15	9	5	9	- 5
10	19	10	3	10	- 6
11	25	11	10	11	9
3-1	5	7-1	-15	11-1	-18
2	1	2	- 9	2	-18
3	7	3	-15	3	-19
4	9	4	-13	4	- 9
5	14	5	- 9	5	-11
6	12	6	-14	6	-13
7	6	7	-17	7	-18
8	9	8	1	8	-13
9	15	9	4	9	- 5
10	10	10	7	10	- 9
11	2	11	17	11	3
4-1	-14	8-1	-11		
2	0	2	-11		
3	8	3	- 7		
4	7	4	- 3		
5	8	5	- 6		
6	10	6	- 5		
7	11	7	- 9		
8	11	8	- 8		
9	10	9	1		
10	13	10	5		
11	17	11	11		

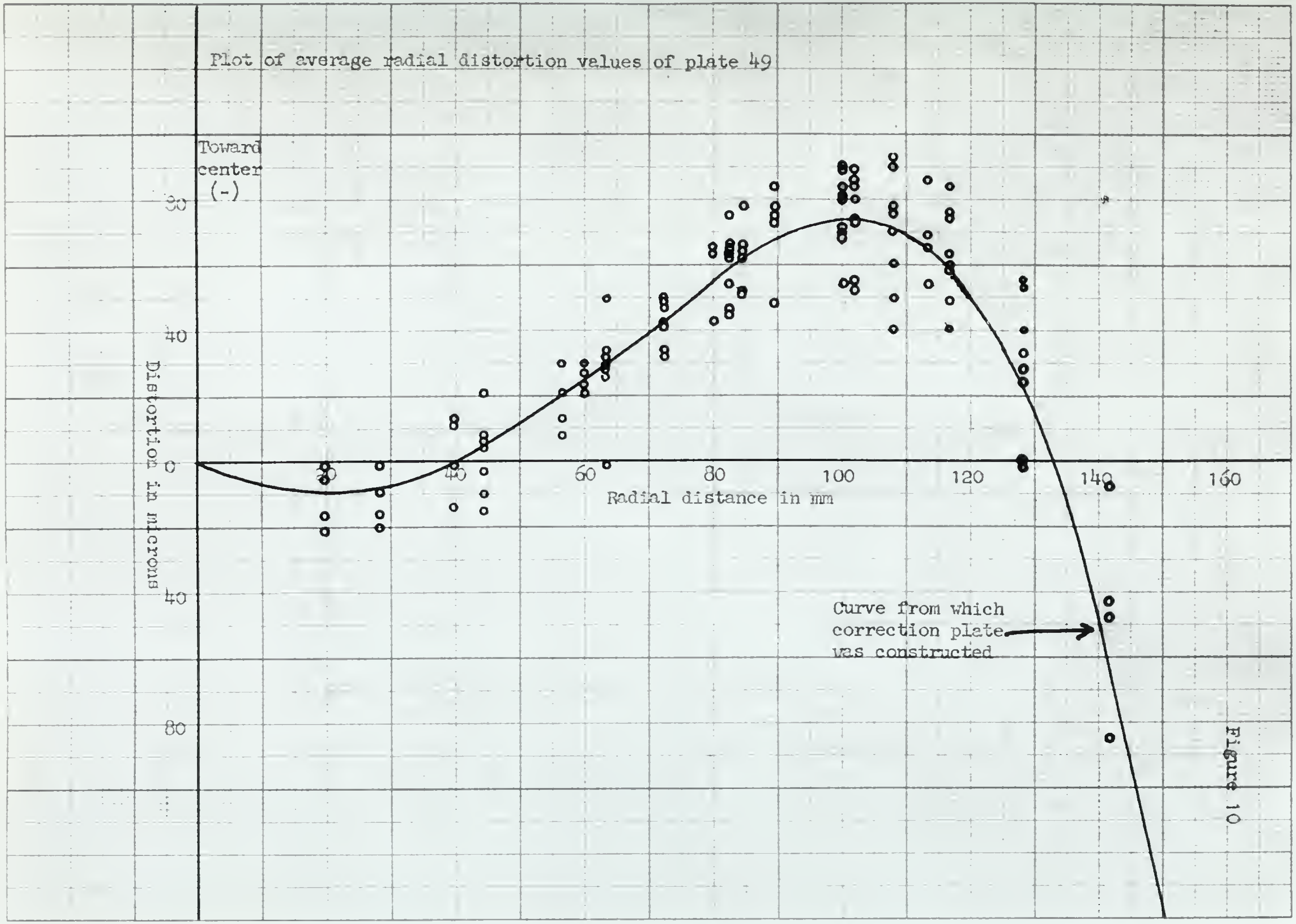
Plot of average radial distortion values of plate 49
Toward center (-)
80
40
0
40
80
Distortion in microns
20
40
60
80
100
120
140
160
Radial distance in mm
Curve from which correction plate was constructed

Figure 10

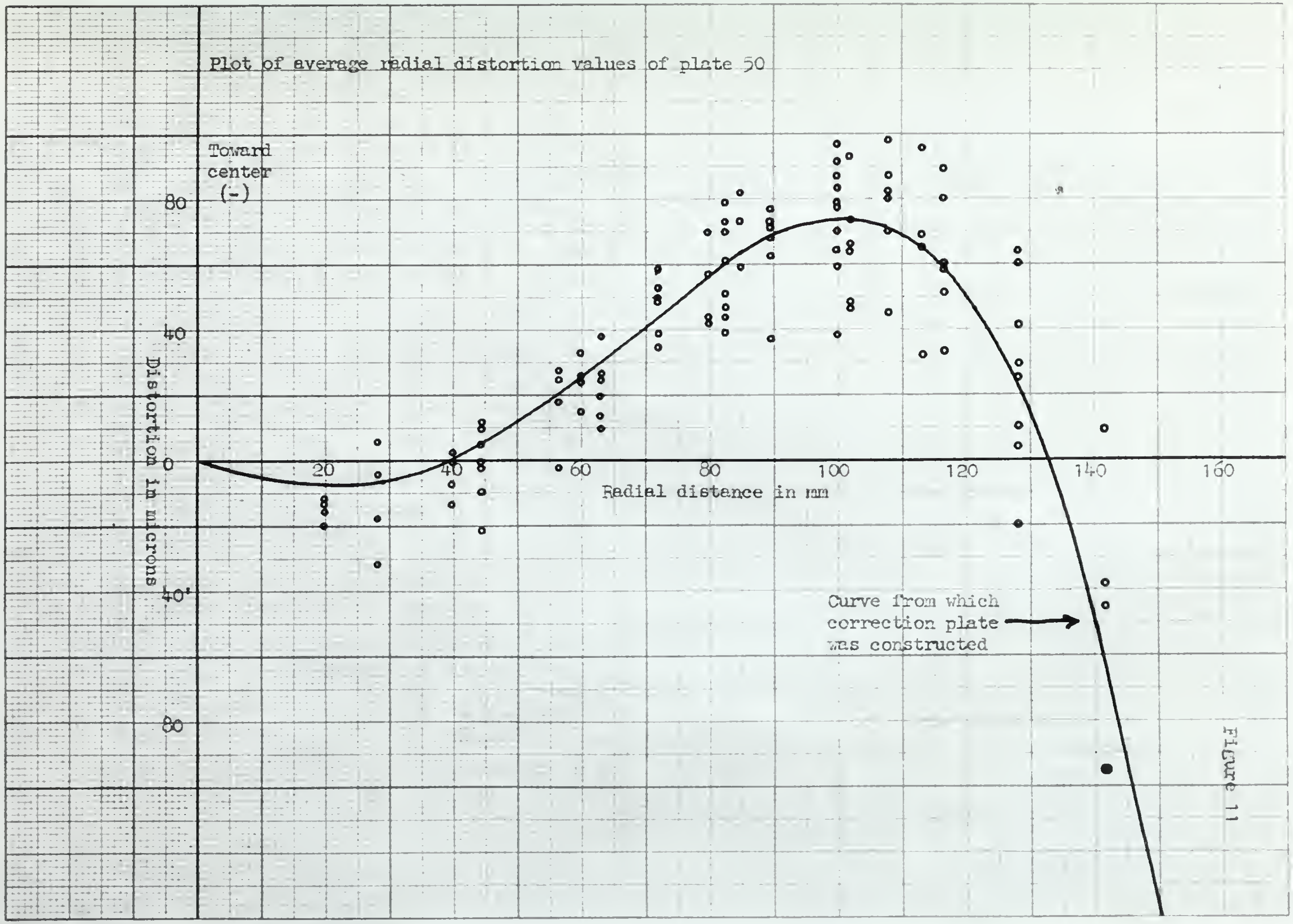

Plot of average radial distortion values of plate 50
Toward center (-)
80
40
0
40
80
Distortion in microns
20
40
60
80
100
120
140
160
Radial distance in mm
Curve from which correction plate was constructed

Figure 11

CONSTRUCTION OF COORDINATE ERROR CURVES

Using the metrogon correction plate curve, as specified for construction, as the reference, the curves of elevation error were computed and tabulated in Table VII. Using these values and the equations for py, dX" and e_o derived in Chapter II, values were computed for points in the model sufficient to construct error curves. Lens 13 is the worst of the 25 lenses in point of view of resultant elevation errors and lens 18 the best. Table XXIV contains these computations which were done for the upper half of the model only due to the symmetry about the X axis. Figures 12 through 20 are the constructed curves. These curves are computed on the basis of an assumed elevation of 4,000 meters above the terrain just as all examples throughout the thesis have been.

In order to provide a more realistic picture of the anticipated errors, the elements of mathematical relative orientation were computed for a dependent pair orientation procedure using the following formulae:

$$d\phi_2 = \frac{3183h}{bd}(p_3 - p_4 - p_5 + p_6)$$

$$d\omega_2 = \frac{1591h}{d^2}(-2p_1 - 2p_2 + p_3 + p_4 + p_5 + p_6$$

$$d\kappa_2 = \frac{2122}{b}(p_1 - p_2 + p_3 - p_4 + p_5 - p_6)$$

$$dbz_2 = \frac{h}{2d}(p_6 - p_4)$$

Where: Quantities are in centesimal minutes and mm.
p = parallax at given point in model
h = projector to model distance

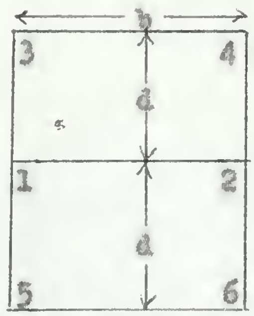

Model

Points 3,4,5,6 are approximately 1 cm from the respective upper and lower edges of the photo. Points 1 and 2 are approximately the nadir points.

Lens	p_1	p_2	p_3	p_4	p_5	p_6
13	0	0	-.037	.037	.037	-.037 mm
Ave.	0	0	.0025	-.0025	-.0025	.0025
18	0	0	.0042	-.0042	-.0042	.0042

Lens	$d\phi_2$	$d\omega_2$	$d\kappa_2$	dbz_2
13	-7.88^c	0	0	-.0564 mm
Ave.	.533	0	0	.0038
18	.895	0	0	.0064

These elements were then introduced into the following equation to solve for the change in e_2, the elevation error of the right projector, caused by relative orientation:

$$dh = \left[\frac{h^2}{b} + \frac{(X-b)^2}{b}\right] d\phi_2 - \frac{(X-b)Y'}{b} d\omega_2 - \frac{hY}{b} d\kappa_2 + \frac{(X-b)}{b} dbz_2$$

As can be seen from the above table of elements of orientation, all elements except $d\phi_2$ and dbz_2 are zero due to the symmetry of the parallax resulting from the model composed of two vertical photos. The dbz_2 element is retained in the computations even though it could be corrected for in the absolute orientation, as it causes a straight line tilt of the model about the Y axis as shown below:

The h^2/b part of the $d\phi_2$ coefficient is a constant elevation change, thus could be compensated in absolute orientation, and the $(X-b)^2/b$ is the variable as shown below:

The absolute orientation will be carried out using three points as near as possible to the points circled in the above diagram in order to compensate in the absolute orientation, as near as possible, for the error in $d\phi_2$ brought about by parallax caused by uncompensated distortion in the camera lens. Also this scheme of points will avoid correcting for any error in $d\omega_2$ caused by distortion parallax, as can be seen from the following diagram of elevation error caused by $d\omega_2$:

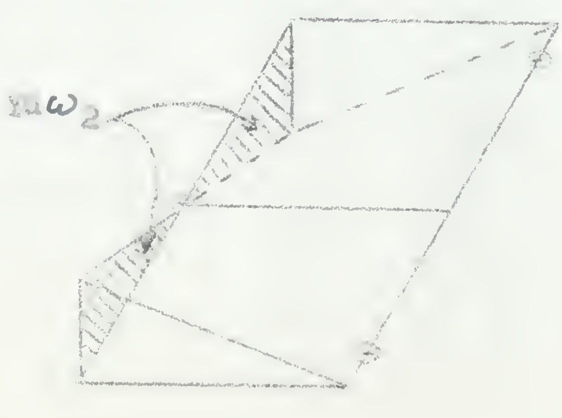

The effect of the warping caused by a $d\phi_2$ error can be seen in Figures 27 through 29. The elevation errors along the X-axis form a curve with a definite change of slope as can be seen in a diagram of the theoretical situation.

Line representing result of levelling in absolute orientation to compensate for $d\phi_2$ error.

As an indication of the effect of the approximation of $d\phi_2$ in absolute orientation, the magnitude of A, the maximum point of separation, is computed for each of the three lenses:

Lens	A at ground scale in meters	Error as a fraction of flying height
13	0.742	1:5400
Ave.	0.050	1:80000
18	0.084	1:47600

Measurement of cross-section graphs through the X-axis of Figures 27 through 29 yields values of A greater than in the above table but approximately equal to A plus the result of dbz_2 at that point. As can be seen from the above table of values, this approximation, in all but the worst lenses, will not introduce errors anywhere near the errors caused by the uncompensated distortion. Measurement of a cross-section through the X-axis of Figure 32, the elevation errors of the actual photography, yielded this curve with a value for A of approximately twice that found for lens 18.

The computations of dh appear in Table XXVI. The curves of the resultant errors appear in Figures 21 through 29. After this false orientation, which has destroyed the true spatial relationship, the errors depicted in Figures 21 through 29 would represent, approximately, what would be observed in models formed with these lenses, except that the model formed with lens 13 would require extensive adjustment to correct the large amount of y-parallax present. The average lens is probably representative of most metrogon lenses.

As a comparison of the data plotted in Figures 12 through 20 and Figures 21 through 29, the following table of maximum errors is presented, in which the errors are stated as fractional parts of the aircraft elevation:

	Elevation Errors	X-direction Errors
True spatial model Fig. 12-20		
Lens 13	1:1300	1:8000
Average lens	1:5000	1:27000
Lens 18	1:20000	1:65000
Oriented model Fig. 21-29		
Lens 13	1:400	1:4000
Average lens	1:2670	1:16000
Lens 18	1:1600	1:10000

The best elevation accuracy attainable would be approximately three halves that of a second order plotter and one half that in a first order instrument. The relative accuracy of using the above metrogon photography in a first order instrument to that in a second order instrument would be approximately

$\sqrt{1.5^2 + 3^2} : \sqrt{1.5^2 + 1^2}$ or 1.88:1.

For comparison purposes, one stereo model was observed and errors computed in Table XXVII. The curves of these errors are plotted in Figures 30 through 32. The photography was taken by the U. S. Coast and Geodetic Survey with a metrogon lens camera of focal length 152.37 mm at a stated altitude of 13750 feet over the McClure, Ohio, photogrammetric test area. The observations were made in the Wild Autograph A7. Relative orientation was completed in the normal manner using 6 points. Absolute orientation was completed using 3 points as previously discussed to minimise the effect that a warped model, caused by ϕ or ω errors, would have upon the absolute orientation.

Model scale was selected as 1:10,000 in order to provide a desirable position of the model in Z column height. Model scaling was performed using the following set of equations:

$\Delta S_1^* = So_1^* - S_1^*$

$\Delta S_2^* = So_2^* - S_2^*$

$\Delta S_3^* = So_3^* - S_3^*$

So^* = observed distance at model scale

S^* = given distance at model scale

$q_1 = \dfrac{\Delta S_1^*}{So_1^*} \qquad q_1 = \dfrac{\Delta S_2^*}{So_1^*} \qquad q_1 = \dfrac{\Delta S_3^*}{So_3^*}$

$q = 1/3(q_1 + q_2 + q_3)$

$bx = bx_o - qbx_o$

$by = by_o - qby_o$

$bz = bz_o - qbz_o$

Model levelling was completed as follows:

$$\Delta H_A = \Delta H_1 + \frac{1-A}{1-2}(\Delta H_2 - \Delta H_1)$$

$$\Delta H_B = \Delta H_3 + \frac{3-B}{3-2}(\Delta H_2 - \Delta H_3)$$

$$\omega = \frac{\Delta H_3 - \Delta H_A}{A-3}$$

$$\phi = \frac{\Delta H_B - \Delta H_1}{B-1}$$

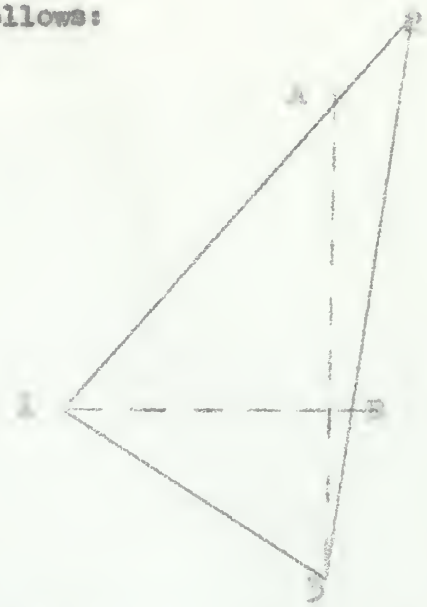

Upon completion of orientation, final observations were made on the above 3 points and the following determined:

Actual model scale: 1:9999.12.

Rotation of model necessary to align model with given coordinate system: $A = 1^\circ\ 42'\ 52''.6$.

Upon completion of observation of all given points in the model, the observed quantities of X and Y were corrected using the following equations, in which m is the scale factor:

$$X' = mX \cos A + my \sin A$$

$$Y' = mY \cos A - mX \sin A.$$

TABLE XXIV

x_{a_1} (cm)	x_{a_2} (cm)	y_a (cm)
-0.71	- 9.85	1.82
1.26	- 7.88	1.51
-2.46	-11.60	3.12
-0.05	- 9.19	4.00
1.92	- 7.22	3.52
3.49	- 5.65	2.00
-1.37	-10.51	5.83
1.05	- 8.09	5.90
3.00	- 6.14	5.19
-2.53	-11.67	7.58
0.20	- 8.94	8.00
2.59	- 6.55	7.59
-2.18	-11.32	9.77
-0.56	- 9.70	9.99
2.14	- 7.00	9.89
1.78	- 7.36	11.85
7.36	- 1.78	11.85
7.00	- 2.14	9.89
9.70	0.56	9.99
11.32	2.18	9.77
6.55	- 2.59	7.59
8.94	- 0.20	8.00
11.67	2.53	7.58
6.14	- 3.00	5.19
8.09	- 1.05	5.90
10.51	1.37	5.83
5.65	- 3.49	2.00
7.22	- 1.92	3.52
9.19	0.05	4.00
11.60	2.46	3.12
7.88	- 1.26	1.51
9.85	0.71	1.82

TABLE XXIV—Continued

Lens 13						
e_1 (m)	e_2 (m)	e_1-e_2 (m)	py (microns)	dX" (m)	fdX''/x_{a_2} (m)	e_o (m)
-2.84	-1.54	-1.30	- 5.9	0.065	-0.10	-1.44
-2.84	-2.68	-0.16	- 6.0	-0.011	0.02	-2.70
-3.13	0.55	-3.68	-28.7	0.747	-0.99	1.54
-3.13	-1.54	-1.59	-15.9	0.005	-0.01	-1.53
-3.13	-2.68	-0.45	-4.0	-0.044	0.09	-2.77
-3.13	-3.28	0.15	+ 0.8	0.021	-0.06	-3.22
-3.28	0.55	-3.83	-55.8	0.392	-0.57	1.12
-3.28	-1.54	-1.74	-25.7	-0.105	0.20	-1.74
-3.28	-2.68	-0.60	- 7.8	-0.079	0.20	-2.88
-2.68	-0.09	-2.59	-49.1	0.544	-0.72	0.63
-2.68	0.55	-3.23	-64.6	-0.041	0.07	0.48
-2.68	-1.54	-1.14	-21.6	-0.138	0.32	-1.86
-1.54	0.19	-1.73	-42.3	0.304	-0.41	0.60
-1.54	-0.09	-1.45	-36.2	0.056	-0.09	0
-1.54	0.55	-2.09	-51.7	-0.223	0.49	0.06
0.55	-0.09	0.64	+19.0	0.060	-0.13	0.04
-0.09	0.55	-0.64	-19.0	-0.060	0.52	0.03
0.55	-1.54	2.09	51.7	0.223	-1.60	0.06
-0.09	-1.54	1.45	36.2	-0.056	-1.54	0
0.19	-1.54	1.73	42.3	-0.304	-2.14	0.60
-1.54	-2.68	1.14	21.6	0.138	-0.82	-1.86
0.55	-2.68	3.23	64.6	0.041	-3.15	0.47
-0.09	-2.68	2.59	49.1	-0.544	-3.31	0.63
-2.68	-3.28	0.60	7.8	0.079	-0.40	-2.88
-1.54	-3.28	1.74	25.7	0.105	-1.54	-1.74
0.55	-3.28	3.83	55.8	-0.392	-4.40	1.12
-3.28	-3.13	-0.15	- 0.8	-0.021	+0.09	-3.22
-2.68	-3.13	0.45	4.0	0.044	-0.35	-2.78
-1.54	-3.13	1.59	15.9	-0.005	-1.60	-1.53
0.55	-3.13	3.68	28.7	-0.747	-4.67	1.54
-2.68	-2.84	0.16	6.0	0.011	-0.13	-2.71
-1.54	-2.84	1.30	5.9	-0.065	-1.41	-1.43

TABLE XXIV—Continued

Lens 18						
e_1 (m)	e_2 (m)	e_1-e_2 (m)	py (microns)	dX" (m)	$f dX''/x_{a_2}$ (m)	e_c (m)
0.56	0	0.56	2.5	−0.028	0.04	−0.04
0.56	−0.20	0.76	2.9	0.054	−0.10	−0.10
0.33	0	0.33	2.6	−0.067	0.09	−0.09
0.33	0	0.33	3.3	−0.001	0	0
0.33	−0.20	0.53	4.7	0.052	−0.11	−0.09
0.33	−0.20	0.53	2.7	0.074	−0.21	0.01
−0.20	0	−0.20	− 2.9	0.020	−0.03	0.03
−0.20	0	−0.20	− 3.0	−0.012	0.02	−0.02
−0.20	−0.20	0	0	0	0	−0.20
−0.20	−0.15	−0.05	− 0.9	0.011	−0.01	−0.14
−0.20	0	−0.20	− 2.0	−0.003	0	0
−0.20	0	−0.20	− 3.6	−0.024	0.06	−0.06
0	−0.24	0.24	5.9	−0.042	0.06	−0.30
0	−0.15	0.15	3.7	−0.006	0.01	−0.16
0	0	0	0	0	0	0
0	−0.15	0.15	4.4	0.014	−0.03	−0.12
−0.15	0	−0.15	− 4.4	−0.014	0.12	−0.12
0	0	0	0	0	0	0
−0.15	0	−0.15	− 3.7	0.006	0.16	−0.16
−0.24	0	−0.24	− 5.9	0.042	0.30	−0.30
0	−0.20	0.20	3.8	0.024	−0.14	−0.06
0	−0.20	0.20	2.0	0.003	−0.21	0.01
−0.15	−0.20	0.05	0.9	−0.011	−0.01	−0.13
−0.20	−0.20	0	0	0	0	−0.20
0	−0.20	0.20	3.0	0.012	−0.18	−0.02
0	−0.20	0.20	2.9	−0.020	−0.22	0.02
−0.20	0.33	−0.53	− 2.7	−0.074	0.33	0
−0.20	0.33	−0.53	− 4.7	−0.052	0.42	−0.09
0	0.33	−0.33	− 3.3	0.001	0.32	0.01
0	0.33	−0.33	− 2.6	0.067	0.42	−0.09
−0.20	0.56	−0.76	− 2.9	−0.054	0.66	−0.10
0	0.56	−0.56	− 2.5	0.028	0.61	−0.05

TABLE XXIV—Continued

Average						
e_1 (m)	e_2 (m)	e_1-e_2 (m)	py (microns)	$\delta X''$ (m)	$f\delta X''/x_{a_2}$ (m)	e_o (m)
−0.54	−0.02	−0.52	− 2.4	0.026	−0.04	0.02
−0.54	−0.55	0.01	0	0.001	0	−0.55
−0.58	+0.27	−0.85	− 6.6	0.173	−0.23	0.50
−0.58	−0.02	−0.56	− 5.6	0.002	0	−0.02
−0.58	−0.55	−0.03	− 0.3	−0.003	+0.01	−0.56
−0.58	−0.80	0.22	1.1	0.031	−0.08	−0.72
−0.80	0.27	−1.07	−15.6	0.110	−0.16	0.43
−0.80	−0.02	−0.78	−11.5	−0.047	+0.09	−0.11
−0.80	−0.55	−0.25	− 3.2	−0.033	+0.08	−0.63
−0.55	−0.12	−0.43	− 8.1	0.091	−0.12	0
−0.55	0.27	−0.82	−16.4	−0.010	+0.02	0.24
−0.55	−0.02	−0.53	−10.1	−0.064	+0.15	−0.17
−0.02	−0.32	0.30	7.3	−0.053	+0.07	−0.39
−0.02	−0.12	0.10	2.5	−0.004	+0.01	−0.13
−0.02	0.27	−0.29	− 4.7	−0.031	+0.07	0.20
0.27	−0.12	0.39	11.6	0.036	−0.08	−0.04
−0.12	0.27	−0.39	−11.6	−0.036	+0.31	−0.04
0.27	−0.02	0.29	4.7	0.031	−0.22	0.20
−0.12	−0.02	−0.10	− 2.5	0.004	+0.11	−0.13
−0.32	−0.02	−0.30	− 7.3	0.053	+0.37	−0.39
−0.02	−0.55	0.53	10.1	0.064	−0.38	−0.17
0.27	−0.55	0.82	16.4	0.010	−0.77	0.22
−0.12	−0.55	0.43	8.1	−0.091	−0.55	0
−0.55	−0.80	0.25	3.2	0.033	−0.17	−0.63
−0.02	−0.80	0.78	11.5	0.047	−0.69	−0.11
0.27	−0.80	1.07	15.6	−0.110	−1.23	0.43
−0.80	−0.58	−0.22	− 1.1	−0.031	+0.14	−0.72
−0.55	−0.58	0.03	0.3	0.003	−0.02	−0.56
−0.02	−0.58	0.56	5.6	−0.002	−0.61	0.03
0.27	−0.58	0.85	6.6	−0.173	−1.08	0.50
−0.55	−0.54	−0.01	0	−0.001	+0.01	−0.55
−0.02	−0.54	0.52	2.4	−0.026	−0.56	0.02

Figure 12

Y-Parallax in microns
Stereo model formed with Lens #13

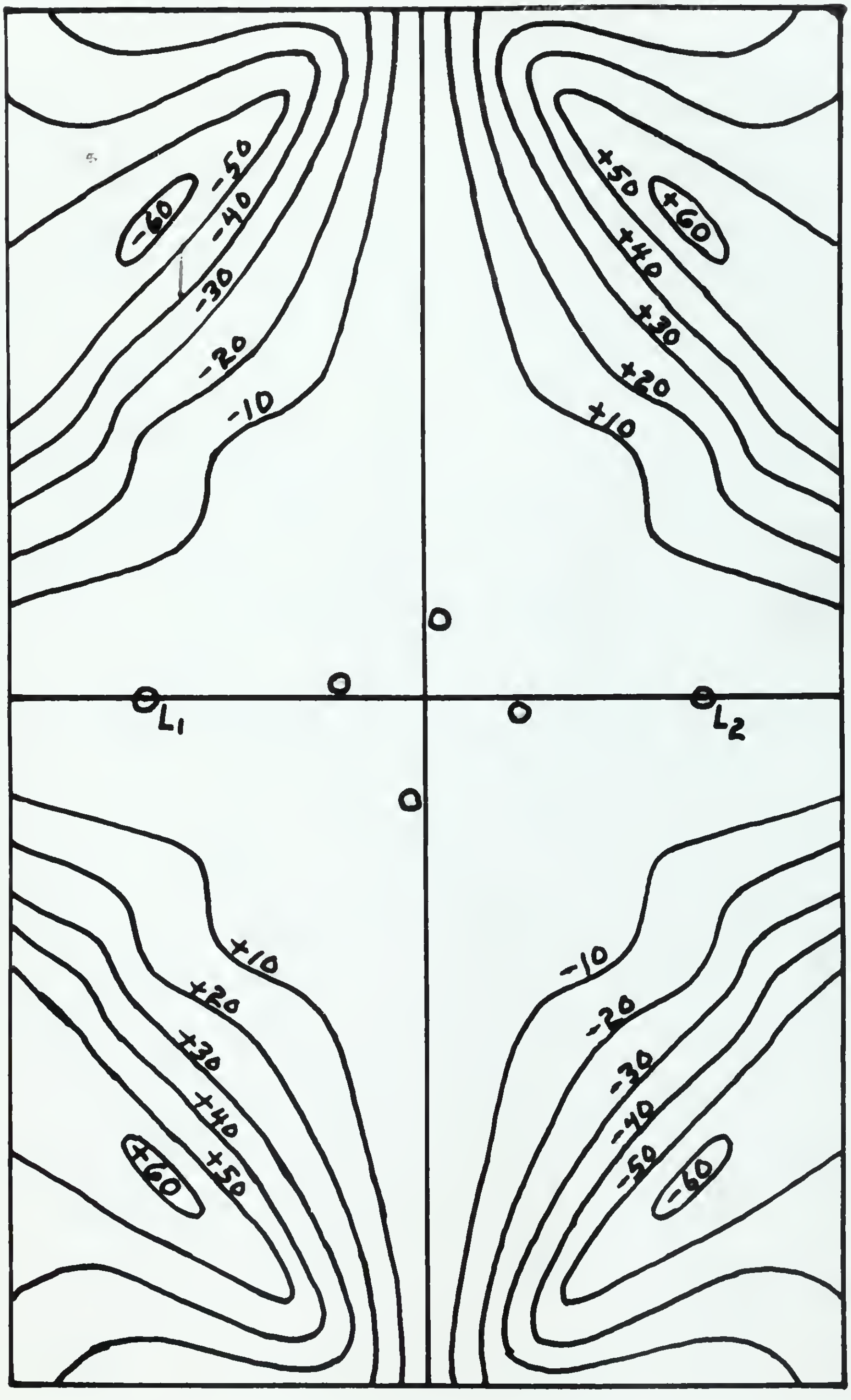

Figure 1[illegible]

Y-Parallax in microns
Stereo model formed with Average Lens

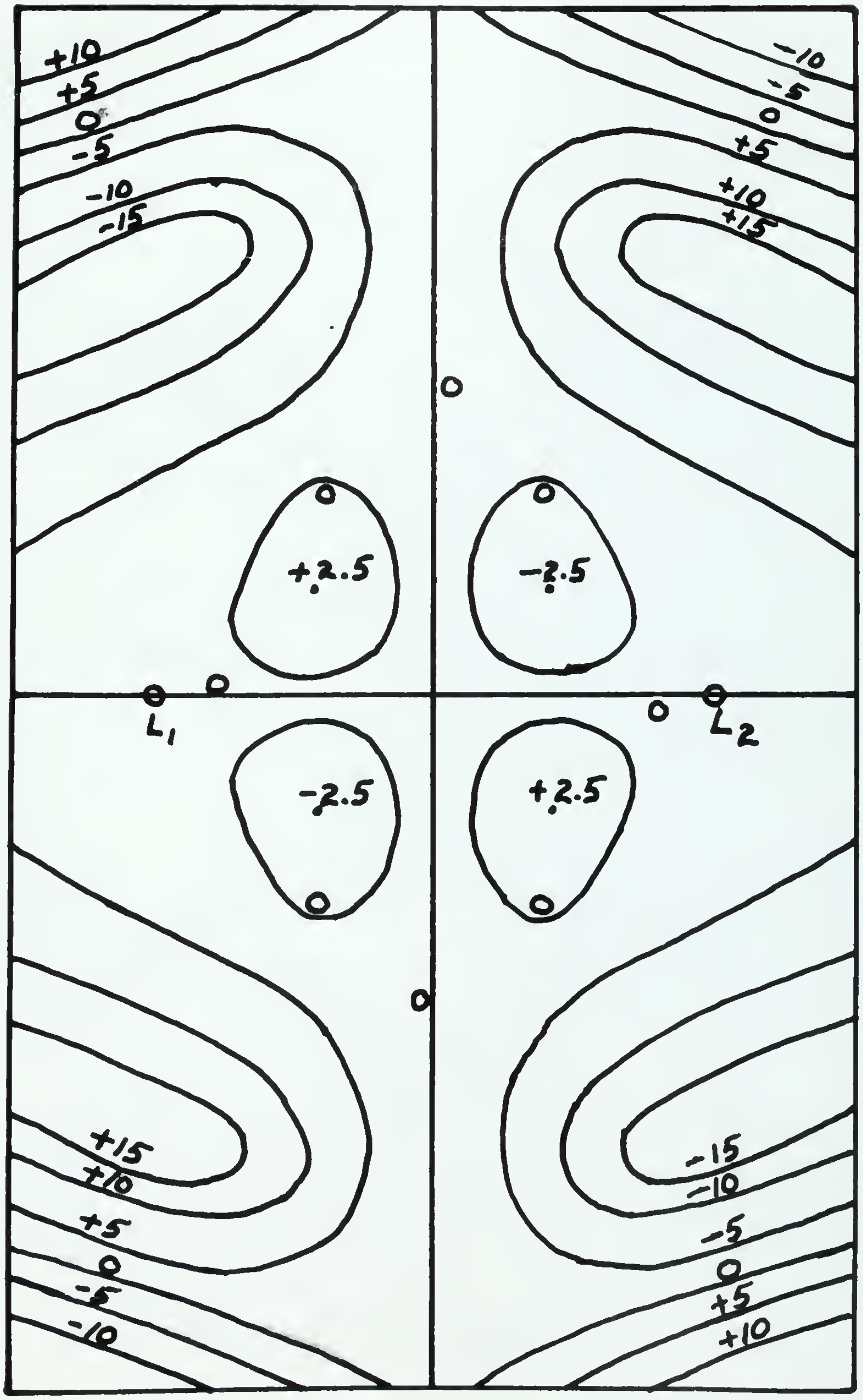

Figure 14

Y-Parallax in microns
Stereo model formed with Lens #18

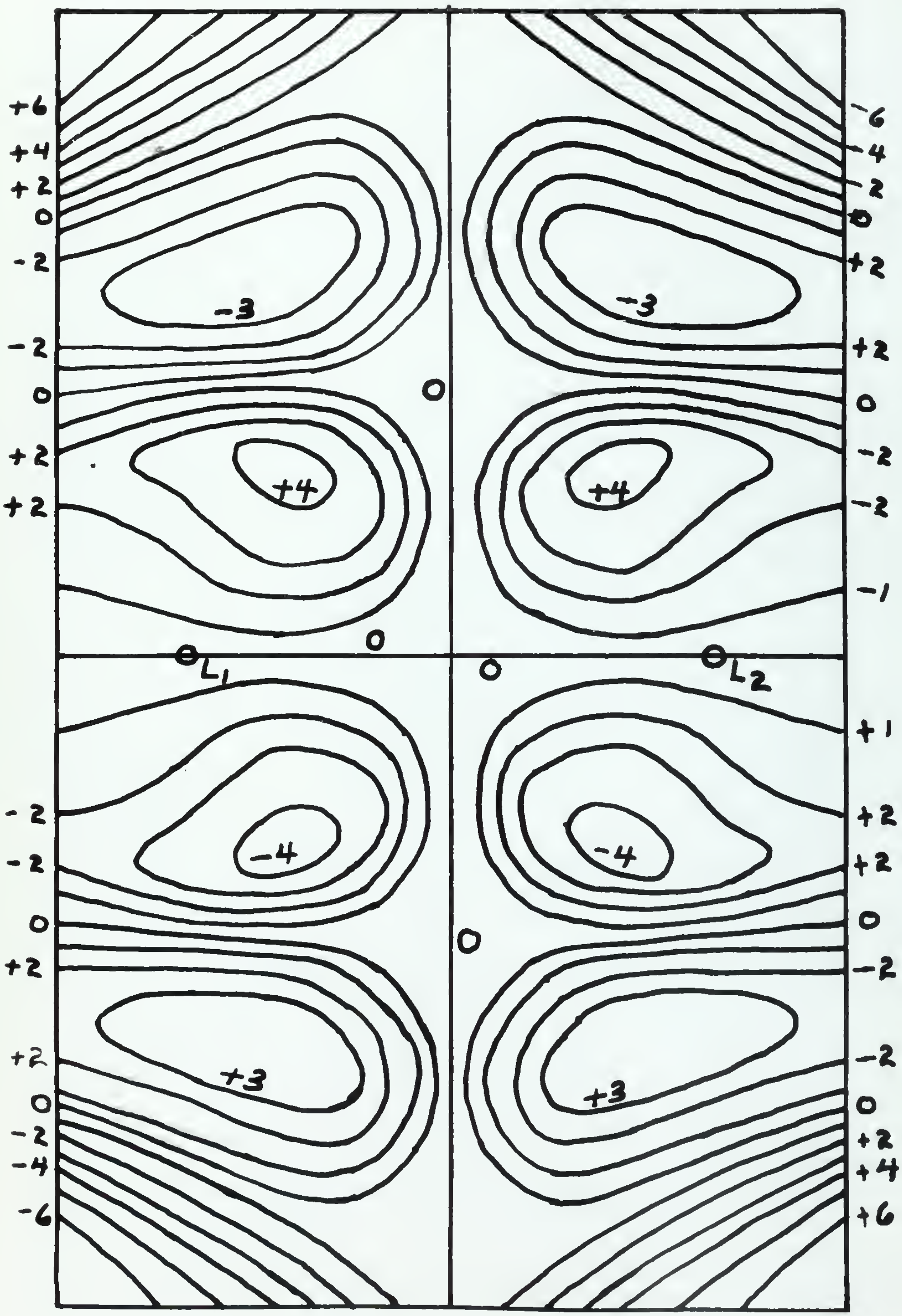

Figure 15

X-direction errors in centimeters
Stereo model formed with Lens #13

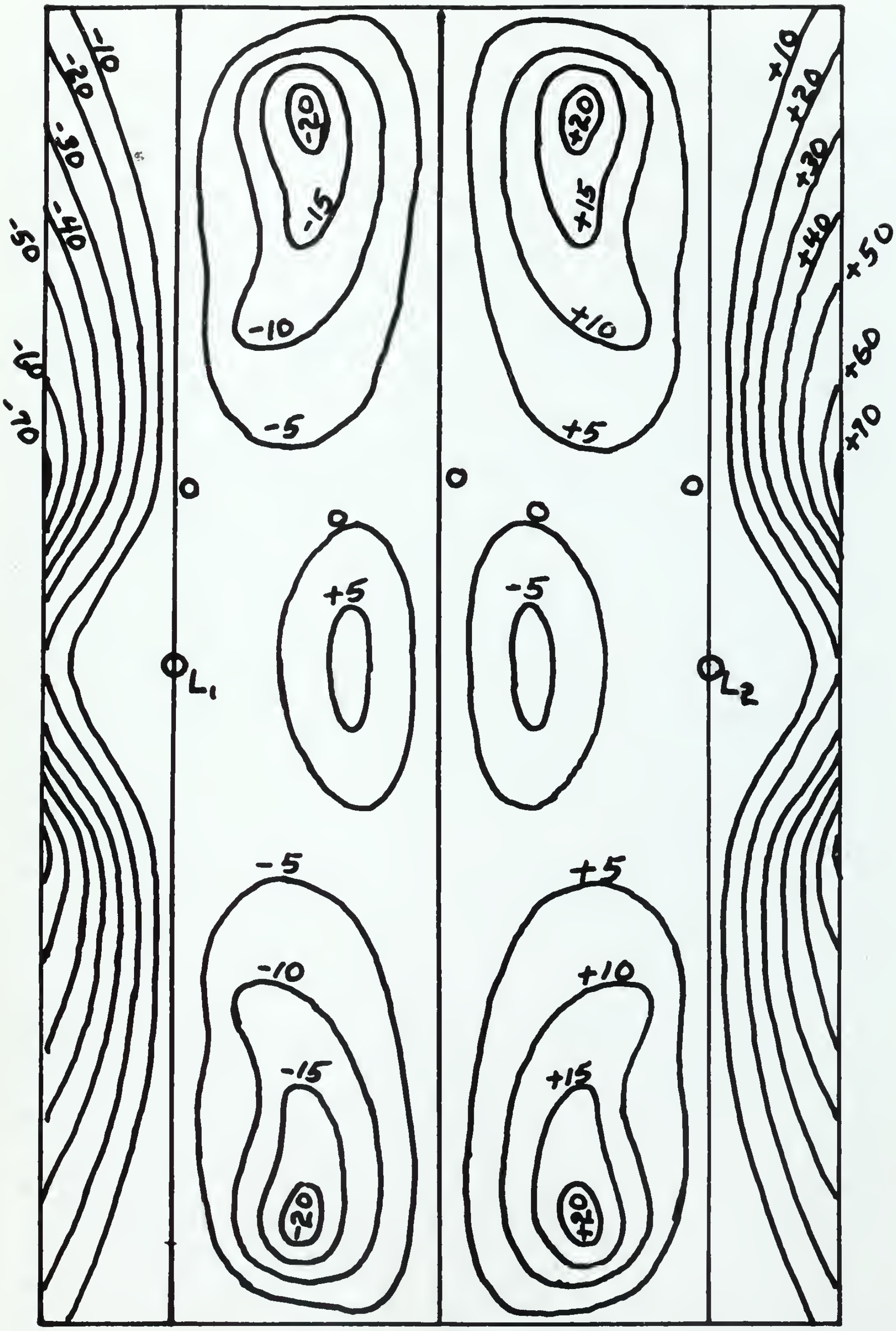

Figure 16

X-direction errors in centimeters
Stereo model formed with Average Lens

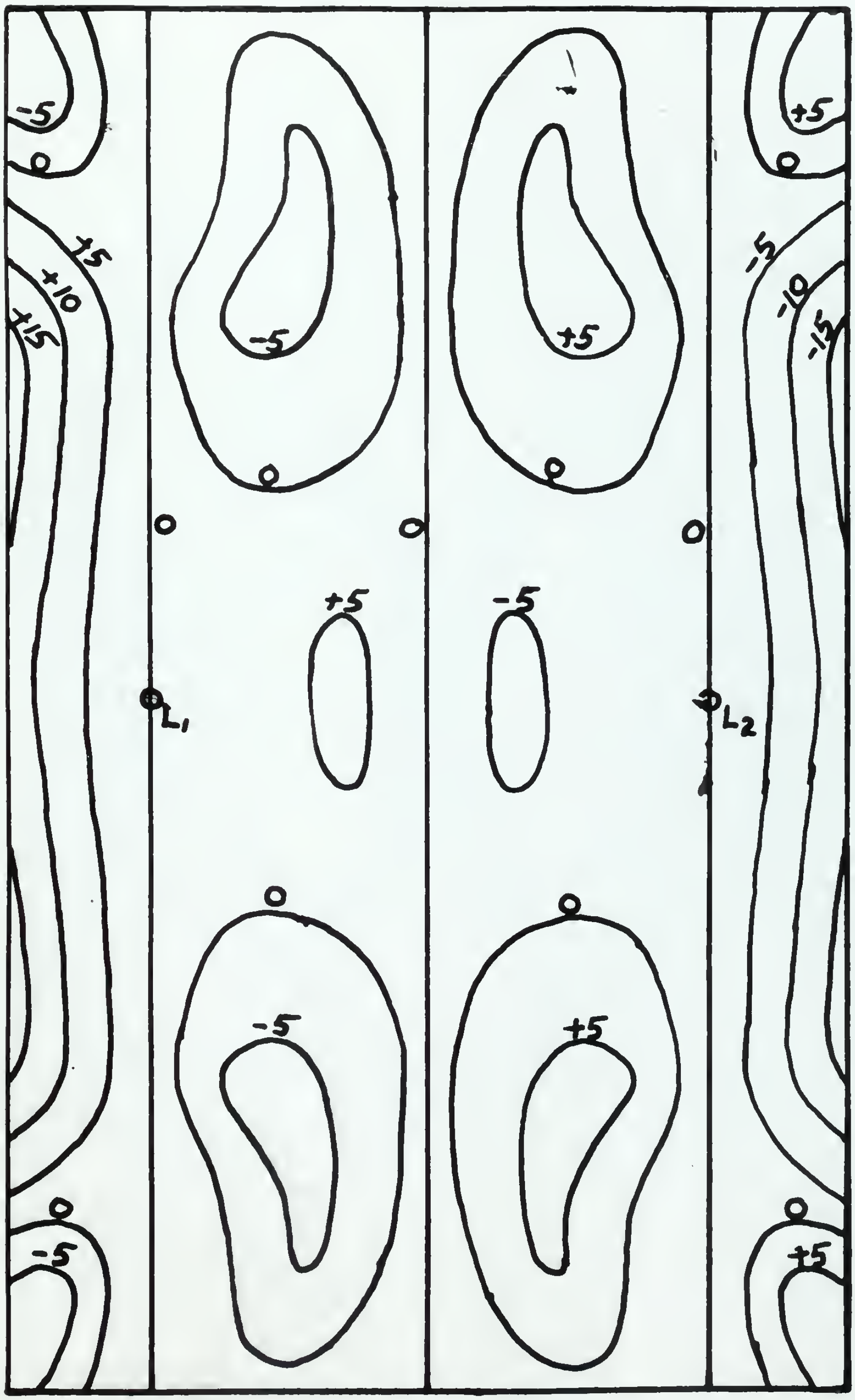

Figure 17

X-direction errors in centimeters
Stereo model formed with Lens #18

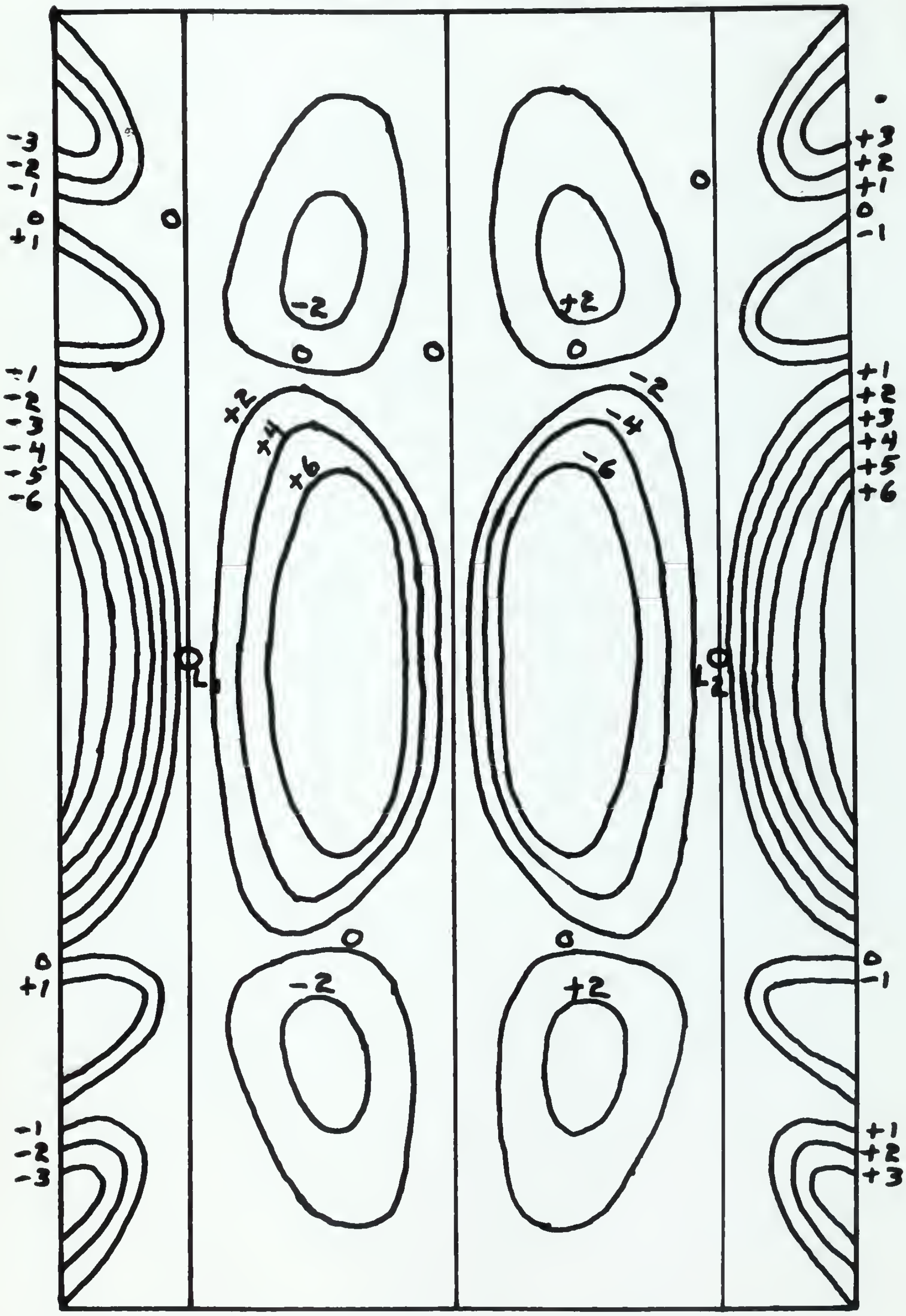

Figure 18

Elevation errors in meters
Stereo model formed with Lens #13

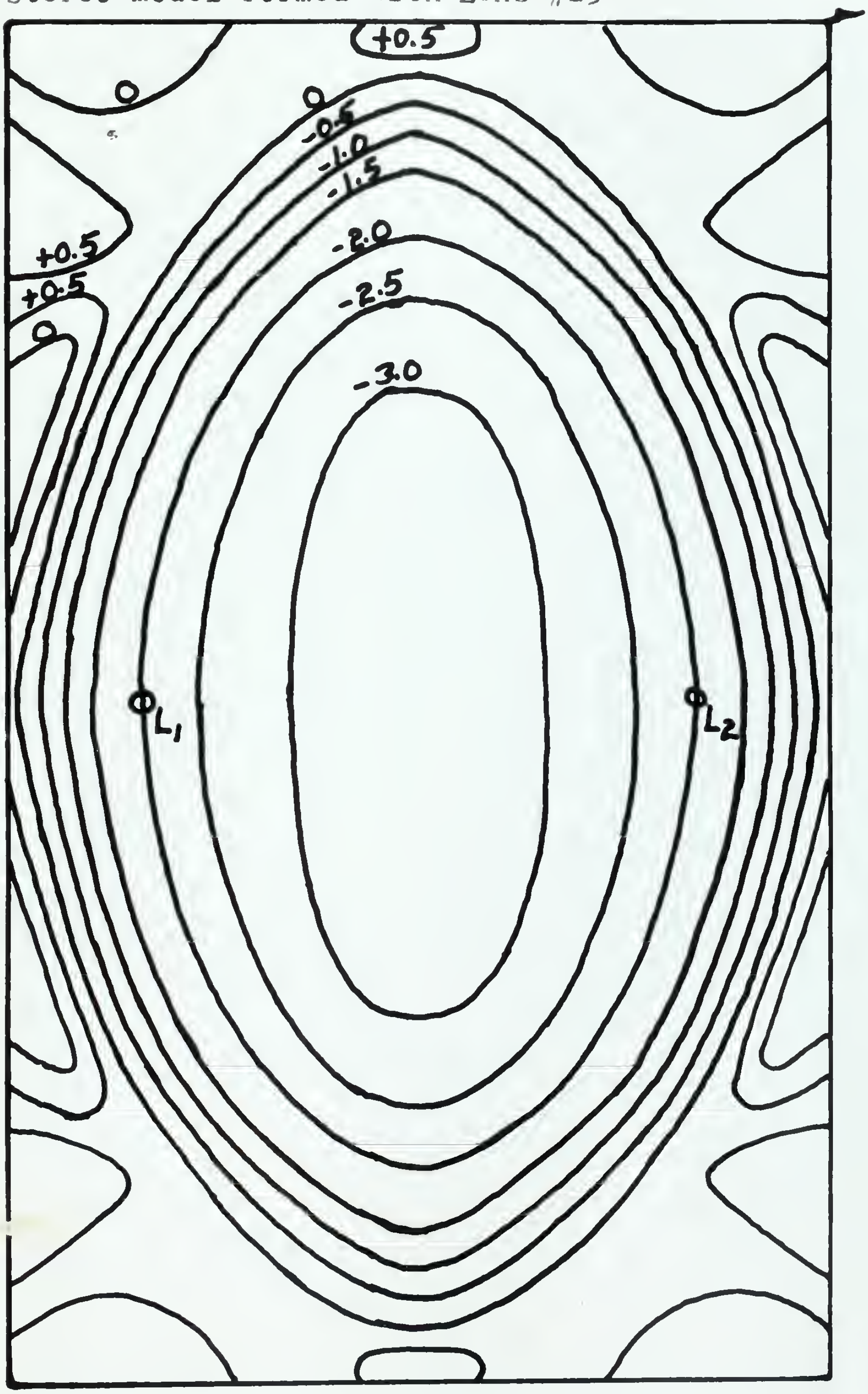

Figure 19

Elevation errors in meters
Stereo model formed with Average Lens

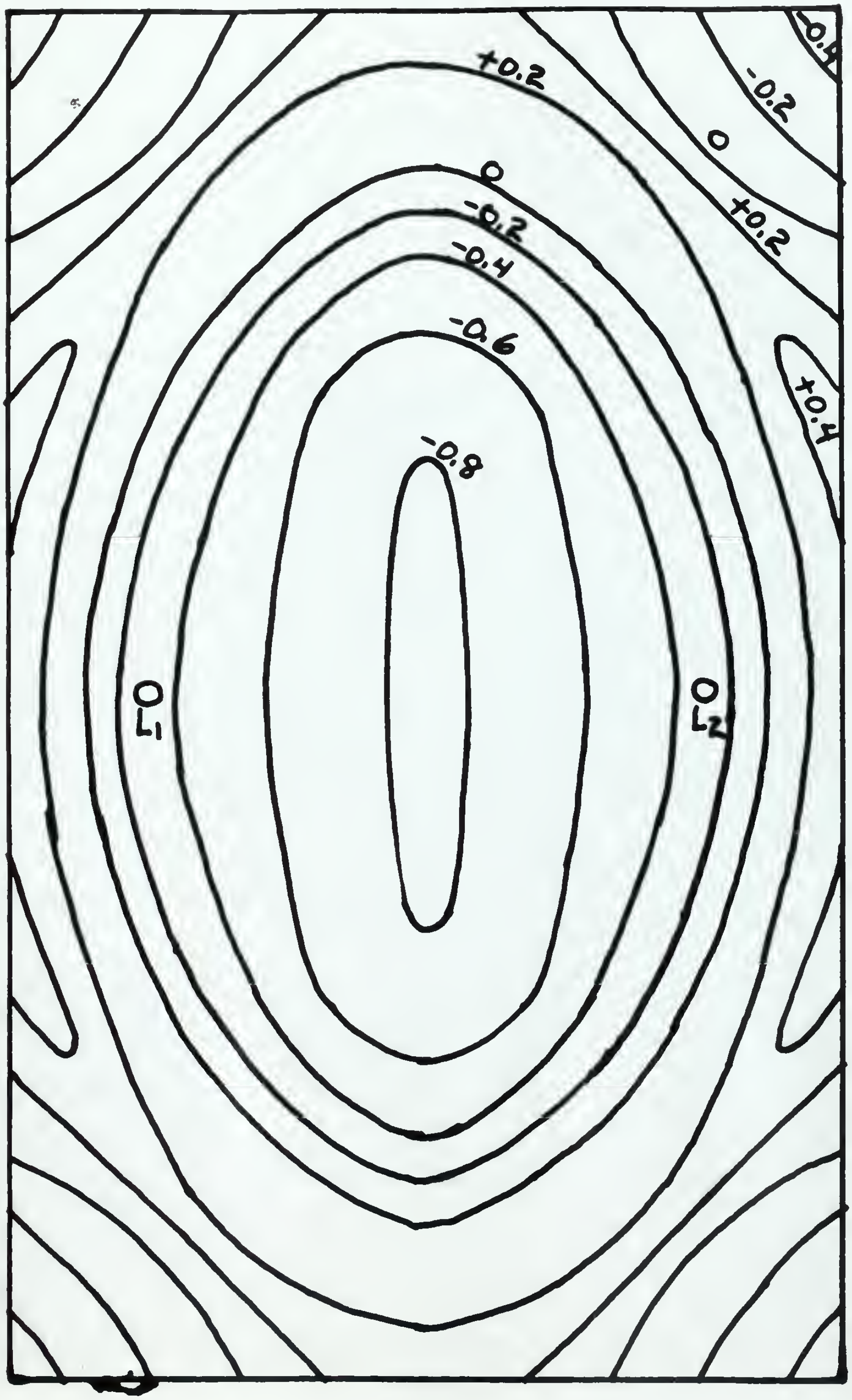

Figure 30

Elevation errors in meters
Stereo model formed with Lens #16

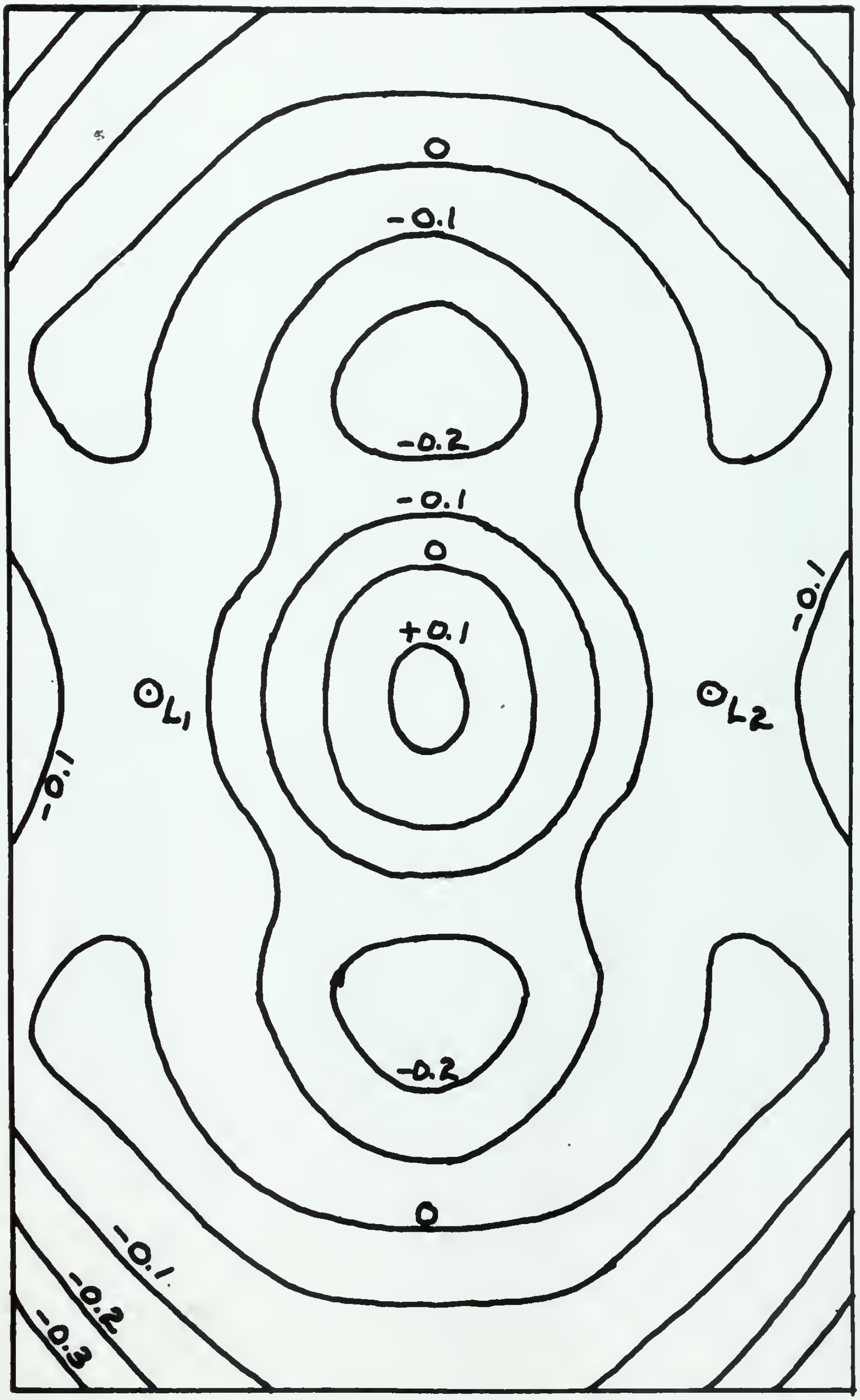

TABLE XXV

x (cm)	(x − b) (mm)	$\frac{(x-b)^2}{b}$ (mm)	2 + 4 (mm)	$\frac{x-b}{b}$ (mm)
− 9.85	−189.9	394.555	648.566	−2.0777
− 7.88	−170.2	316.929	570.940	−1.8621
−11.60	−207.4	470.611	724.622	−2.2691
− 9.19	−183.3	367.608	621.619	−2.0055
− 7.22	−163.6	292.828	546.839	−1.7899
− 5.65	−147.9	239.332	493.343	−1.6182
−10.51	−196.5	422.455	676.466	−2.1499
− 8.09	−172.3	324.803	578.814	−1.8851
− 6.14	−152.8	255.451	509.462	−1.6718
−11.67	−208.1	473.802	727.813	−2.2768
− 8.94	−180.8	357.640	611.651	−1.9781
− 6.55	−156.9	269.335	523.346	−1.7166
−11.32	−204.6	457.997	712.008	−2.2385
− 9.70	−188.4	388.349	642.360	−2.0613
− 7.00	−161.4	285.016	539.027	−1.7659
− 7.36	−165.0	297.875	551.886	−1.8053
−1.78	−109.2	130.461	384.472	−1.1947
−2.14	−112.8	139.206	393.217	−1.2341
0.56	− 85.8	80.540	334.551	−0.9387
2.18	− 69.6	53.000	307.011	−0.7615
−2.59	−117.3	150.543	404.554	−1.2834
−0.20	− 93.4	95.445	349.456	−1.0219
2.53	− 66.1	46.429	300.440	−0.7024
−3.00	−121.4	161.243	415.254	−1.3282
−1.05	−101.9	113.608	367.619	−1.1149
1.37	− 77.7	66.053	320.064	−0.8501
−3.49	−126.3	174.521	428.532	−1.3818
−1.92	−110.6	133.837	387.848	−1.2101
0.05	− 90.9	90.400	344.411	−0.9945
2.46	− 66.8	48.824	302.835	−0.7309
−1.26	−104.0	118.342	372.353	−1.1379
0.71	− 84.3	77.750	331.761	−0.9223

TABLE XXV—Continued

Lens 13 dh (m)	Ave.Lens dh (m)	Lens 18 dh (m)	Lens 13 e_2 (m)	Ave.Lens e_2 (m)	Lens 18 e_2 (m)
-18.00	1.22	2.05	16.46	-1.24	-2.05
-15.80	1.07	1.80	13.12	-1.62	-2.00
-20.19	1.37	2.30	19.64	-1.10	-2.30
-17.23	1.17	1.96	15.69	-1.19	-1.96
-15.12	1.02	1.72	12.44	-1.57	-1.92
-13.64	0.92	1.55	10.36	-1.72	-1.75
-18.80	1.27	2.14	18.25	-1.00	-2.14
-16.02	1.08	1.82	14.48	-1.10	-1.82
-14.08	0.95	1.60	11.40	-1.50	-1.80
-20.28	1.37	2.31	20.19	-1.49	-2.46
-16.94	1.15	1.93	16.39	-0.88	-1.93
-14.46	0.98	1.65	12.92	-1.00	-1.65
-19.82	1.34	2.26	19.63	-1.66	-2.50
-17.82	1.21	2.03	17.73	-1.33	-2.18
-14.90	1.01	1.70	14.35	-0.74	-1.70
-15.26	1.03	1.74	15.17	-1.15	-1.89
-10.72	0.73	1.22	10.17	-0.46	-1.22
-10.95	0.74	1.25	9.41	-0.76	-1.25
- 9.48	0.64	1.08	7.94	-0.66	-1.08
- 8.85	0.60	1.01	7.31	-0.62	-1.01
-11.25	0.76	1.28	8.57	-1.15	-1.48
- 9.84	0.67	1.12	7.16	-1.22	-1.32
- 8.72	0.59	0.99	6.04	-1.14	-1.19
-11.53	0.78	1.31	8.25	-1.58	-0.98
-10.30	0.70	1.17	7.02	-1.50	-1.37
- 9.14	0.62	1.04	5.86	-1.42	-1.24
-11.88	0.80	1.35	8.75	-1.38	-1.02
-10.81	0.73	1.23	7.68	-1.31	-0.90
- 9.72	0.67	1.11	6.59	-1.25	-0.78
- 8.76	0.59	1.00	5.63	-1.17	-0.67
-10.41	0.71	1.19	7.57	-1.25	-0.63
- 9.42	0.73	1.07	6.58	-1.27	-0.51

TABLE XXVI

x_{a_1} (cm)	x_{a_2} (cm)	y_a (cm)
-0.71	- 9.85	1.82
1.26	- 7.88	1.51
-2.46	-11.60	3.12
-0.05	- 9.19	4.00
1.92	- 7.22	3.52
3.49	- 5.65	2.00
-1.37	-10.51	5.83
1.05	- 8.09	5.90
3.00	- 6.14	5.19
-2.53	-11.67	7.58
0.20	- 8.94	8.00
2.59	- 6.55	7.59
-2.18	-11.32	9.77
-0.56	- 9.70	9.99
2.14	- 7.00	9.89
1.78	- 7.36	11.85
7.36	- 1.78	11.85
7.00	-2.14	9.89
9.70	0.56	9.99
11.32	2.18	9.77
6.55	- 2.59	7.59
8.94	- 0.20	8.00
11.67	2.53	7.58
6.14	- 3.00	5.19
8.09	- 1.05	5.90
10.51	1.37	5.83
5.65	- 3.49	2.00
7.22	-1.92	3.52
9.19	0.05	4.00
11.60	2.46	3.12
7.88	- 1.26	1.51
9.85	0.71	1.82

TABLE XXVI—Continued

Lens 13						
e_1 (m)	e_2 (m)	$e_1 - e_2$ (m)	py (microns)	dX" (m)	fdX''/x_{a_2} (m)	e_o (m)
-2.84	16.46	-19.30	- 87.8	0.961	-1.50	17.96
-2.84	13.12	-15.96	- 60.2	-1.128	2.20	10.92
-3.13	19.64	-22.77	-177.6	4.624	-6.13	25.77
-3.13	15.69	-18.82	-188.2	0.062	-0.10	15.79
-3.13	12.44	-15.57	-137.1	-1.536	3.27	9.17
-3.13	10.36	-13.49	- 67.5	-1.893	5.15	5.21
-3.28	18.25	-21.53	-313.8	2.206	-3.23	21.48
-3.28	14.48	-17.76	-261.9	-1.074	2.04	12.44
-3.28	11.40	-14.68	-190.5	-1.924	4.82	6.58
-2.68	20.19	-22.87	-433.4	4.805	-1.53	21.72
-2.68	16.39	-19.07	-381.4	-0.243	0.42	15.97
-2.68	12.92	-15.60	-296.0	-1.883	4.42	8.50
-1.54	19.63	-21.17	-517.1	3.718	-5.05	24.68
-1.54	17.73	-19.27	-481.3	0.745	-1.18	18.91
-1.54	14.35	-15.89	-392.9	-1.694	3.72	10.63
0.55	15.17	-15.72	-465.7	-1.465	3.06	12.11
-0.09	10.17	-10.26	-303.9	-0.956	8.26	1.91
0.55	9.41	- 8.86	-219.1	-0.944	6.78	2.63
-0.09	7.94	- 8.03	-200.5	0.310	8.51	-0.57
0.19	7.31	- 7.12	-173.9	1.250	8.82	-1.51
-1.54	8.57	-10.11	-191.8	-1.220	7.24	1.33
0.55	7.16	- 6.61	-132.2	-0.084	6.46	0.70
-0.09	6.04	- 6.13	-116.2	1.288	7.83	-1.79
-2.68	8.25	-10.93	-141.8	-1.433	7.34	0.91
-1.54	7.02	- 8.56	-126.3	-0.517	7.57	-0.55
0.55	5.86	- 5.31	- 77.4	0.544	6.11	-0.25
-3.28	8.75	-12.03	- 60.2	-1.688	7.44	1.31
-2.68	7.68	-10.36	- 91.2	-1.022	8.18	-0.50
-1.54	6.59	- 8.13	- 81.3	0.027	8.30	-1.71
0.55	5.63	- 5.08	- 39.6	1.032	6.45	-0.82
-2.68	7.57	-10.25	- 38.7	-0.724	8.83	-1.26
-1.54	6.58	- 8.12	- 36.9	0.404	8.75	-2.17

TABLE XXVI—Continued

Lens 18						
e_1 (m)	e_2 (m)	e_1-e_2 (m)	py (microns)	dX" (m)	$f\delta X''/x_{a_2}$ (m)	e_o (m)
0.56	−2.05	2.61	11.9	−0.130	0.20	−2.25
0.56	−2.00	2.56	9.7	0.181	−0.35	−1.65
0.33	−2.30	2.63	20.5	−0.534	0.71	−3.01
0.33	−1.96	2.29	22.9	−0.007	0.01	−1.97
0.33	−1.92	2.15	18.9	0.212	−0.45	−1.47
0.33	−1.75	2.08	10.4	0.292	−0.79	−0.96
0.20	−2.14	2.34	34.1	−0.240	0.35	−2.49
0.20	−1.82	2.02	29.8	0.122	−0.23	−1.59
0.20	−1.80	2.00	26.0	0.262	−0.66	−1.14
0.20	−2.46	2.66	50.4	−0.559	0.74	−3.20
0.20	−1.93	2.13	42.6	0.027	−0.05	−1.88
0.20	−1.65	1.85	35.1	0.223	−0.52	−1.13
0	−2.50	2.50	61.1	−0.439	0.60	−3.10
0	−2.18	2.18	54.4	−0.084	0.13	−2.31
0	−1.70	1.70	42.0	0.184	−0.40	−1.30
0	−1.89	1.89	56.0	0.176	−0.37	−1.52
−0.15	−1.22	1.07	31.7	0.100	−0.86	−0.36
0	−1.25	1.25	30.9	0.133	−0.95	−0.30
−0.15	−1.08	0.93	23.2	−0.036	−0.99	−0.09
−0.24	−1.01	0.77	18.8	−0.135	−0.95	−0.06
0	−1.48	1.48	28.1	0.179	−1.06	−0.42
0	−1.32	1.32	26.4	0.017	−1.31	−0.01
−0.15	−1.19	1.04	19.7	−0.219	−1.33	0.14
−0.20	−0.98	0.78	10.1	0.102	−0.52	−0.46
0	−1.37	1.37	20.2	0.083	−1.21	−0.16
0	−1.24	1.24	18.1	−0.127	−1.42	0.18
−0.20	−1.02	0.82	4.1	0.115	−0.51	−0.51
−0.20	−0.90	0.70	6.2	0.069	−0.55	−0.35
0	−0.78	0.78	7.8	−0.003	−0.92	0.14
0	−0.67	0.67	5.2	−0.136	−0.85	0.18
−0.20	−0.63	0.43	1.6	0.030	−0.37	−0.26
0	−0.51	0.51	2.3	−0.001	−0.02	−0.49

TABLE XXVI—Continued

Average						
e_1 (m)	e_2 (m)	e_1-e_2 (m)	py (microns)	dX" (m)	fdX"/x_{a_2} (m)	e_c (m)
-0.54	-1.24	0.70	3.2	-0.035	0.05	-1.29
-0.54	-1.62	1.08	4.1	0.076	-0.15	-1.47
-0.58	-1.10	0.52	4.1	-0.106	0.14	-1.24
-0.58	-1.19	0.61	6.1	-0.002	0	-1.19
-0.58	-1.57	0.99	8.7	0.098	-0.21	-1.36
-0.58	-1.72	1.14	5.7	0.160	-0.43	-1.29
-0.80	-1.00	0.20	2.9	-0.021	0.03	-1.03
-0.80	-1.10	0.30	4.4	0.018	-0.03	-1.07
-0.80	-1.50	0.70	9.1	0.092	-0.23	-1.27
-0.55	-1.49	0.94	17.8	-0.198	0.26	-1.75
-0.55	-0.88	0.33	6.6	0.004	-0.01	-0.87
-0.55	-1.00	0.45	8.5	0.054	-0.13	-0.87
-0.02	-1.66	1.64	40.1	-0.289	0.39	-2.05
-0.02	-1.33	1.31	32.7	-0.051	0.08	-1.41
-0.02	-0.74	0.72	17.8	0.078	-0.17	-0.57
0.27	-1.15	1.42	42.1	0.133	-0.28	-0.87
-0.12	-0.46	0.34	10.1	0.032	-0.28	-0.18
0.27	-0.76	1.03	25.5	0.110	-0.79	0.03
-0.12	-0.66	0.54	13.5	-0.021	-0.58	-0.08
-0.32	-0.62	0.30	7.3	-0.053	-0.37	-0.25
-0.02	-1.15	1.13	21.4	0.137	-0.81	-0.31
0.27	-1.22	1.49	29.8	0.019	-1.46	0.24
-0.12	-1.14	1.02	19.3	-0.215	-1.30	0.16
-0.55	-1.58	1.03	13.4	0.135	-0.69	-0.89
-0.02	-1.50	1.48	21.8	0.090	-1.32	-0.18
0.27	-1.42	1.69	24.6	-0.174	-1.95	0.53
-0.80	-1.38	0.58	2.9	0.082	-0.36	-1.02
-0.55	-1.31	0.76	6.7	0.075	-0.60	-0.71
-0.02	-1.25	1.23	12.3	-0.004	-1.23	-0.02
0.27	-1.17	1.44	11.2	-0.293	-1.83	0.66
-0.55	-1.25	0.70	2.6	0.050	-0.61	-0.64
-0.02	-1.27	1.25	5.7	-0.062	-1.34	0.07

Figure 21

Y-Parallax in microns
Model formed with lens 13

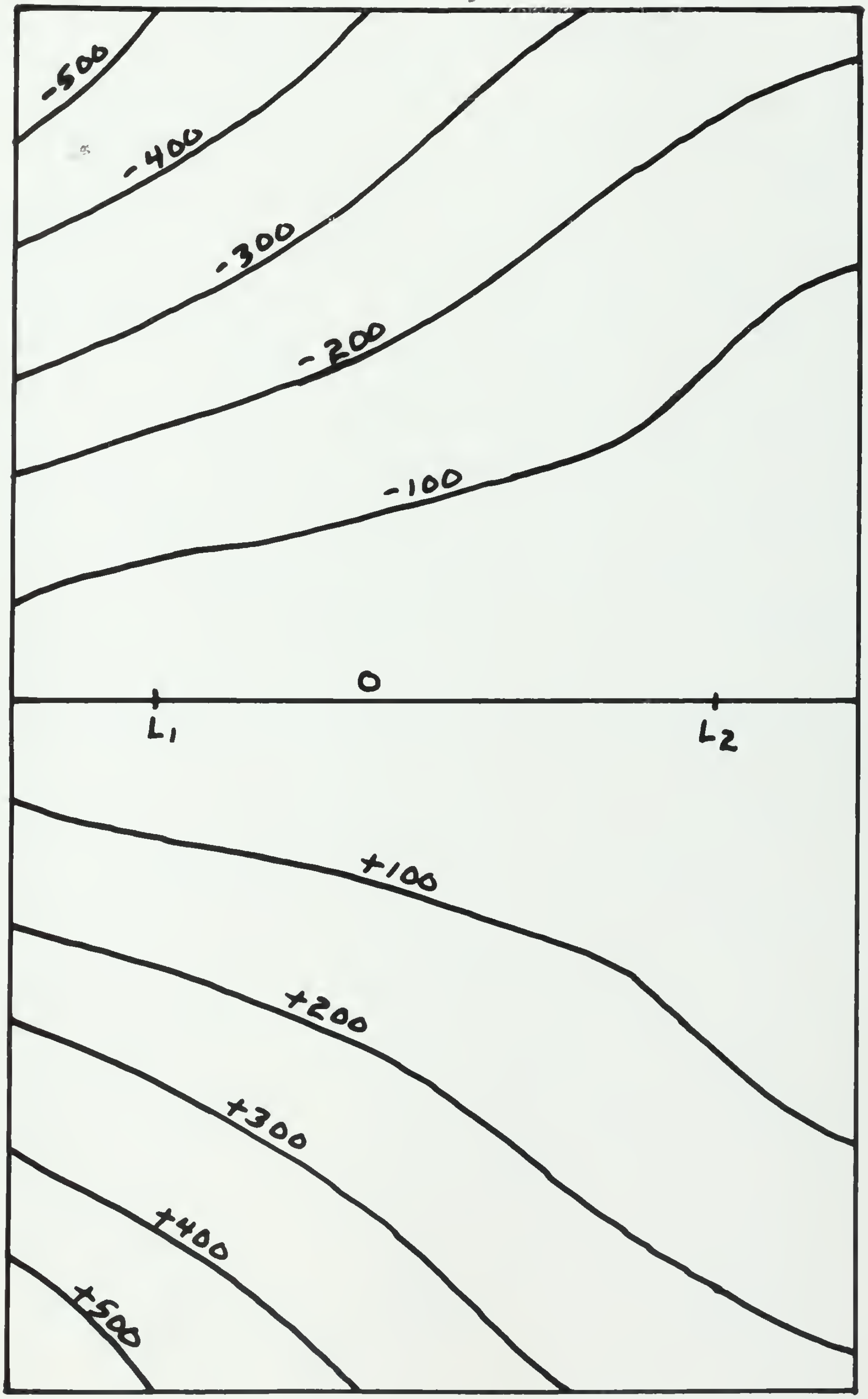

Figure 22

Y-Parallax in microns
Model formed with the average lens

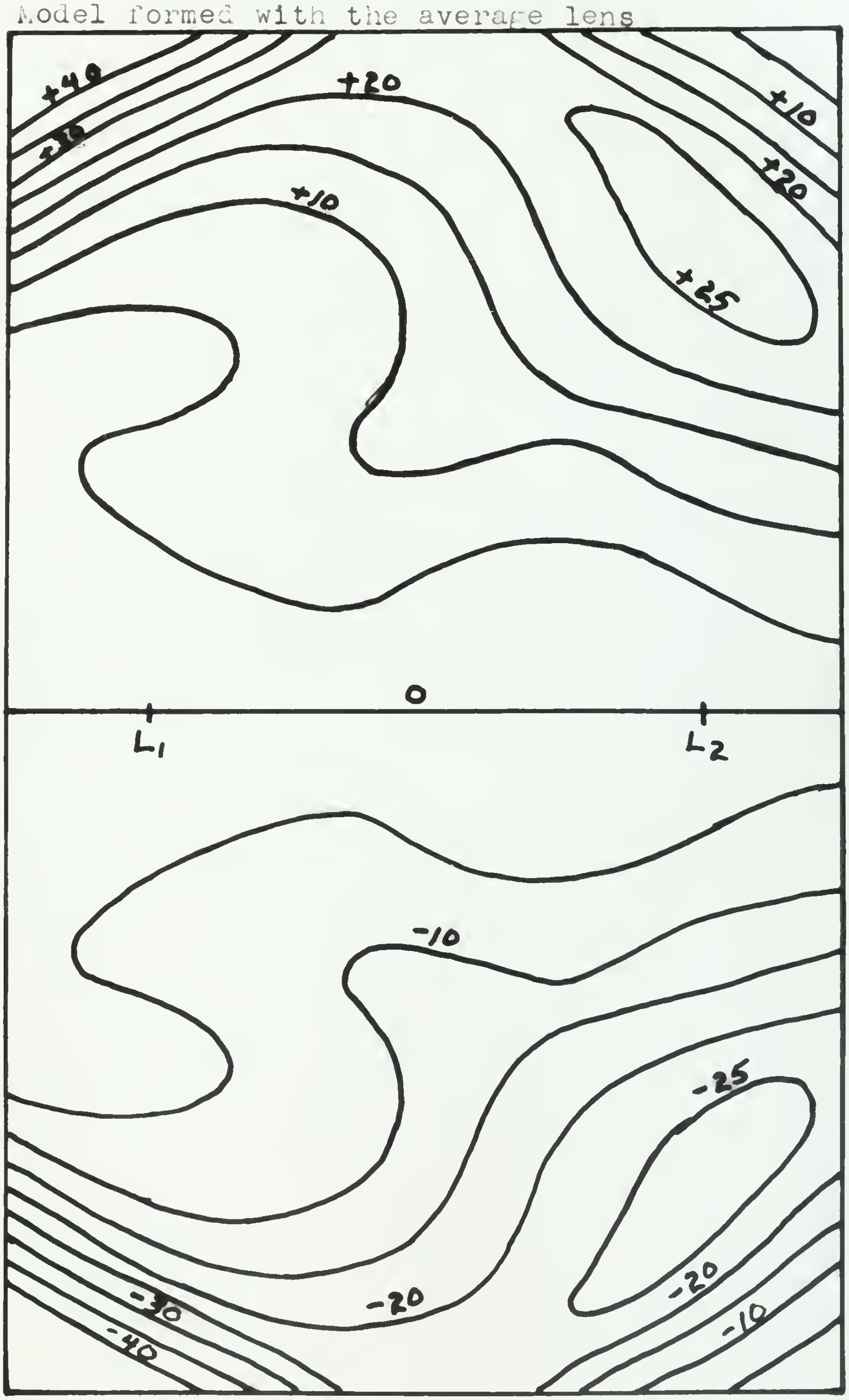

Figure 23

Y-Parallax in microns
Model formed with lens 1(

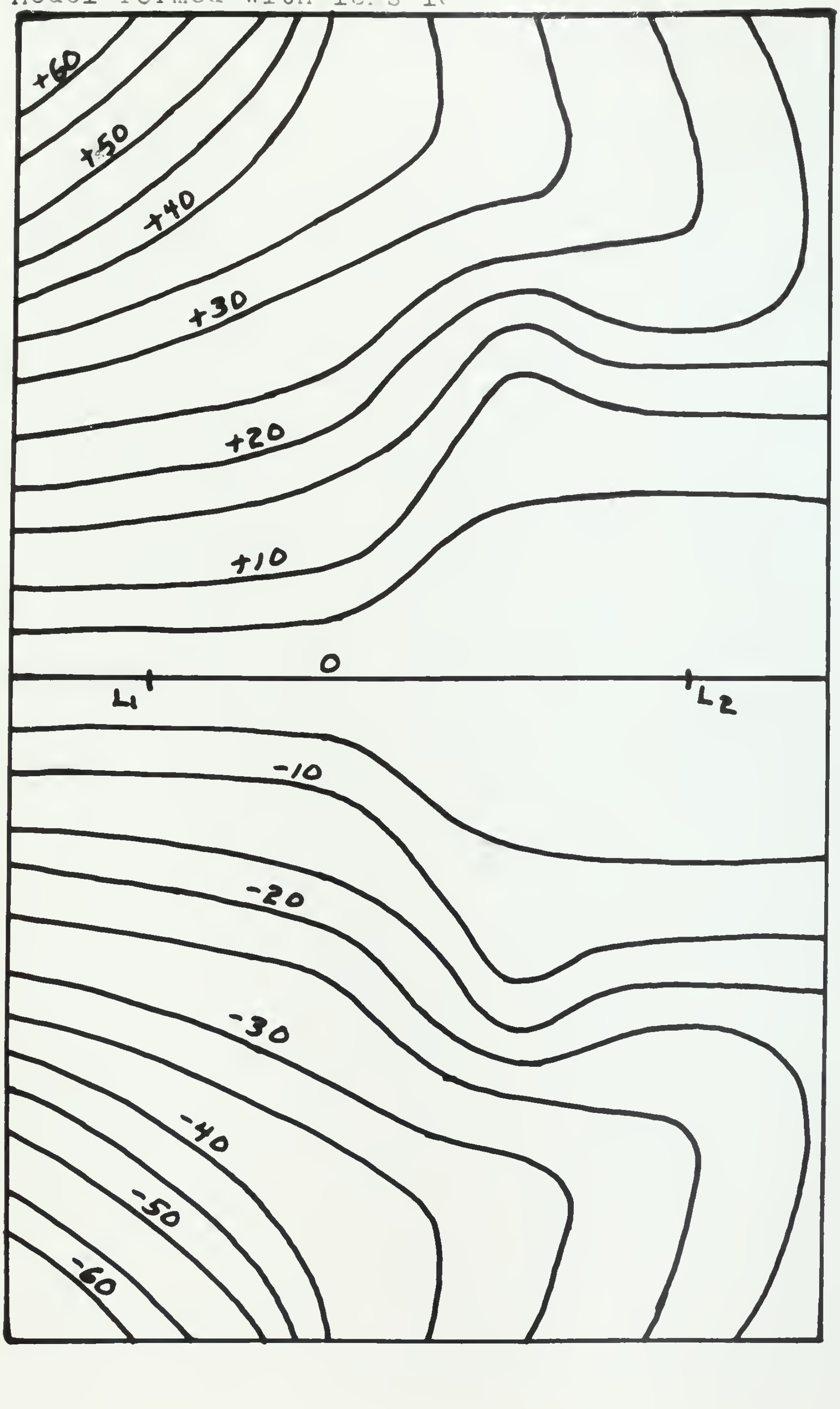

Figure 24

X-direction errors in meters
Model formed with lens 13

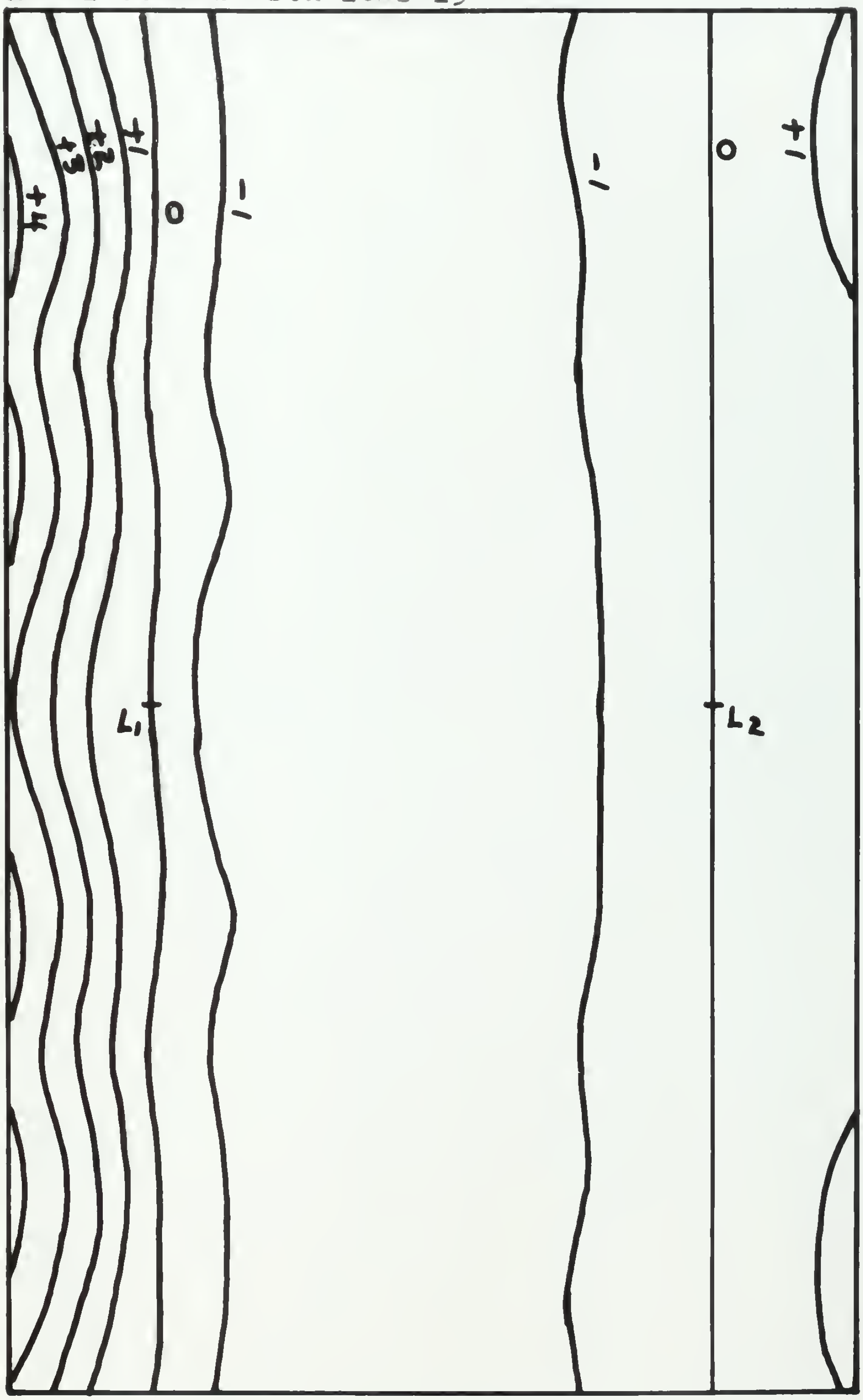

Figure 25

X-direction errors in centimeters
Model formed with the average lens

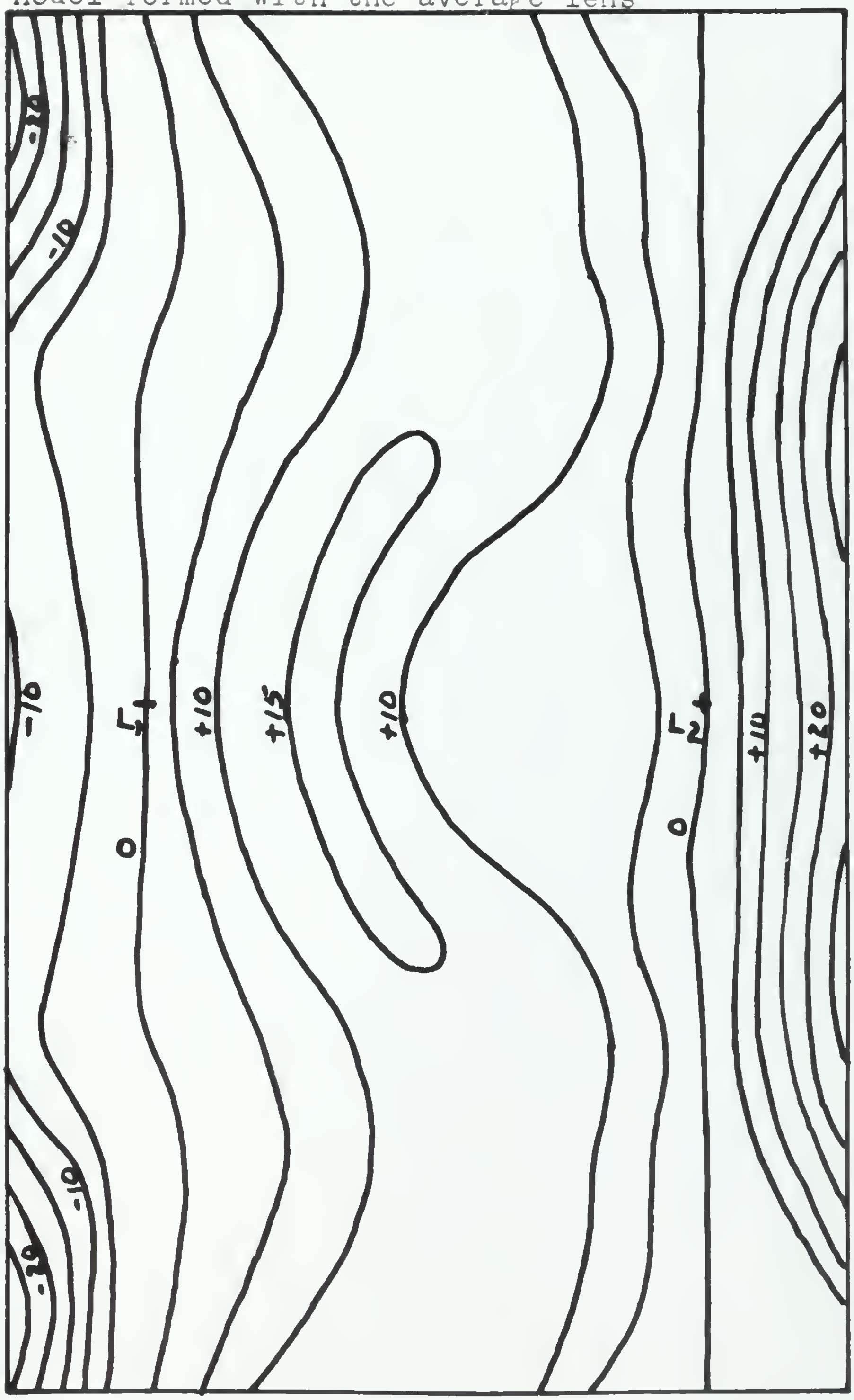

Figure 26

X-direction errors in centimeters
Model formed with lens 18

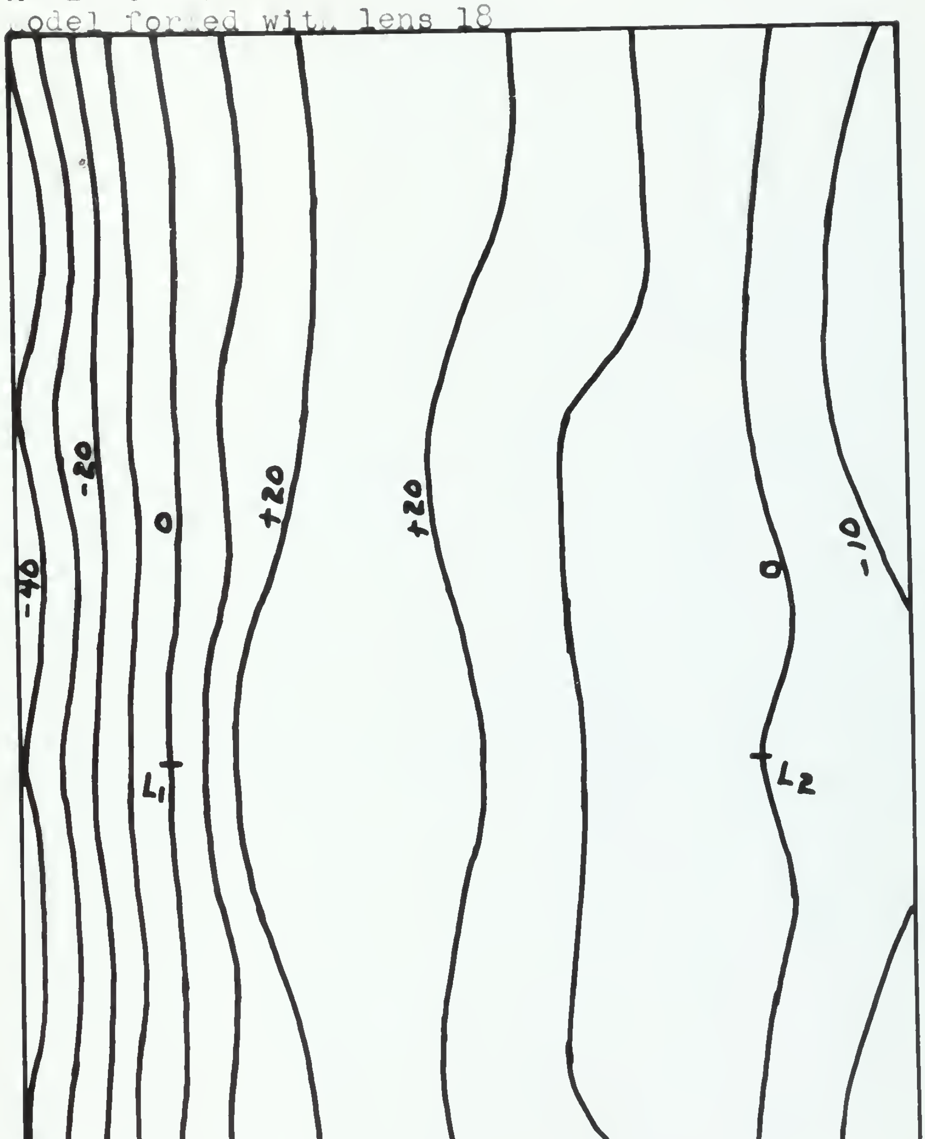

Figure 27

Elevation errors in meters
Model formed with lens 13

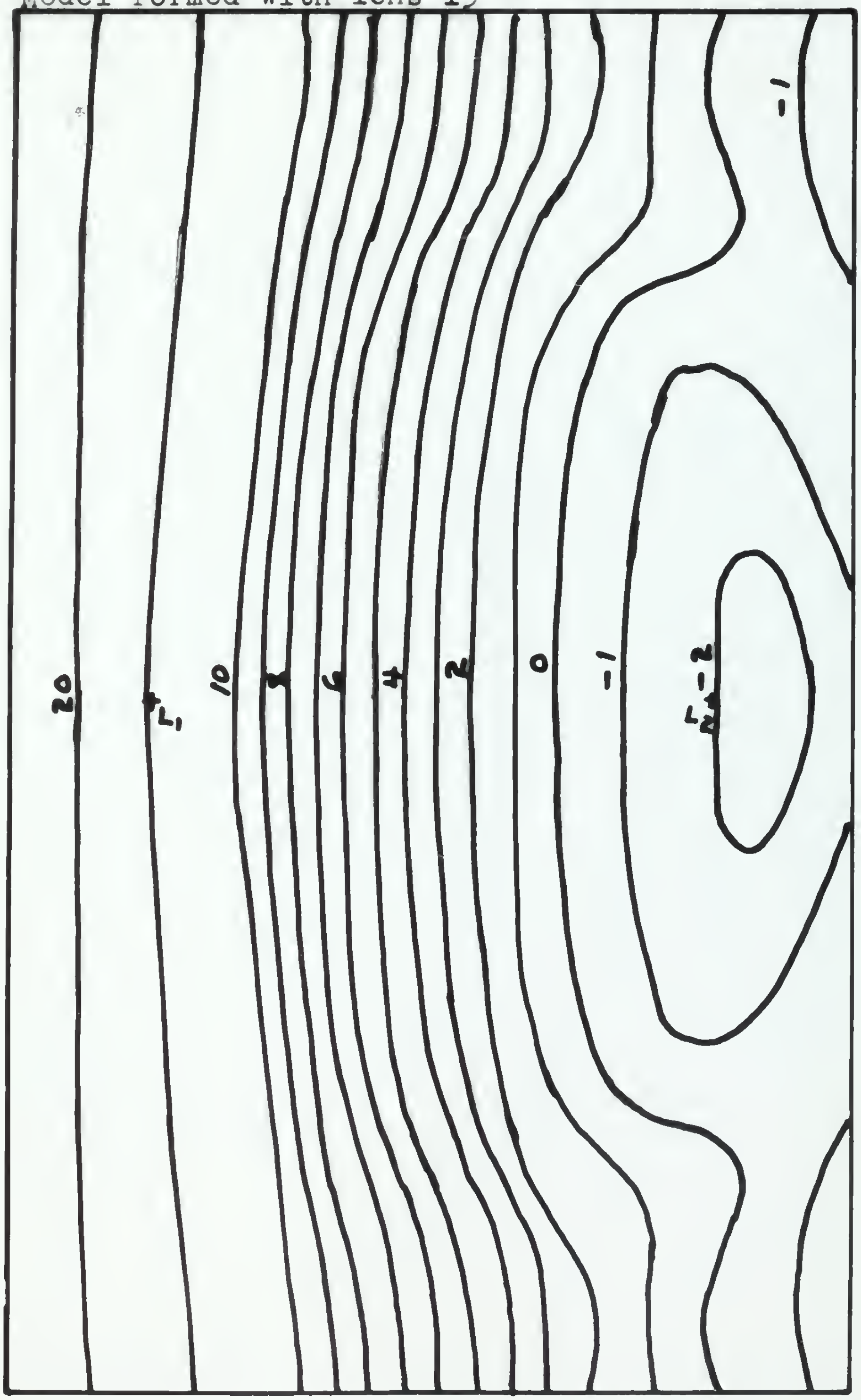

Figure 28

Elevation errors in meters
Model formed with the average lens

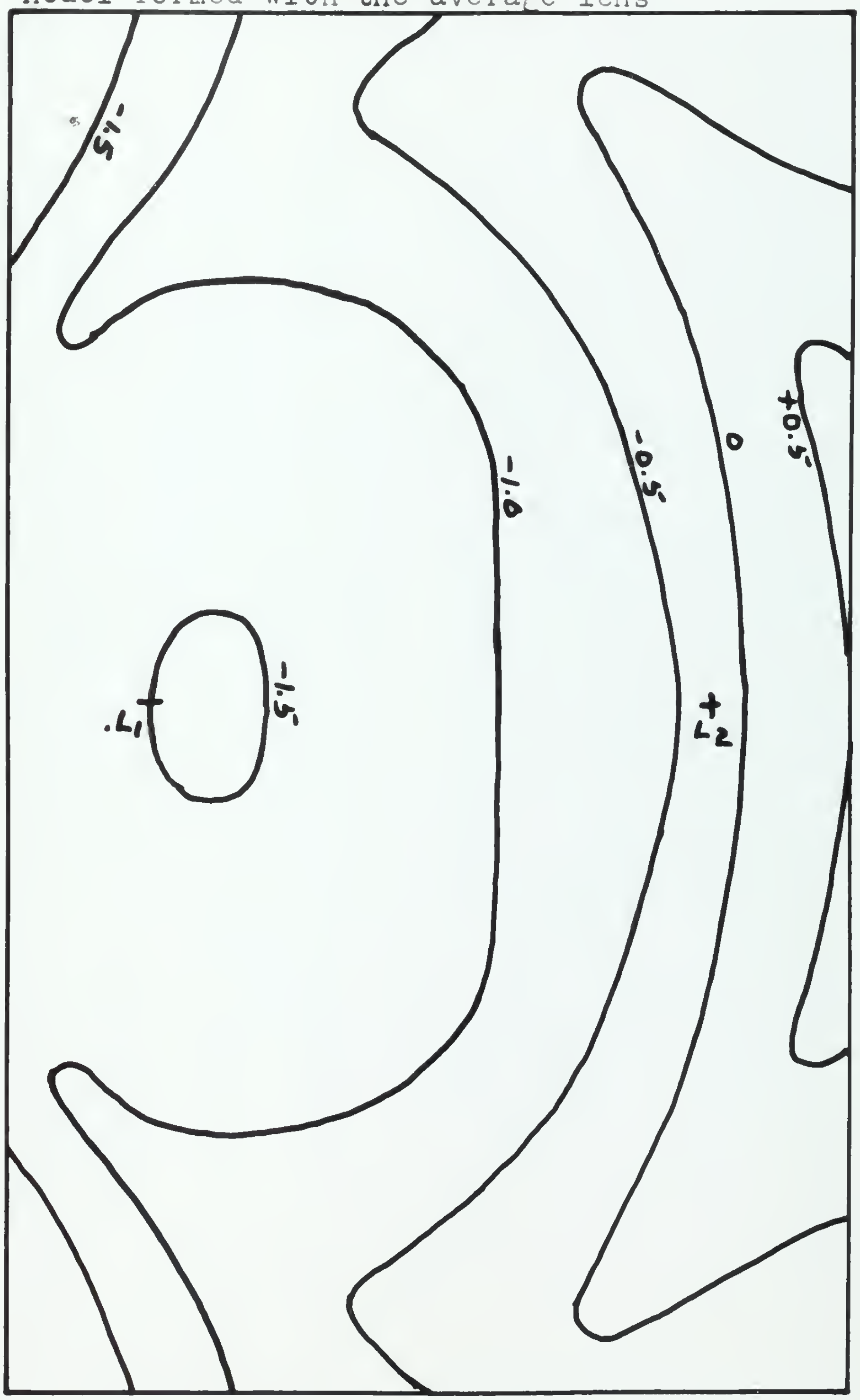

Figure 29

Elevation errors in meters
Model formed with lens 18

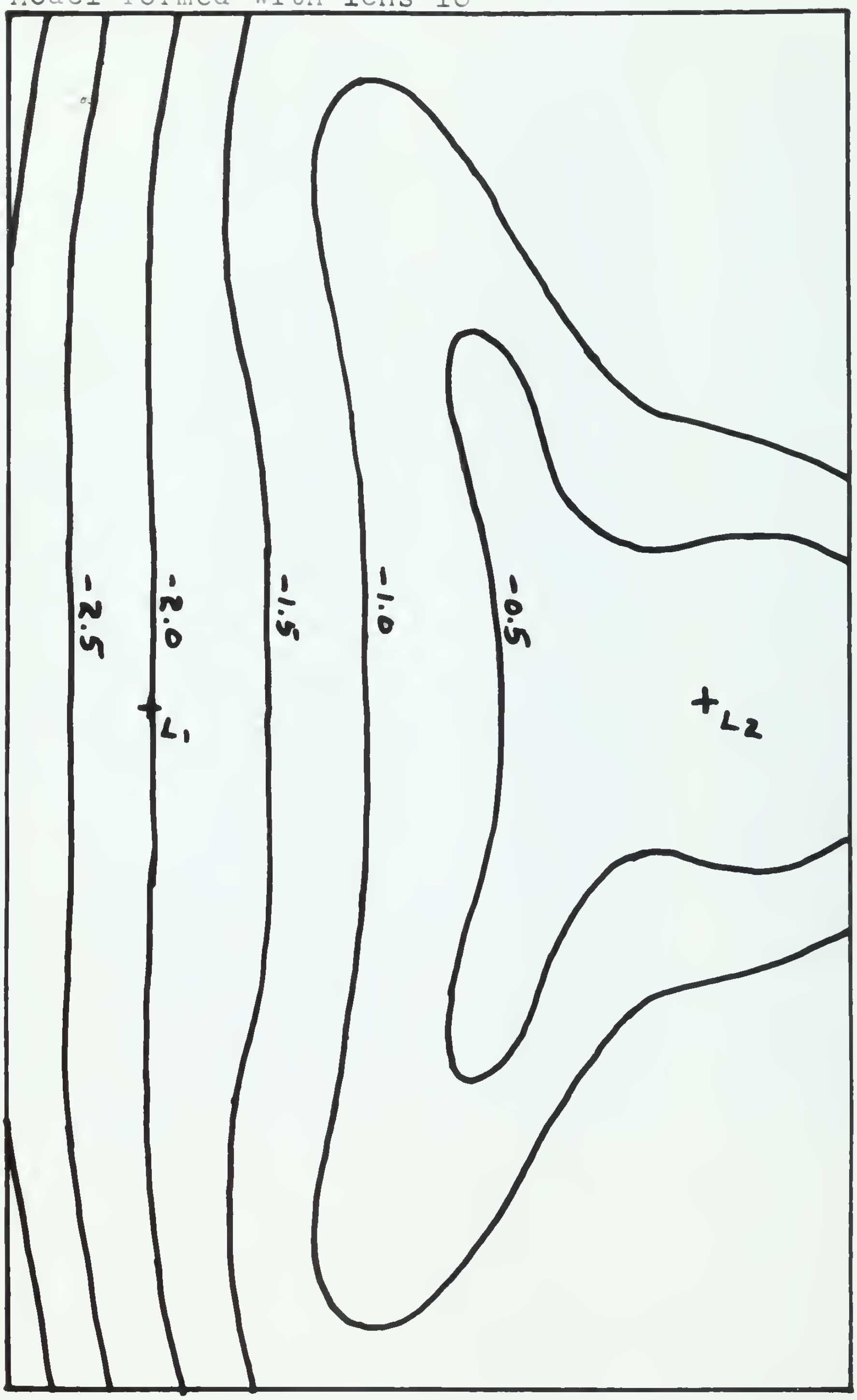

TABLE XXVII

	Given in Feet		
	X(E)	Y(N)	Z
Sprow	1,593,463.81	604,404.94	684.8
Garner	1,593,451.33	603,023.15	686.2
Albert	1,594,756.93	603,076.95	685.3
Hoof	1,593,453.70	601,744.91	686.5
Weasel	1,593,375.11	600,236.17	694.5
Sarah	1,593,442.88	599,093.65	692.0
Young	1,594,738.14	599,159.21	692.3
School	1,593,438.27	597,797.52	693.0
Seigfred	1,593,421.23	595,098.23	692.4
Gentes	1,593,406.32	593,761.58	693.7
Dickmander	1,596,071.06	597,814.30	690.1
Froese	1,597,404.30	597,760.06	690.1
Hastedt	1,598,651.10	593,773.10	694.5
John	1,598,740.74	595,063.89	692.3
Field	1,598,749.86	596,380.53	691.6
Fickle	1,598,754.96	597,752.22	690.6
Bickmeier	1,600,361.16	597,694.69	693.4
Alvah	1,601,378.97	597,752.70	691.8
Austin	1,598,690.78	598,893.28	689.2
Rich	1,598,810.24	600,368.86	687.1
Thompson	1,598,758.48	601,701.38	685.9
Richard	1,598,684.02	603,122.47	685.4
Florence	1,598,786.36	604,340.80	687.0
Blue	1,602,746.73	602,984.10	684.8
Meyers	1,604,049.62	604,317.81	683.9
R-116	1,604,103.93	603,038.92	684.9
Rowland	1,604,025.50	601,508.11	685.5
Fuller	1,604,018.30	600,357.58	686.7
Father	1,602,719.26	599,039.58	688.6
Hasko	1,604,065.99	595,788.10	691.8
Winner	1,603,997.86	594,194.80	695.7
Hoskinson	1,609,391.79	600,332.56	686.9
Lange	1,593,421.79	596,401.23	693.4

TABLE XXVII—Continued

Observed			Observed at Ground Scale in Feet	
X(E) (mm)	Y(E) (mm)	Z (ft)	E	N
808.66	1,284.24	685.1	42,133.86	26,530.84
766.57	1,283.41	684.6	42,106.63	25,149.94
769.43	1,243.66	685.1	40,802.49	25,243.77
727.62	1,282.13	685.1	42,064.63	23,872.05
681.60	1,283.16	693.1	42,098.43	22,362.21
646.83	1,280.13	688.3	41,999.02	21,221.46
650.02	1,240.74	688.8	40,706.69	21,326.12
607.32	1,279.12	686.1	41,965.88	19,925.20
525.00	1,277.16	682.8	41,901.58	17,224.41
484.26	1,276.47	684.3	41,878.94	15,887.80
610.23	1,198.90	687.7	39,333.99	20,020.67
609.75	1,158.27	689.5	38,000.99	20,004.92
489.37	1,116.75	674.2	36,638.78	16,055.45
528.84	1,115.10	695.3	36,584.65	17,350.39
568.98	1,116.03	694.5	36,615.16	18,667.32
610.77	1,117.10	694.3	36,650.26	20,038.39
610.52	1,068.17	697.2	35,044.95	20,030.18
613.19	1,037.23	695.7	34,029.86	20,117.78
645.50	1,120.08	689.3	36,748.03	21,177.82
690.60	1,117.82	686.4	36,673.89	22,657.48
731.11	1,120.60	686.7	36,765.09	23,986.55
774.38	1,124.12	684.2	36,880.58	25,406.17
811.58	1,122.16	683.7	36,816.27	26,626.64
773.90	1,000.33	686.3	32,819.23	25,390.42
815.72	961.80	681.5	31,555.12	26,762.47
776.80	959.03	686.8	31,464.24	25,485.57
730.07	959.97	684.5	31,495.08	23,952.43
695.00	959.15	685.3	31,468.18	22,801.84
653.66	997.54	690.5	32,727.69	21,445.54
555.80	953.61	699.3	31,286.42	18,234.91
507.26	954.28	707.3	31,308.40	16,642.39
699.12	795.45	689.8	26,097.44	22,937.01
564.70	1,278.31	689.2	41,939.31	18,526.90

TABLE XXVII—Continued

Observed at Given Origin		Observed at Local Origin	
E	N	E	N
1,593,304.95	604,246.30	-5,385.83	5,353.02
1,593,332.18	602,865.40	-5,358.60	3,972.12
1,594,636.32	602,959.23	-4,054.46	4,065.95
1,593,374.18	601,587.51	-5,316.60	2,694.23
1,593,340.38	600,077.67	-5,350.40	1,184.39
1,593,439.79	598,936.92	-5,250.99	43.64
1,594,732.12	599,041.58	-3,958.66	148.30
1,593,472.93	597,640.66	-5,217.85	-1,252.62
1,593,537.23	594,939.87	-5,153.55	-3,953.41
1,593,559.87	593,603.26	-5,130.91	-5,290.02
1,596,104.82	597,736.13	-2,585.96	-1,157.15
1,597,437.82	597,720.38	-1,252.96	-1,172.90
1,598,800.03	593,770.91	109.25	-5,122.37
1,598,854.16	595,065.85	163.38	-3,827.43
1,598,823.65	596,382.78	132.87	-2,510.50
1,598,788.55	597,753.85	97.77	-1,139.43
1,600,393.86	597,745.64	1,703.08	-1,147.64
1,601,408.95	597,833.24	2,718.17	-1,060.04
1,598,690.78	598,893.28	0	0
1,598,764.92	600,372.94	74.14	1,479.66
1,598,673.72	601,702.01	- 17.06	2,808.73
1,598,558.23	603,121.63	- 132.55	4,228.35
1,598,620.54	604,342.10	- 70.24	5,448.82
1,602,619.58	603,105.88	3,928.80	4,212.60
1,603,883.69	604,477.93	5,192.91	5,584.65
1,603,974.57	603,201.03	5,283.79	4,307.75
1,603,943.73	601,667.89	5,252.95	2,774.61
1,603,970.63	600,517.30	5,279.85	1,624.02
1,602,711.12	599,161.00	4,020.34	267.72
1,604,152.39	595,950.37	5,461.61	-2,942.91
1,604,130.41	594,357.85	5,439.63	-4,535.43
1,609,341.37	600,652.47	10,650.59	1,759.19
1,593,499.50	596,242.36	-5,191.28	-2,650.92

TABLE XXVII—Continued

Corrected Local Coordinates		Corrected Observed Coordinates	
E	N	E	N
-5,222.98	5,511.13	1,593,467.80	604,404.41
-5,237.02	4,130.15	1,593,453.76	603,023.43
-3,930.77	4,184.95	1,594,760.01	603,078.23
-5,233.23	2,851.69	1,593,457.55	601,744.97
-5,312.14	1,343.67	1,593,378.64	600,236.95
-5,246.88	200.55	1,593,443.90	599,093.83
-3,952.11	266.53	1,594,738.67	599,159.81
-5,250.49	-1,096.00	1,593,440.29	597,797.28
-5,268.95	-3,797.27	1,593,421.83	595,096.01
-5,286.27	-5,133.84	1,593,404.51	593,759.44
-2,888.15	-1,079.24	1,595,802.63	597,814.04
-1,287.34	-1,134.83	1,597,403.44	597,758.45
- 43.90	-5,122.90	1,598,646.88	593,770.38
48.90	-3,830.27	1,598,739.68	595,063.01
57.77	-2,513.13	1,598,748.55	596,380.15
63.66	-1,141.74	1,598,754.44	597,751.54
1,667.87	-1,182.60	1,600,358.65	597,710.68
2,685.04	-1,140.71	1,601,375.82	597,752.57
0	0	1,598,690.78	598,893.28
118.32	1,476.65	1,598,809.10	600,369.93
66.89	2,807.74	1,598,757.67	601,701.02
- 6.11	4,230.05	1,598,684.67	603,123.33
92.65	5,448.01	1,598,783.43	604,341.29
4,052.60	4,092.93	1,602,743.38	602,986.21
5,357.04	5,426.46	1,604,047.82	604,319.74
5,409.71	4,147.53	1,604,100.49	603,040.81
5,333.07	2,616.13	1,604,023.85	601,509.41
5,325.56	1,465.35	1,604,016.34	600,358.63
4,018.19	147.42	1,602,708.91	599,040.70
5,370.73	-3,104.57	1,604,061.51	595,788.71
5,301.17	-4,695.58	1,603,991.95	594,197.70
10,697.47	1,439.93	1,609,388.25	600,333.21
-5,267.73	-2,494.35	1,593,423.05	596,398.93

TABLE XXVII—Continued

Errors of Observations E(ft)	N(ft)	Z(ft)
+3.99	-0.53	0.3
+2.43	+0.28	-1.6
+3.08	+1.28	-0.2
+3.85	+0.06	-1.4
+3.53	-0.78	-1.4
+1.02	+0.18	-3.7
+0.53	+0.60	-3.5
+2.02	-0.24	-6.9
+0.60	-2.22	-9.6
-1.81	-2.14	-9.4
X	-0.26	-2.4
-0.86	-1.61	-0.6
-4.22	-2.72	X
-1.06	-0.88	3.0
-1.31	-0.38	2.9
-0.52	-0.68	0.7
-2.51	X	3.8
-3.15	-0.13	3.9
0	0	0.1
-1.14	+1.07	-0.7
-0.81	-0.36	0.8
+0.65	+0.86	-1.2
-2.93	+0.49	-3.3
-3.35	+1.89	1.5
-1.80	+1.93	-2.4
-3.44	+1.89	1.9
-1.65	+1.30	-1.0
-1.96	+1.05	-1.4
X	+1.12	1.9
-4.48	+0.61	-0.5
-5.91	+2.90	X
-3.54	+0.65	2.9
+1.26	-2.30	-4.2

X Apparent observation error.

Y-direction errors in feet Figure 30

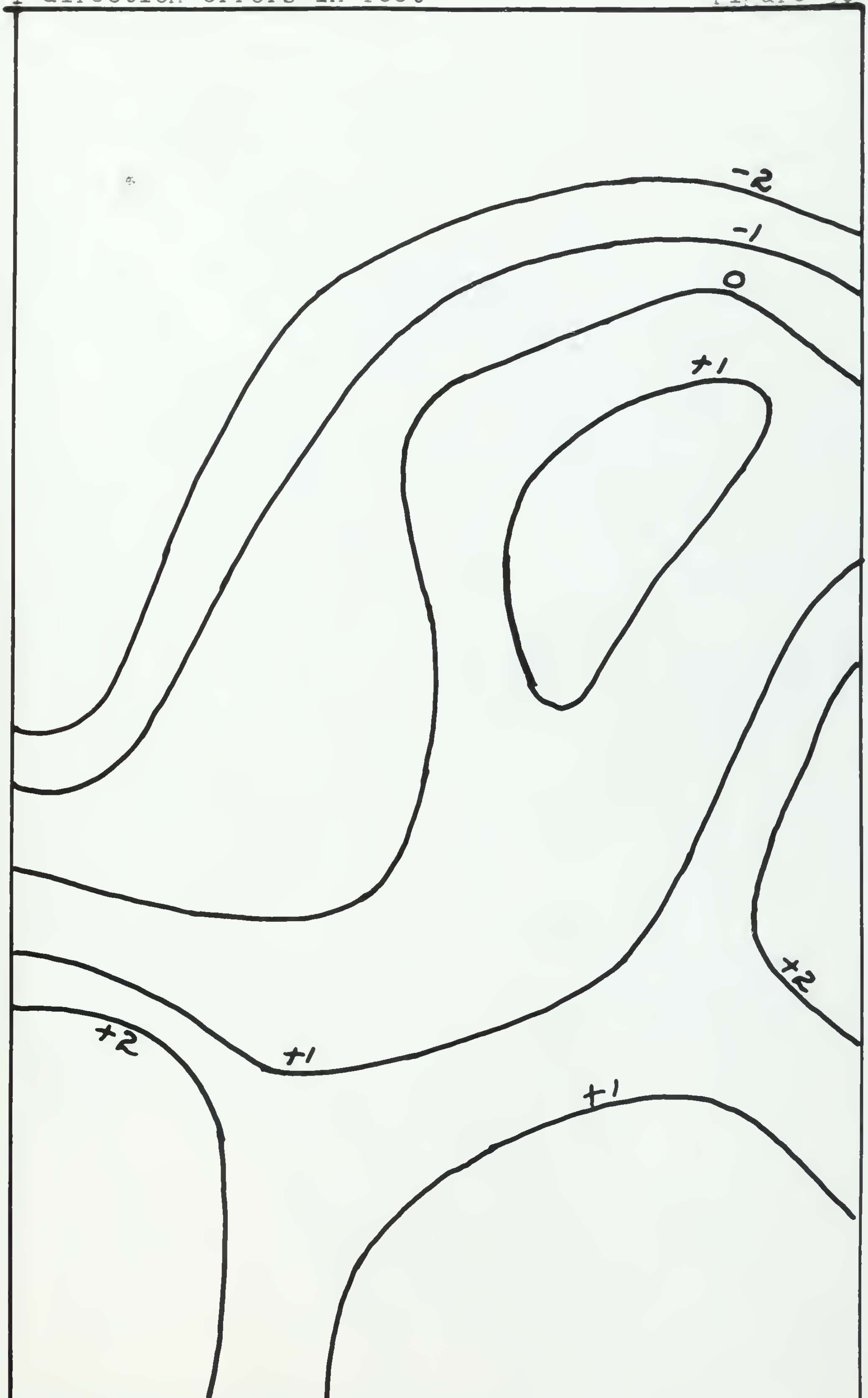

X-direction errors in feet Figure 31

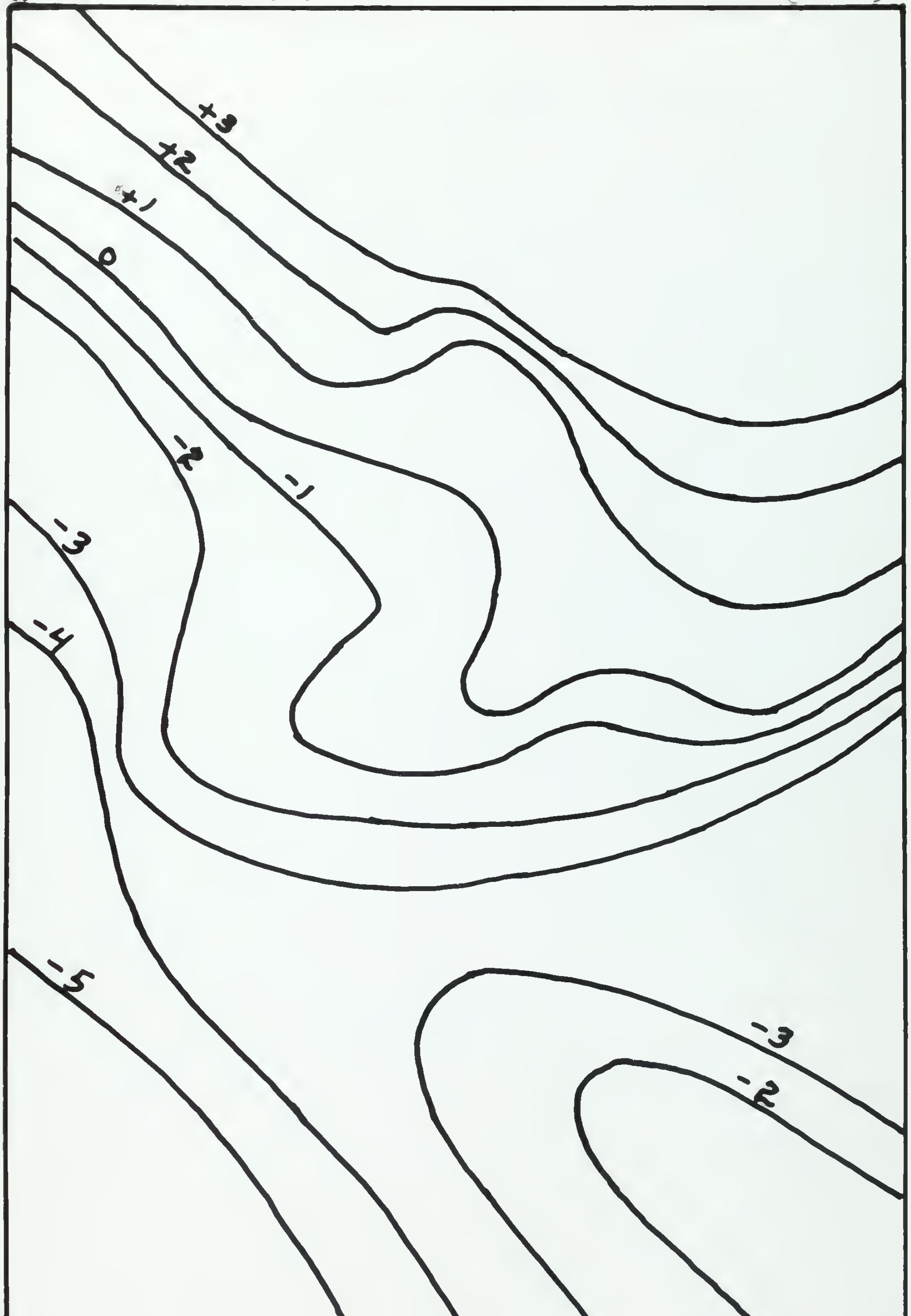

Elevation errors in feet Figure 32

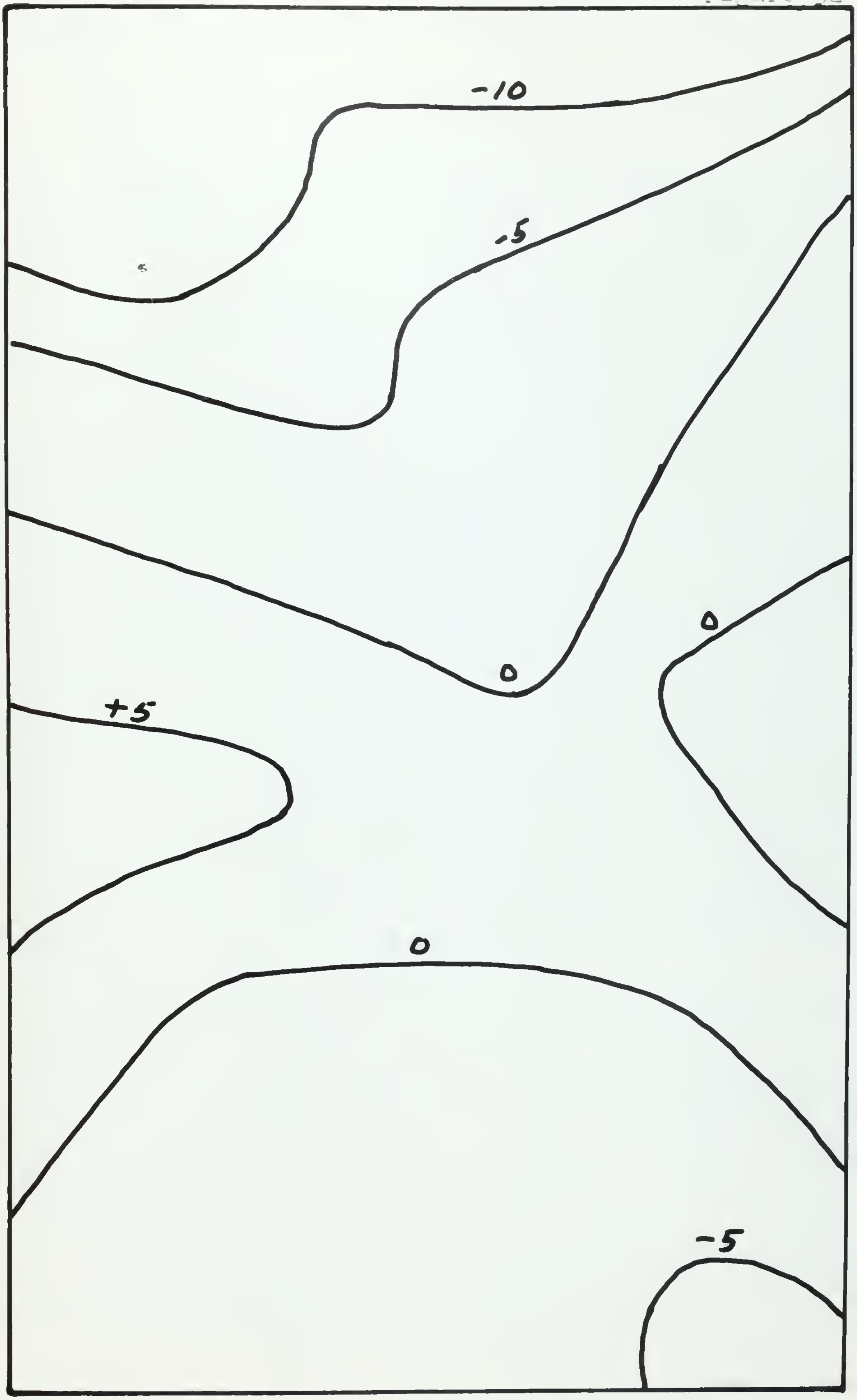

CONCLUSIONS

Assuming that the lens used in the photography measured is comparable to the average lens computed, a comparison of errors can be made, inasmuch as the elevation, 13,750', is approximately equal to the 4,000 m elevation assumed for other computations.

As is obvious from the difference in magnitude and pattern of error, the lack of a true spatial model prevents any meaningful comparison. With the exception of corner points, the elevation errors obtained were relatively close to being within the maximum computed for the average lens, however the range of errors was greater than computed for the average lens. The X-direction errors bore no resemblance to the computed graphs in either pattern or magnitude. The Y-direction errors cannot be computed, as previously discussed, due to the lack of ability to predict just where along the line between the two images, as separated by parallax, the point would be chosen. The magnitude of Y-direction errors, measured in the actual photography, is considerably less than the X-direction and elevation errors measured. The maximum predominant error in all coordinates was approximately 5 feet, which would put the accuracy at one part in 2,750 parts of elevation above the terrain. This accuracy would only be acceptable for most mapping requirements if flown at very low altitude above the terrain and controlled by

CONCLUSIONS

Assuming that the lens used in the photography examined is comparable to the average lens computed, a comparison of errors can be made, inasmuch as the elevation, 13,750', is approximately equal to the 4,000 m elevation assumed for other computations.

It is evident from the differences in magnitude and patterns of error, the lack of a true conical model prevents any meaningful comparisons. With the exception of summit points, the elevation errors obtained were relatively close to being within the maximum computed for the average lens; however the range of errors was greater than computed for the average lens. The X-direction errors bear no resemblance to the computed errors in either pattern or magnitude. The Y-direction errors cannot be compared, as previously discussed, due to the lack of ability to predict path shape along the line between the two images, as expressed by parallax, the points would be chosen. The magnitude of Y-direction errors, measured in the actual photography, is considerably less than the X-direction and elevation errors measured. The maximum predominant error in all coordinates was approximately 3 feet, which would put the accuracy at one part in 4,750 parts of elevation above the terrain. This accuracy would only be acceptable for most mapping requirements if flown at very low altitude above the terrain and controlled by

sufficient geodetic control or by high altitude normal angle photography.

Without the ability to obtain a true spatial model in the stereo plotter, the relatively high accuracy as computed for the X values of the average lens will not be achieved. Any tendency to warp the model to eliminate the parallax caused by lens distortion will tend to decrease the X coordinate accuracy. The elevation accuracy is also adversely affected by this warping but not to the same extent. The plus to minus range of errors is increased considerably but absolute errors are not increased too greatly. The Y-direction errors which would be obtained with a true spatial model would probably not be too great but cannot be predicted due to the range of possibilities of Y-positions due to parallax. The maximum of 15 microns parallax computed for the average lens would create a maximum Y-direction error of approximately one part in 10,000 of elevation above terrain. Thus to map with the above photographs taken at 13,000 feet above the terrain, the maximum mapping scale which could be used with mapping accuracy of 0.2 mm would be 1:6,000.

Thus metrogon photography is suitable for low altitude mapping with the altitude determined by the mapping accuracy required, but is not suitable for any control extension work. The only case in which metrogon photography would be suitable would be in case the distortion curve of the lens used was sufficiently close to the metrogon correction plates to be used to bring uncompensated errors throughout the model area to less than 10 microns.